

GEORGIA INSTITUTE OF TECHNOLOGY
OFFICE OF CONTRACT ADMINISTRATION

NOTICE OF PROJECT CLOSEOUT

Closeout Notice Date 01/09/92

Project No. E-20-622_____ Center No. 10/24-6-R7188-0A0_
Project Director MAYNE P W_____ School/Lab CIVIL ENGR_____
Sponsor US DEPT OF TRANSPORTATION/FED AVIATION ADMIN_____
Contract/Grant No. DTFA06-89-F-32199_____ Contract Entity GTRC
Prime Contract No. DTFA06-89-C-30008_____
Title OPTIMIZING THE DESIGN OF LLWAS FOUNDATIONS_____
Effective Completion Date 911231 (Performance) 911231 (Reports)

Closeout Actions Required:	Y/N	Date Submitted
Final Invoice or Copy of Final Invoice	Y	_____
Final Report of Inventions and/or Subcontracts	N	_____
Government Property Inventory & Related Certificate	N	_____
Classified Material Certificate	N	_____
Release and Assignment	N	_____
Other _____	N	_____
Comments _____		

Subproject Under Main Project No. _____

Continues Project No. _____

Distribution Required:

Project Director	Y
Administrative Network Representative	Y
GTRI Accounting/Grants and Contracts	Y
Procurement/Supply Services	Y
Research Property Management	Y
Research Security Services	N
Reports Coordinator (OCA)	N
GTRC	Y
Project File	Y
Other _____	N
_____	N

TA
7
.GA5X
E-20-622
M386

GTA

Georgia Tech Research Corporation
Georgia Institute of Technology
School of Civil Engineering
Atlanta, GA 30332-0355

**Geotechnical Design Manual
for LLWAS Tower Foundations
Under Lateral and Moment Loading**

submitted to

Federal Aviation Administration
Southern Region
Atlanta, GA 30320

FAA Project No. D3794
FAA Contract No. DTFA06-89-F-32199
GTRC Project No. E-20-622

December 31, 1991



Georgia Tech Research Corporation
Georgia Institute of Technology
School of Civil Engineering
Atlanta, GA 30332-0355

**Geotechnical Design Manual
for LLWAS Tower Foundations
Under Lateral and Moment Loading**

submitted to

Federal Aviation Administration
Southern Region
Atlanta, GA 30320

FAA Project No. D3794
FAA Contract No. DTFA06-89-F-32199
GTRC Project No. E-20-622

December 31, 1991

**Geotechnical Design Manual
for LLWAS Tower Foundations
Under Lateral and Moment Loading**

**FAA Project No. D3794
FAA Contract No. DTFA06-89-F-32199
GTRC Project No. E-20-622**

December 1991

Prepared by

**GEORGIA TECH RESEARCH CORPORATION
Georgia Institute of Technology
School of Civil Engineering
Geotechnical Engineering Division
Atlanta, Georgia 30332-0355**

**Authors
D.G. Blaydes
B.S.Y. Chen
J.S. Fang
P.W. Mayne**

**Principal Investigator
P.W. Mayne**

Prepared for

**Federal Aviation Administration
Southern Region, ASO 462
P.O. Box 20636
Atlanta, Georgia 30320**

**FAA Technical Officer
A.G. Stensland**

EXECUTIVE SUMMARY

Current practice for supporting a 150-foot high FAA LLWAS tower involves the construction of a single drilled shaft foundation with a 4-foot diameter embedded 20 feet into soil and/or rock, depending upon the specific site and local geology. Large overturning moments are imposed on the shafts during storm events. Specific concerns include the ultimate lateral capacity and groundline displacements of the foundations during wind shear and microbursts, since the LLWAS system must perform as a warning system for these conditions.

In the FAA Southern Region, a total of 37 airports have been outfitted with a basic array of 6 LLWAS towers. For most of these sites, the LLWAS tower foundation systems have proven to be adequate in capacity and overall performance. At 16 of these airports, an additional 5 LLWAS towers have been installed or are currently under construction. The remaining 21 airports will also be provided with additional LLWAS towers over the next few years. Of particular interest to FAA are sites where: (1) the standard foundation design may be inadequate for load-deflection response due to poor soil conditions and (2) shallow bedrock conditions which result in significant cost overruns during construction in order to achieve the standard design foundation lengths.

This design manual summarizes procedures to be taken by field personnel during the initiation and construction of future LLWAS towers. The text of this manual is a synopsis of a companion *Final Report* addressing a geotechnical analysis of the LLWAS drilled shaft foundation system which has been prepared by GTRC for the FAA Southern Region. The geotechnical study was performed to evaluate the probable lateral capacity and load-deflection response under a variety of common geologic settings, soil types, and bedrock conditions. The effort was separated into three primary tasks to address specific issues raised by the FAA Technical Officer, including: (1) the expected performance of standard LLWAS foundations under critical loading conditions, (2) an assessment of available analytical and numerical modelling capabilities, and (3) recommendations for

minimum required socket lengths of shaft foundations at sites where shallow rock is encountered. These task items are discussed in detail in the *Final Report*.

SOIL PROFILES

Analytical Design Charts

For LLWAS towers installed at sites underlain by firm soils, the standard 4-foot diameter by 20-foot long drilled shaft foundations appear adequate. These dimensions constitute relatively rigid foundation members due to their low length to diameter ratio ($L/d = 5$). Their anticipated performance has been evaluated from a load test database on rigid drilled shaft foundations subjected to lateral/moment loading that were compiled from the geotechnical literature and published reports. These load test results have been analyzed within a framework of elastic continuum mechanics, and a simple hyperbolic model was shown to effectively describe the nonlinear load-deflection behavior. Backcalculated design parameters were formulated in terms of soil strength and soil modulus, which in turn have been related to the simple and common standard penetration test (SPT).

The results of the analytical study are summarized in Figures 1 and 2 for clayey soils and sandy soils, respectively. As discussed in the *Final Report*, a maximum groundline deflection $\delta = 0.5$ inches has been established as the acceptance criterion for foundation performance. The analyses show that, in general, the standard LLWAS foundation is capable of adequate or superior performance under critical loading conditions, except where the soil overburden profile consists of soft/firm clays or loose sands below the water table.

Problem Soils

Specifically, the numerical analysis indicated problems could exist where the results of soil test borings (ASTM D-1586) showed standard penetration test (SPT) resistances consistently less than 7 blows per foot in clays and less than 8 blows per foot in sands. For LLWAS sites not meeting these criteria, more extensive geotechnical analyses should be performed to evaluate the need for installing deeper (or wider) foundations at these sites.

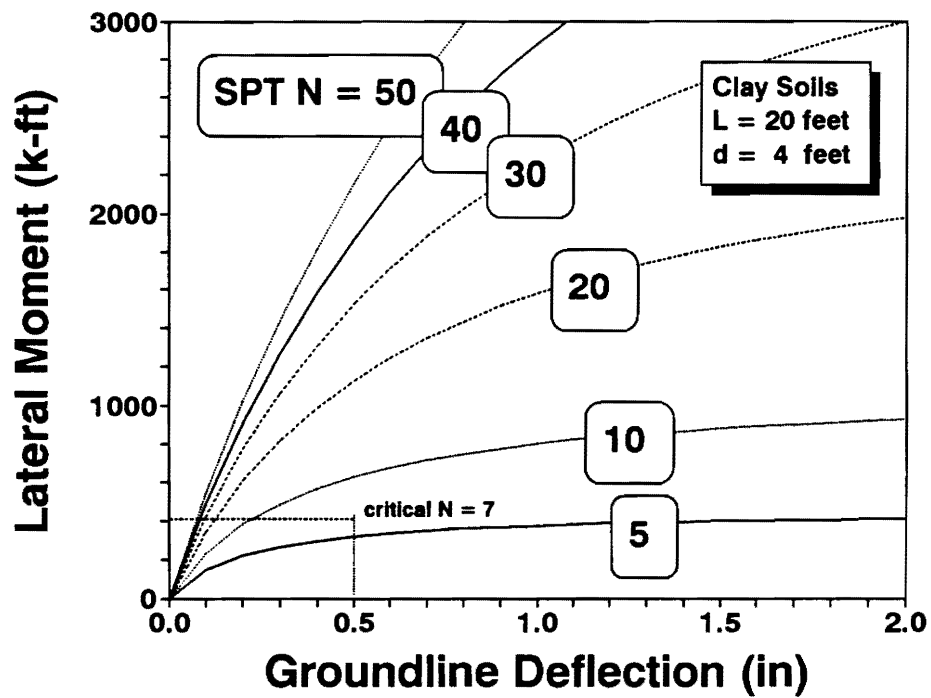


Figure 1. Predicted Moment-Deflection Behavior of Shafts at Clay Sites.

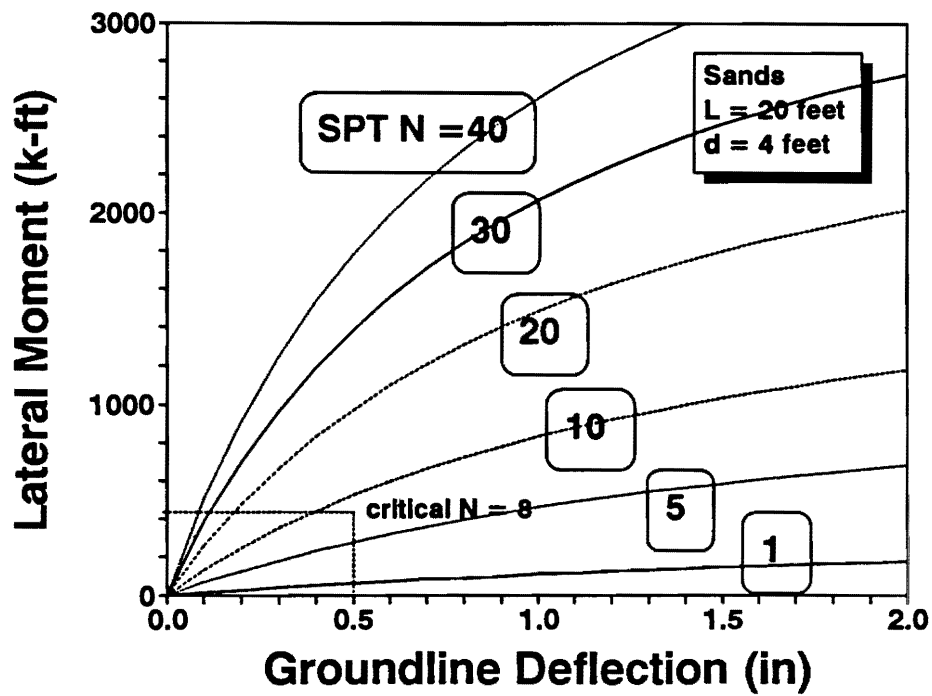


Figure 2. Predicted Moment-Deflection Behavior of Shafts at Sand Sites.

Field Inspection

Visual examination of auger cuttings of excavated soils should provide warning to the FAA field inspector as to the necessity for more detailed geotechnical analyses and possible need for a modified foundation design. Of particular concern, the field inspector should be wary of wet, soft, and plastic clays, black and dark-colored clays with organics, peats, uniform silts, loose clean to silty sands, and soils which cave upon excavation by the caisson rig (Reference ASTM D-2488 standards for soil classification). Also, sites having been previously filled and containing debris, rubble, waste, and man-made buried objects should be suspect as not meeting the criteria for acceptable ground.

In many cases, the field inspector may be able to discern the problem soil types, yet not be confident in estimating the degree of penetration resistance without actually performing an SPT. For these situations, the helix probe test (HPT) may provide a simple and economical means of obtaining a numerical value of the soil consistency. The HPT measures the torque required to advance a 0.75-inch diameter auger (Yokel and Mayne, 1988). Approximately five feet of soil depth can be investigated in about 5 to 10 minutes with readings typically taken on 0.5-foot increments. The measured torque (t_{12}) has been correlated with standard penetration test (SPT) resistance, as well as cone penetration test (CPT), dilatometer test (DMT), and in-place density measurements. The entire instrument weighs only 5 lbs and easily carried by a field inspector. A modified version with rod extensions has also been built which is capable of achieving test depths of up to 20 feet.

Advanced Geotechnical Analyses

If the field inspector has determined the need for additional and more extensive foundation analyses, a qualified geotechnical consultant should be retained to perform the necessary in-situ testing and computer simulations. Based on the findings of the *Final Report*, it is recommended that the consultant perform a series of flat dilatometer tests (DMT) or pressuremeter tests (PMT) at the LLWAS site in question. Test procedures for the DMT and PMT are given by Schmertmann (1986) and ASTM (1990). The results of these tests provide information on the soil strength and modulus properties.

The use of the computer programs: LTBASE (North Carolina State University, Raleigh, NC) or MFAD (Electric Power Research Institute, Palo Alto, CA) appear appropriate for analyzing LLWAS foundations because both have been specifically developed for short and rigid drilled shafts.

In the event that the standard design is suspected to be inadequate, the following remedial measures may be considered: (1) increase foundation length, (2) increase foundation diameter, (3) soil improvement, or (4) move the tower location. Considering the practicality of drilling operations and feasibility of construction, selection of choice (1) appears the most economical. Therefore, modified designs and analyses should be directed at solutions which investigate $L = 30$ feet, or longer, or similar such alternatives.

SHALLOW BEDROCK PROFILES

Analytical Approach

The design and construction of LLWAS foundations at sites with soil over shallow bedrock has also been addressed in the *Final Report*. In the LLWAS program, no current procedures or guidelines exist for terminating shaft lengths less than the standard design length of 20 feet, even if sound rock is encountered beforehand. Available analytical tools for evaluating rock-socketed shafts have been reviewed and these are based on boundary element and finite element solutions to elastic continuum formulations of the problem. A computer program (DEFPIG) has been used to develop a design chart, presented as Figure 3, which rationally minimizes the required length of the rock socket. The chart is valuable to the FAA field inspector in selecting a suitable total length of shaft and mitigating cost overruns during drilled shaft construction.

In the event that bedrock is encountered at the ground surface, the recommended minimum length of the shaft should be 1.5 times the foundation diameter. Recent unpublished moment load tests on rock-socketed shafts conducted by EPRI support this recommendation. Therefore, for the standard 4-foot diameter shaft, a minimum 6-foot embedment length is recommended.

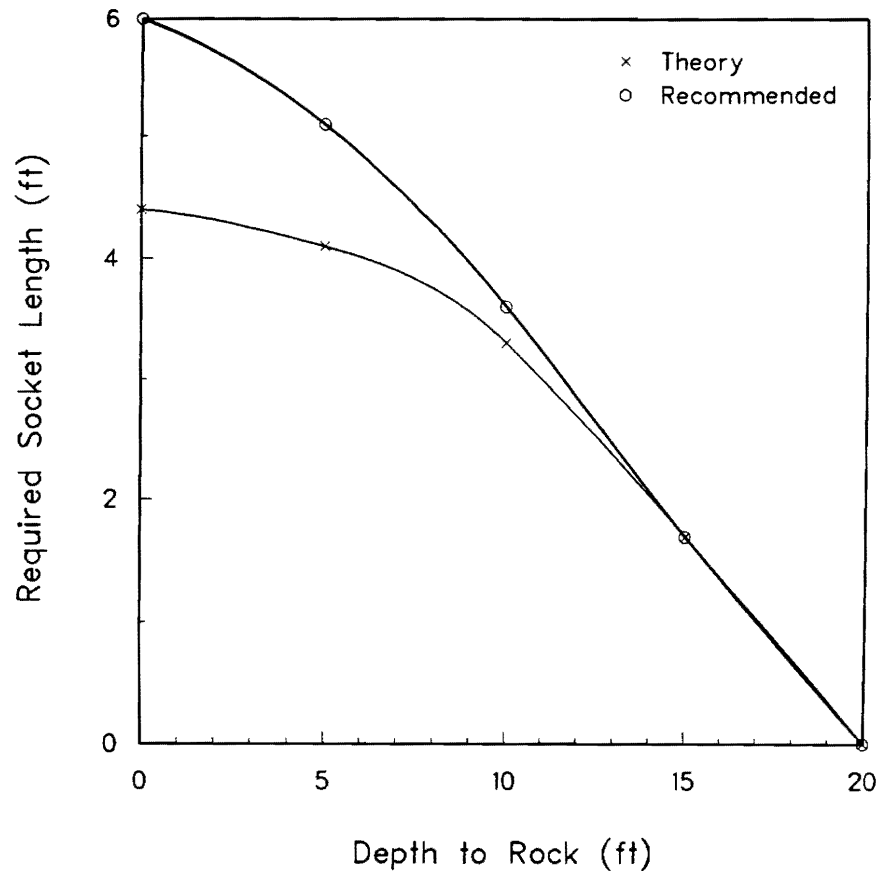


Figure 3. Recommended Minimum Length of Rock Socket for Drilled Shaft Foundations Constructed at Shallow Bedrock Sites.

Detailed Geotechnical Analysis

If more detailed analyses are desired, the following procedure is suggested for implementation by a qualified geotechnical consultant. Soil test borings with standard penetration testing (SPT) should be advanced to the top of bedrock (ASTM D-1586). The SPT values may be used to evaluate the relevant soil moduli from relationships given in Section 2 of the *Final Report*. Upon SPT refusal, core samples of the underlying rock should be taken (ASTM D-2113) and the rock quality designation (RQD) should be determined. Selected specimens from the recovered core should be subjected to uniaxial compression tests to determine the elastic modulus of the intact rock (ASTM D-3148). The RQD value should be utilized to obtain a reduction factor per Section 4 of the *Final Report* and appropriate value of the modulus of the rock mass in-situ. Finally, the computer program DEFPIG (University of Sydney, Australia) should be used to evaluate the load-deflection behavior of the rock-socketed foundations.

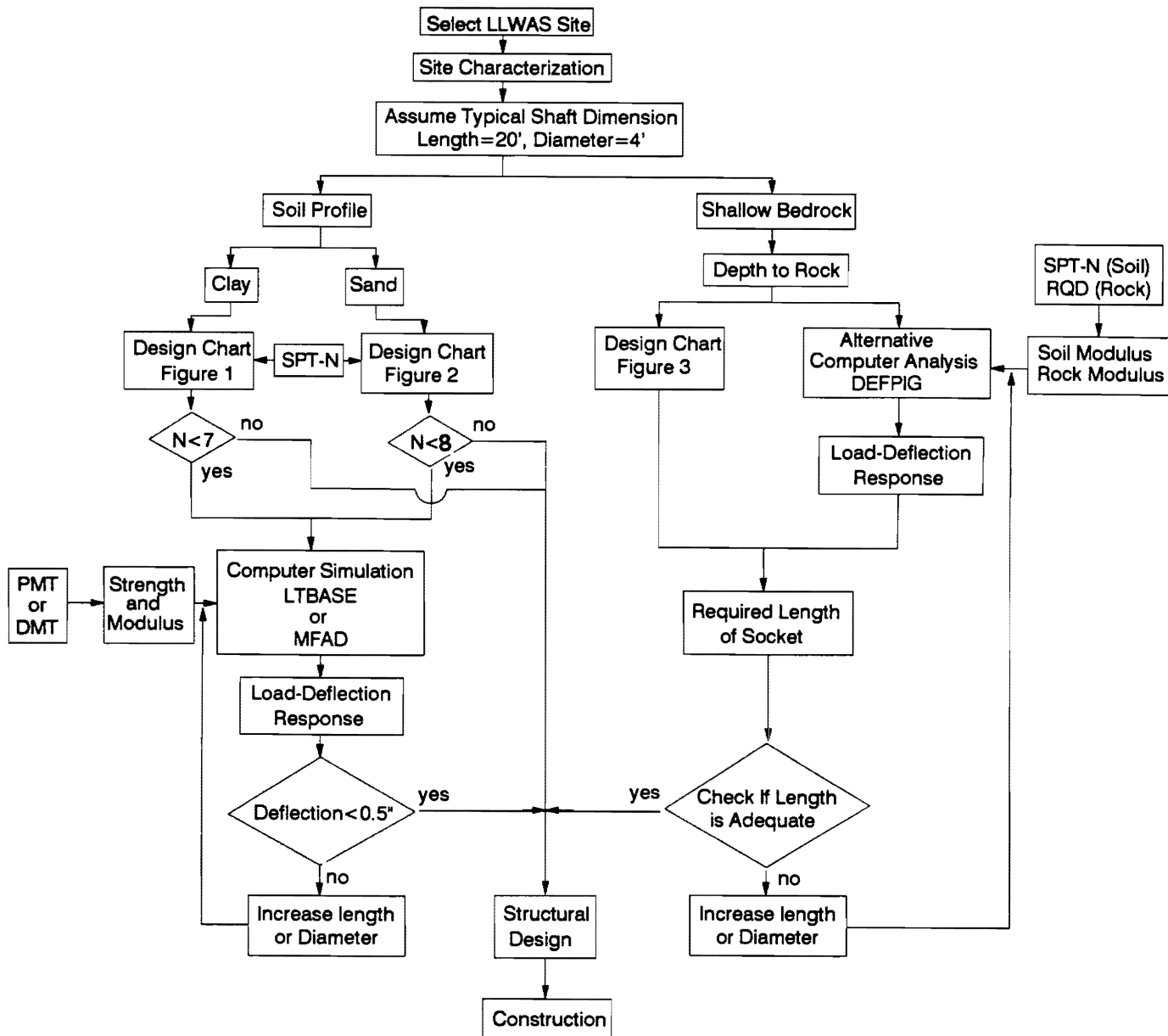


Figure 4. Systematic Procedure for Geotechnical Evaluation of LLWAS Site.

FLOW CHART

A synopsis of the recommended procedures for evaluating the suitability of geotechnical conditions at specific LLWAS tower foundation locations is given on the flow chart in Figure 4. This flow chart may be used by the field inspection and FAA engineer in

assessing the adequacy of the standard LLWAS foundation design, the need for more extensive geotechnical studies, and/or the modification of the drilled shaft foundation to meet the desired performance.

Based on numerical and analytical calculations, the standard LLWAS drilled foundation ($L = 20$ feet, $d = 4$ feet) appears adequate or superior for its intended use, except at sites underlain by soft/firm clays and silts or loose sands below the water table. The field inspector should be trained to discern unacceptable soil conditions and may find assistance in evaluating poor ground conditions by use of the helix probe test (HPT).

At shallow bedrock sites, conservative estimates of rock mass properties and numerical analyses indicate that the total length of the LLWAS foundation may be reduced. The required length of the rock socket will depend upon the particular depth to bedrock.

REFERENCES

American Society for Testing and Materials (1990), ASTM D-3148: "Standard Test Method for Elastic Moduli of Intact Rock Core Specimens", Annual Book of ASTM Standards, Vol. 04.08, Philadelphia, PA, 391-394.

American Society for Testing and Materials (1990), ASTM D-2113: "Standard Practice for Diamond Core Drilling for Site Investigation", Annual Book of ASTM Standards, Vol. 04.08, Philadelphia, PA, 256-259.

American Society for Testing and Materials (1990), ASTM D-1586: "Standard Method for Penetration Test and Split-Barrel Sampling of Soils", Annual Book of ASTM Standards, Vol. 04.08, Philadelphia, PA, 228-232.

American Society for Testing and Materials (1990), ASTM D-4719: "Standard Test Method for Pressuremeter Testing in Soils", Annual Book of ASTM Standards, Vol. 04.08, Philadelphia, PA, 896-903.

American Society for Testing and Materials (1990), ASTM D-2488: "Standard Practice for Description and Identification of Soils", Annual Book of ASTM Standards, Vol. 04.08, Philadelphia, PA, 305-314.

Borden, R.H. and Gabr, M.A. (1987), "LTBASE: Computer Program for Laterally-Loaded Pier Analysis Including Base and Slope Effects", Research No. HRP 86-5, North Carolina State University, Raleigh, NC, 48 p.

Chen, B.S-Y., Fang, J.S., Blaydes, D.G., and Mayne, P.W. (1991), "Final Report, Geotechnical Evaluation of LLWAS Tower Foundations Under Lateral and Moment Loading", Georgia Tech Research Corporation Report E-20-622 to FAA Southern Region, Atlanta, Georgia, 113 p.

Davidson, H.L., et al. (1990), "TL Workstation Code: Version 2.0, Volume 17, MFAD Manual", EPRI Report EL-6420, Electric Power Research Institute, Palo Alto, CA.

Poulos, H.G. (1978), "User's Guide to Program DEFPIG", University of Sydney, School of Civil Engineering, Australia, 77 p.

Schmertmann, J.H. (1986), "Suggested Method for Performing the Flat Dilatometer Test", ASTM Geotechnical Testing Journal, Vol. 9 (2), 93-101.

Yokel, F.Y. and Mayne, P.W. (1988), "Helical Probe Tests: Initial Test Calibration", ASTM Geotechnical Testing Journal, Vol. 11 (3), 179-186.

Georgia Tech Research Corporation
Georgia Institute of Technology
School of Civil Engineering
Atlanta, GA 30332-0355

Final Report
Geotechnical Evaluation of LLWAS Tower
Foundations Under Lateral and Moment Loading

submitted to

Federal Aviation Administration
Southern Region
Atlanta, GA 30320

FAA Project No. D3794
FAA Contract No. DTFA06-89-F-32199
GTRC Project No. E-20-622

December 31, 1991



***Georgia Tech Research Corporation
Georgia Institute of Technology
School of Civil Engineering
Atlanta, GA 30332-0355***

**Final Report
Geotechnical Evaluation of LLWAS Tower
Foundations Under Lateral and Moment Loading**

submitted to

***Federal Aviation Administration
Southern Region
Atlanta, GA 30320***

**FAA Project No. D3794
FAA Contract No. DTFA06-89-F-32199
GTRC Project No. E-20-622**

December 31, 1991

Geotechnical Evaluation of LLWAS Tower Foundations Under Lateral and Moment Loading

**FAA Project No. D3794
FAA Contract No. DTFA06-89-F-32199
GTRC Project No. E-20-622**

Final Report, December 1991

Prepared by

**GEORGIA TECH RESEARCH CORPORATION
Georgia Institute of Technology
School of Civil Engineering
Geotechnical Engineering Division
Atlanta, Georgia 30332-0355**

**Authors
B.S.Y. Chen
J.S. Fang
D.G. Blaydes
P.W. Mayne**

**Principal Investigator
P.W. Mayne**

Prepared for

**Federal Aviation Administration
Southern Region, ASO 462
P.O. Box 20636
Atlanta, Georgia 30320**

**FAA Technical Officer
A.G. Stensland**

ACKNOWLEDGMENTS

Several individuals provided valuable assistance to the authors during the development of this study and preparation of this manuscript. In particular, Mr. Alan Stensland of FAA met with the principal investigator and co-authors to detail the scope of the geotechnical evaluation and critique a presentation on the group's findings. In addition, Mr. Stensland provided a site tour of existing and presently-constructed LLWAS towers at the Atlanta Hartsfield Airport. Dr. R.C. Bachus prepared the initial proposal to FAA and reviewed a draft version of the report prior to publication. In addition, Dr. F.H. Kulhawy of Cornell University, Ithaca, NY, Dr. S.W. Agaiby of Cairo University, Egypt, Dr. C.H. Trautmann of the Ithaca Sciencenter, NY, Dr. L. Roja-Gonzales of GAI Consultants, Pittsburgh, PA, and Mr. V.J. Longo of EPRI, Palo Alto, CA, all contributed to providing information, data, published documents, and stimulating discussions during the project development.

ABSTRACT

The standard FAA LLWAS tower foundation includes a single drilled shaft foundation supporting a 150-foot high hollow metal pole outfitted with anemometers to detect wind shear. Each foundation consists of a 4-foot diameter shaft embedded 20 feet into soil and/or rock, depending upon the specific site and local geology. Large overturning moments are imposed on the shafts during storm events. Specific concerns include an evaluation of the ultimate lateral capacity of these foundations under storm loading, as well as the magnitude of groundline displacement, since excessive deflections may result in false indications of microburst activity or impaired transmission of signals during potentially critical events. An allowable groundline deflection of 0.5 inches has been adopted as the tolerance criterion for acceptable performance of LLWAS foundations.

In this study, a geotechnical analysis of the LLWAS drilled shaft foundation system was performed to evaluate the probable lateral capacity and load-deflection response. The effort was separated into three primary tasks to address specific issues raised by the FAA Technical Officer, including: (1) the expected performance of standard LLWAS foundations under critical loading conditions, (2) an assessment of available analytical and numerical modelling capabilities, and (3) recommendations for minimum required socket lengths of shaft foundations at sites where shallow rock is encountered. These task items are discussed in detail in the report sections.

Section 1 provides an introduction to the drilled shaft foundation system and imposed loading conditions peculiar to the LLWAS tower situation. In particular, the critical mode of loading involves high overturning moments on relatively rigid foundations. Section 2 presents a load test database on rigid drilled shaft foundations subjected to lateral/moment loading. Load test data were compiled from the geotechnical literature and published reports. These load test results are evaluated within a framework of elastic

continuum mechanics and a simple hyperbolic model is shown to effectively describe nonlinear load-deflection behavior. Backcalculated design parameters are formulated in terms of soil strength and soil modulus, which in turn are related to the most common of the in-situ test methods, the standard penetration test (SPT). Analyses show that, in general, the standard LLWAS foundation is capable of adequate or superior performance under critical loading conditions, except where the soil overburden profile exhibits SPT resistances consistently less than 7 blows per foot in clays and less than 8 blows per foot in sands. For these cases, more extensive geotechnical analyses should be performed to evaluate the need for installing deeper (or wider) foundations at these sites.

Section 3 includes a parametric assessment of the shaft geometry of LLWAS foundations using available computer methods. Four different commercial programs (COM624, MFAD, LTBASE, and PIGLET) all address the predicted behavior of deep foundations under lateral and moment loading. The benefits and limitations of these programs are reviewed and examined for selected examples. Two programs have been specifically developed for rigid drilled shaft behavior (MFAD and LTBASE), and these are applied to several case studies to compare the predicted behavior with actual load test results obtained from the published literature. Since the computer methods require a relatively high level of input data, the focus of work in Section 3 investigates the use of sophisticated in-situ test devices, such as the pressuremeter test (PMT) and flat dilatometer test (DMT).

Section 4 addresses the design and construction of LLWAS foundations at sites with shallow bedrock. In the LLWAS program, no current procedures or guidelines exist for terminating shaft lengths less than the standard design length of 20 feet, even if sound rock is encountered beforehand. Available analytical tools for evaluating rock-socketed shafts are reviewed. Essentially, these methods are based on boundary element and finite element solutions to elastic continuum theory formulations of the problem. A computer program (DEFPIG) is used to aid in developing design charts which rationally minimizes the required length of the rock socket.

	Table of Contents	Page
	ACKNOWLEDGMENTS	i
	ABSTRACT	ii
	TABLE OF CONTENTS	iv
	LIST OF FIGURES	vii
	LIST OF TABLES	ix
1.	INTRODUCTION	1
	1.1. LLWAS TOWER STRUCTURES	1
	1.2. STRUCTURAL LOADING OF POLE STRUCTURES	2
	1.3. LATERAL AND MOMENT LOADING OF DEEP FOUNDATIONS	3
	1.4. TOLERANCE CRITERION	7
	1.5. SCOPE OF STUDY	9
	1.6. REFERENCES	10
2.	BEHAVIOR OF LATERALLY-LOADED DRILLED SHAFTS	12
	2.1. LLWAS FOUNDATIONS	13
	2.1.1. Lateral Capacity Criteria	13
	2.1.2. Rigidity Criteria	14
	2.1.3. Soil Shearing Mode	16
	2.2. LOAD TEST DATABASE	19
	2.3. FOUNDATION LOAD-DEFLECTION RESPONSE	23
	2.3.1. Hyperbolic Load-Deflection Model	23
	2.3.2. Limit Equilibrium Analysis	27
	2.3.3. Elastic Continuum Theory	30
	2.3.4. Interpretation of Undrained Strength and Soil Modulus . . .	33
	2.3.5. Interpretation of Drained Strength	34
	2.4. UTILIZATION OF LOAD TEST DATABASE	35
	2.4.1. Standard Penetration Test Correlations	40
	2.4.2. Prediction of Load-Deflection Curves	47
	2.5. CONCLUSIONS	50
	2.6. REFERENCES	51
3.	COMPUTER MODELLING OF LATERALLY-LOADED DRILLED SHAFTS	54
	3.1. ANALYTICAL METHODOLOGIES FOR LATERAL PILE PROBLEM	54
	3.2. COMPARISON OF COMPUTER PROGRAMS	55
	3.2.1. COM624	56
	3.2.2. LTBASE	58
	3.2.3. PIGLET	58
	3.2.4. MFAD	58

	Table of Contents (Continued)	Page
3.3.	CAPABILITIES AND LIMITATIONS	59
3.4.	COMPARISONS OF PREDICTIONS FROM COMPUTER PROGRAMS	62
3.4.1.	Case 1 - Undrained Lateral Loading Condition	63
3.4.2.	Case 2 - Drained Lateral Loading Condition	65
3.4.3.	Discussion of Results	65
3.5.	CASE STUDIES	67
3.5.1.	Texas A&M University Campus Site	67
3.5.2.	Barnhart Island Site	71
3.5.3.	Delta Site	73
3.5.4.	Alamo Site	75
3.5.5.	North Carolina Highway Site	75
3.6.	CONCLUSIONS	78
3.7.	REFERENCES	79
4.	ELASTIC SOLUTIONS FOR ROCK-SOCKETED SHAFTS	81
4.1.	METHODS OF ANALYSIS	81
4.1.1.	Poulos (1972) Solution	81
4.1.2.	Carter and Kulhawy (1988) Solution	87
4.1.3.	DEFPIG Computer Solution	91
4.2.	LOAD TEST DATA	92
4.2.1.	Load Tests in Texas	92
4.2.2.	Load Tests in the United Kingdom	96
4.2.3.	Load Tests on Shafts in Surface Exposed Rock	98
4.3.	DETERMINATION OF MATERIAL PARAMETERS	99
4.3.1.	Elastic Parameters For Soils	100
4.3.2.	Elastic Parameters for Rock Masses	100
4.4.	ANALYSIS AND DISCUSSION	103
4.4.1.	Comparison of Methods	103
4.4.2.	Recommended Design Procedure	106
4.4.3.	Example Application	107
4.4.4.	Analysis of the Load Test Data	110
4.5.	DESIGN CHARTS	110
4.6.	CONCLUSIONS	113
4.7.	REFERENCES	113
5.	EXECUTIVE SUMMARY	115
5.1.	SOIL PROFILES	116
5.1.1.	Analytical Design Charts	116
5.1.2.	Problem Soils	116
5.1.3.	Field Inspection	118
5.1.4.	Advanced Geotechnical Analysis	118
5.2.	SHALLOW BEDROCK PROFILES	119

5.2.1. Analytical Approach	119
5.3. FLOW CHART	121
5.4. REFERENCES	122

List of Figures

Page

Fig. 1.1.	Structural Loading Components of an LLWAS Pole Tower.	2
Fig. 1.2.	Terminology Used for Drilled Shaft Foundations	4
Fig. 1.3.	Head Fixity Conditions of Drilled Shafts Under Lateral Loading . . .	5
Fig. 1.4.	Modelling Soil Stiffness by Subgrade Reaction and Elastic Theory . .	6
Fig. 2.1.	Structural Loads on the LLWAS Tower Foundations	12
Fig. 2.2.	Comparison of Lateral Load Interpretation Criteria	13
Fig. 2.3.	Concept of Rigid versus Flexible Shaft Behavior	14
Fig. 2.4.	Relevance of Laboratory Strength Tests to Field Conditions	18
Fig. 2.5.	Hyperbolic Fit of Load-Deflection Curve	26
Fig. 2.6.	Derivation of Hyperbolic Parameters	27
Fig. 2.7.	Rigorous Method of Limit Equilibrium Analysis	28
Fig. 2.8.	Recommended Profiles of Lateral Soil Resistance	29
Fig. 2.9.	Example of Spreadsheet Used to Evaluate Load Test Data	37
Fig. 2.10.	Undrained Strength Ratio as a Function of Test Type	39
Fig. 2.11.	Correlation 1 between s_u and SPT-N Value for Cohesive Soils	42
Fig. 2.12.	Correlation 2 between s_u and SPT-N Value for Cohesive Soils. . . .	42
Fig. 2.13.	Correlation 3 between s_u and SPT-N Value for Cohesive Soils. . . .	43
Fig. 2.14.	Correlation Between Modulus E_t and SPT-N Value for Clays	43
Fig. 2.15.	Correlation 1 between Sand Strength and SPT-N Value	44
Fig. 2.16.	Correlation 2 between Sand Strength and SPT-N Value	44
Fig. 2.17.	Correlation 3 between Sand Strength and SPT-N Value	45
Fig. 2.18.	Correlation between Modulus E_t and SPT-N Value for Sands	45
Fig. 2.19.	Predicted Load-Deflection Curves for Cohesive Soils	49
Fig. 2.20.	Predicted Load-Deflection Curves for Cohesionless Soils	49
Fig. 3.1.	Theoretical Basis for Soil Stiffness of the Computer Programs	57
Fig. 3.2.	Shaft Geometry and Clay Properties for Case 1	64
Fig. 3.3.	Results of Case 1 Analyses for Pier in Clay	64
Fig. 3.4.	Shaft Geometry and Sand Properties for Case 2	66
Fig. 3.5.	Results of Case 2 Analyses for Pier in Sand	66
Fig. 3.6.	Results of In-Situ Testing at Texas A&M Campus Site	69
Fig. 3.7.	Measured and Predicted Deflections for Texas A&M Site	69
Fig. 3.8.	Summary of In-Situ PMT and DMT Results at Barnhart Site, NY. . .	71
Fig. 3.9.	Measured and Predicted Response for Barnhart Island Site, NY	72
Fig. 3.10.	Measured and Predicted Response for Shaft 1 at Delta Site	74
Fig. 3.11.	Measured and Predicted Response for Shaft 2 at Delta Site	74
Fig. 3.12.	Measured and Predicted Response for Pier 1 at Alamo Site	76
Fig. 3.13.	Measured and Predicted Response for Pier 2 at Alamo Site	76
Fig. 3.14.	Measured and Predicted Response for Pier at North Carolina	78
Fig. 4.1.	Various Boundary conditions for Laterally-Loaded Shafts	81
Fig. 4.2.	Influence factors I_{rH} from Poulos (1972)	84

	Page
List of Figures (Continued)	
Fig. 4.3. Influence factors I_{pM} and $I_{\theta H}$ from Poulos (1972)	85
Fig. 4.4. Influence factors $I_{\theta M}$ from Poulos (1972)	85
Fig. 4.5. Fixing Moment at Drilled Shaft Tip/Base	87
Fig. 4.6. Horizontal Force at Drilled Shaft Tip/Base	88
Fig. 4.7. Profiles for Socketed Shafts A and B	93
Fig. 4.8. Profiles for Socketed Shafts C and D	93
Fig. 4.9. Load-Deflection Curve for Socketed Shaft A	94
Fig. 4.10. Load-Deflection Curve for Socketed Shaft B	95
Fig. 4.11. Load-Deflection Curve for Socketed Shaft C	95
Fig. 4.12. Load-Deflection Curve for Socketed Shaft D	96
Fig. 4.13. Details for Socketed Drilled Shafts E and F in the U.K.	97
Fig. 4.14. Load-Deflection Curves for Socketed Shafts E and F	97
Fig. 4.15. Details for Rock-Socketed Shafts G and H	98
Fig. 4.16. Load-deflection Curves for Socketed Shafts G and H	99
Fig. 4.17. Modulus Reduction Factor vs. Rock Quality Designation (RQD) . .	102
Fig. 4.18. Rock Mass Modulus vs. Rock Mass Rating (RMR).	102
Fig. 4.19. Comparison of Predicted Deflections from the Three Solutions . . .	105
Fig. 4.20. Theoretical Deflection vs. Socket Length for Rock Depth = 5 ft . .	111
Fig. 4.21. Theoretical Deflection vs. Socket Length for Rock Depth = 10 ft .	111
Fig. 4.22. Theoretical Deflection vs. Socket Length for Rock Depth = 15 ft. .	112
Fig. 4.23. Recommended Minimum Required Socket Length vs. Rock Depth .	112
Fig. 5.1. Predicted Moment-Deflection Behavior of Shafts at Clay Sites	117
Fig. 5.2. Predicted Moment-Deflection Behavior of Shafts at Sand Sites . . .	117
Fig. 5.3. Recommended Minimum Length of Rock Socket for Drilled Shaft Foundations Constructed at Shallow Bedrock Sites	120
Fig. 5.4. Systematic Procedure for Geotechnical Evaluation of LLWAS Site .	121

	List of Tables	Page
Table 1.1.	Resultant Loading on LLWAS Tower Structures	3
Table 1.2.	Various Ultimate Load Criteria for Lateral Loading	8
Table 2.1.	Alternative Criteria of Foundation Rigidity	17
Table 2.2.	Load Test Database on Laterally-Loaded Drilled Shafts in Clays . .	20
Table 2.3.	Load Test Database on Laterally-Loaded Drilled Shafts in Sands . .	21
Table 2.4.	Rigidity of Drilled Shafts in Cohesive Soils	22
Table 2.5.	Rigidity of Drilled Shafts in Cohesionless Soils	23
Table 2.6.	Summary of Lab and Field Tests from Load Test Sites in Clays . .	24
Table 2.7.	Summary of Lab and Field Tests from Load Test Sites in Sands . .	25
Table 2.8.	Relative Values of Effective Stress Friction Angle	34
Table 2.9.	Backcalculated Hyperbolic Parameters and Clay Properties	38
Table 2.10.	Backcalculated Hyperbolic Parameters and Sand Properties	39
Table 2.11.	SPT Correction Factors for Field Procedures	41
Table 3.1.	Different Approaches for the Analysis of Laterally-Loaded Piles . .	55
Table 3.2.	Theoretical and Mathematical Basis for the Computer Programs . .	56
Table 3.3.	Capabilities and Limitations of the Computer Programs	60
Table 3.4.	Input Soil Parameters for the Four Computer Programs	61
Table 3.5.	Representative Values of k_h for Different Soils	62
Table 3.6.	Representative Values of ϵ_{50} for Clay Soils	63
Table 3.7.	Summary of the Case Studies and Load Test Data Reviewed	68
Table 3.8.	Summary of the Parameters from In-Situ PMT at the Four Sites . .	70
Table 3.9.	Summary of Soil Parameters from In-Situ DMT at Barnhart	73
Table 3.10.	Summary of Soil Parameters from In-Situ DMT Soundings	77
Table 4.1.	Summary of Load Tests on Rock-Socketed Drilled Shafts	92
Table 4.2.	Intact Rock Modulus Values	101
Table 4.3.	Analysis of the Load Test Data on Socketed Shafts Using the DEFPIG Program and the Hybrid Solution	110

SECTION 1

INTRODUCTION

This report presents a geotechnical evaluation of the standard FAA LLWAS tower foundation system under critical loading conditions. The acronym LLWAS is an abbreviation for "Low Level Windshear Alert System" and involves an array of 6 to 16 sensor stations situated strategically around a candidate airport. The sensors consist of anemometers perched atop tall steel poles, typically 130 to 150 feet in height. Sensor stations are spaced approximately 8000 feet apart along the runway approach path and landing corridor. The anemometers are networked to a central microprocessor unit at the airport control tower for evaluating the immediate potential of dangerous microburst and windshear events. These evaluations are conveyed to commercial, military, and private pilots using the airport runways for takeoff and landings.

The LLWAS program is, in effect, an advisory warning system for detecting severe wind conditions. The events are notably recognized as potential life-threatening situations. Consequently, during storm conditions, the structural components of the LLWAS system should be able to withstand critical loading conditions so that the system remains operational and of full service to the airport control tower. Furthermore, it is necessary that the system be sufficiently stable such that false warning signals are not given during less significant events. This report addresses a geotechnical evaluation of the drilled shaft foundation component of the LLWAS system.

1.1 LLWAS TOWER STRUCTURES

The standard LLWAS pole structure consists of a hollow steel pole of 70 to 150 feet in height. The poles are provided in segmental sections. For a 150-foot high tower, the pole sections taper from about 25 inches in diameter at the bottom to about 7 inches at the top. The lowest section is comprised of a hexagonal base plate which can be bolted to the foundation.

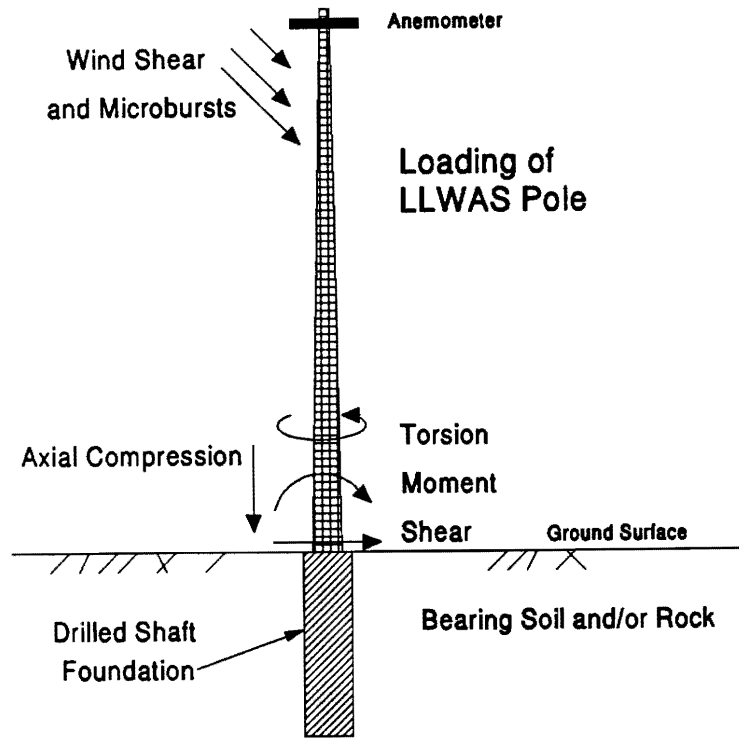


Figure 1.1. Structural Loading Components of an LLWAS Pole Tower.

The LLWAS foundation system consists of a 4-foot diameter by 20-foot long drilled shaft. Drilled shafts are also commonly referred to as bored piles, drilled piers, and caissons. They are often used to support large structural loads for buildings, bridges, and transmission tower structures. The shaft is formed by excavating a circular hole to the required depth with a caisson rig. Typically, the dry method (open hole) is used to facilitate construction operations. A reinforcing cage is installed in the upper section of the excavated hole and the shaft is cast-in-place using 4000 psi strength concrete. After sufficient curing in the field, the pole is mounted to the foundation by anchor bolts.

1.2 STRUCTURAL LOADING OF POLE STRUCTURES

A foundation element supporting a high pole is subjected to several modes of loading, including axial, lateral, torsional, and moment, as shown by Figure 1.1. The dead load imposed by the pole structure itself produces a relatively small axial compression load component. For the LLWAS tower, the significant loads are due to cyclic winds that

produce an unevenly distribution of horizontal forces, resulting in high overturning moments. Although these winds produce dynamic loading conditions, DiGioia et al. (1981) have shown that the resulting foundation deflections can be evaluated using a pseudo-static analysis. The magnitudes of the imposed structural loads are functions of the wind speed, as indicated by Table 1.1

Table 1.1. Resultant Loading on LLWAS Tower Structures

<u>Wind Speed:</u>	<u>Pole Height = 130 ft</u>		<u>Pole Height = 150 ft</u>	
	<u>60 mph</u>	<u>100 mph</u>	<u>60 mph</u>	<u>100 mph</u>
Moment (k-ft):	101.0	278.0	147.0	404.0
Shear (kips):	1.4	3.9	1.8	5.0
Torsion (k-ft):	0.2	0.6	0.2	0.6
Axial (kips):	7.3	7.2	9.5	9.3

1.3 LATERAL AND MOMENT LOADING OF DEEP FOUNDATIONS

The analysis of overturning moments is a subset of the more general case of lateral loading, where the horizontal force (H) is applied with a height of eccentricity of loading (e) above the groundline. Consequently, the applied moment (M) is considered to be $M = H e$. For example, at 100 mph wind speed, the 150-foot LLWAS tower is subjected to a horizontal shear force of 5 kips, applied at an eccentricity of 80.8 feet above the ground, resulting in a moment of 404 kip-feet at groundline. Further details on this procedure are given in Poulos and Davis (1980).

Terminology related to the drilled shaft foundation is given in Figure 1.2. The completed shaft is considered to have an embedded length (L) and effective diameter or width (d). The top of the shaft is termed the head (or butt) and the bottom of the foundation is referred to as the tip or base. Horizontal deflections (δ) are taken at groundline level. The analyses described herein focus strictly on straight-shaft pier foundations, so that belled piers are not considered.

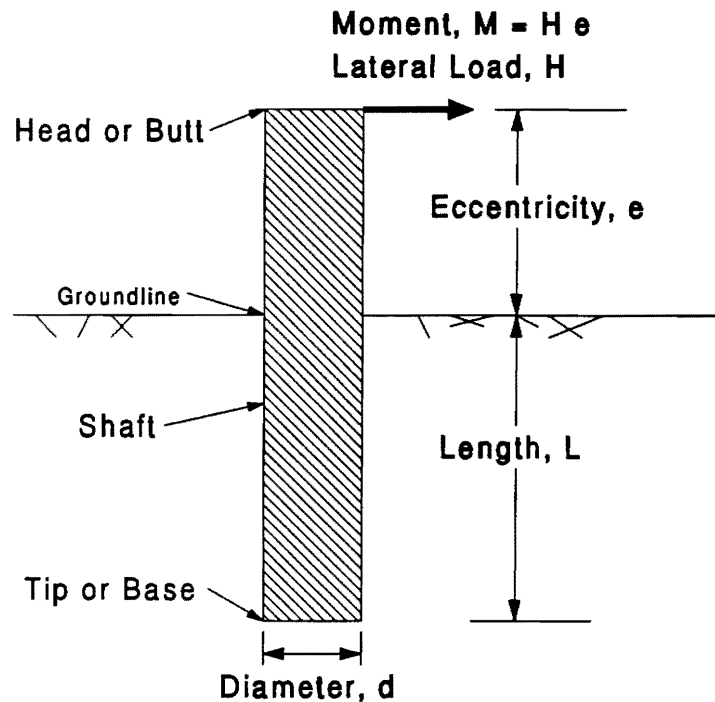


Figure 1.2. Terminology Used for Drilled Shaft Foundations

The lateral and moment behavior of deep foundations is determined by several factors, including: (1) passive soil (and/or rock) resistance, (2) relative rigidity or flexibility of the foundation system, (3) head fixity, and (4) base fixity. Generally, for shafts embedded solely in soil, the base of the foundation is considered to be free to move. Analyses given in Sections 2 and 3 of this report adopt this assumption. If the shaft is constructed into bedrock, the base may be considered to be either pinned (rotation allowed) or fixed (socketed into rock with no deflection or rotation permitted). In Section 4, fixed-tip conditions are assumed for rock-socketed shafts.

The head fixity conditions of deep foundations may be restrained (fixed-head) or unrestrained (free-head). Shafts which are restrained at the head can translate, but not rotate, under lateral and moment loading, as shown by Figure 1.3(a). Unrestrained shafts both deflect and rotate, as illustrated by Figure 1.3(b). Since the LLWAS pole is a single structure, the head or top of the drilled shaft is considered free and unrestrained. Consequently, Section 2, 3, and 4 all assume a free-head condition for analyses.

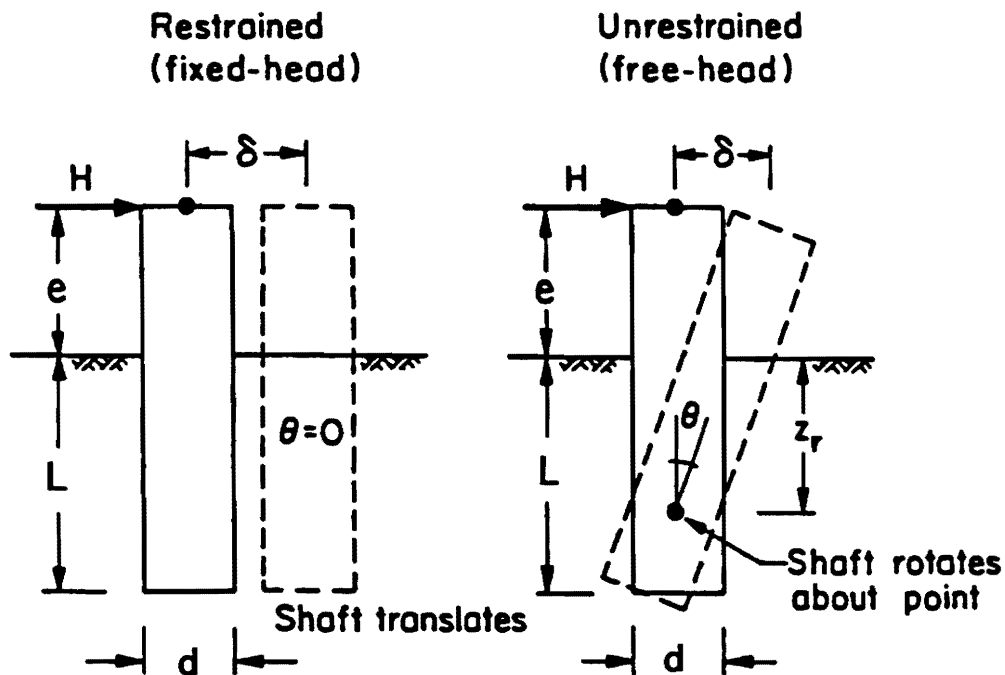


Figure 1.3. Head Fixity Conditions of Drilled Shafts Under Lateral Loading Showing (a) Fixed-Head or Restrained Shafts and (b) Free-Head or Unrestrained Shafts.

The relative rigidity between the foundation and supporting medium (soil or rock) is also an important factor in assessing the system response. Long slender foundations, such as driven steel-H piles, typically behave in a flexible manner under lateral-type loading. In contrast, short and stubby foundations, such as the reinforced concrete LLWAS drilled shafts, act as relatively rigid bodies. The differences between flexible and rigid foundation behavior and a detailed discussion of rigidity criteria are provided later in Section 2 of this report.

Lateral soil resistance plays a significant role in the lateral load-deflection-capacity analysis of deep foundations. For evaluating the ultimate capacity, the passive soil resistance depends upon the type of soil, layering profile, rate of loading, drainage conditions, interface friction characteristics of the foundation material, and modelling technique. For clays, an undrained behavior is assumed, whilst for sands, a drained

response is adopted. In the long term, however, a drained response in clay is also feasible. Passive soil resistance is considered to be a function of the undrained shear strength (s_u) in clays and effective stress friction angle (ϕ') in sands.

The lateral load-deflection behavior at service load levels is often approached using one of two primary analytical models: (1) subgrade reaction method or (2) elastic continuum theory. The subgrade reaction approach represents the soil reaction by a series of simple and unconnected springs. In these cases, the soil stiffness is often expressed as a spring constant, in units of force per unit deflection. Alternatively, a coefficient of subgrade reaction is defined in terms of stress per unit deflection. Continuum theory uses an equivalent elastic modulus (E_s), in units of stress per unit strain, to represent the soil stiffness. Figure 1.4 illustrates the basic distinctions in representing soil stiffness by these two methods. The advantages and limitations of the subgrade reaction and elastic continuum models are discussed within each section of this report, as appropriate.

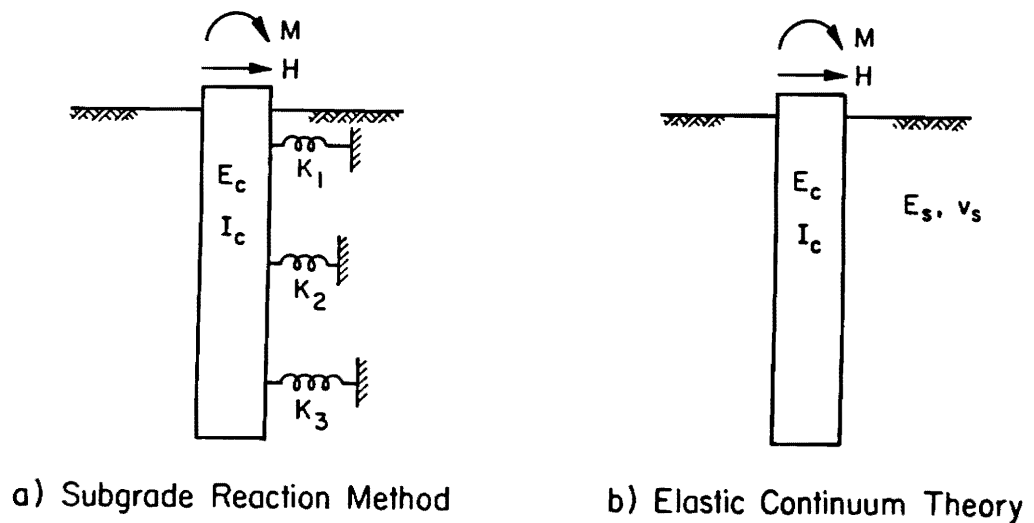


Figure 1.4. Modelling Soil Stiffness by (a) Subgrade Reaction and (b) Elastic Continuum

1.4 TOLERANCE CRITERION

The acceptable tolerance level in the performance of a foundation system depends upon its serviceability and specific use. In addition to maintaining an adequate factor of safety (FS) against total collapse of the foundation system, the LLWAS program can be effective only if the system performs well under situations less than and equal to severe wind loading conditions. In this case, the tower must not deflect or rotate excessively during a 100-mph wind. The movements experienced by the anemometers and transmitting devices at the top of the pole depend upon both the response of the hollow steel pole and supporting drilled shaft foundation. For the foundation, an acceptable groundline deflection has been adopted as $\delta \leq 0.5$ inches, and is based on the following arguments.

A number of different criteria for defining ultimate lateral capacity have been proposed. Since lateral and moment load tests show no well-defined peak, the ultimate value has often been determined by somewhat arbitrary rules. A recent study by Hirany and Kulhawy (1988) indicate at least 12 such criteria in use by practicing engineers. Certain of these criteria are based on the absolute magnitude of groundline deflection (δ), foundation rotation (Θ), or lateral deflection corresponding to a percentage of the foundation diameter (δ/d). Table 1.2 lists several of the more commonly-used criteria for defining ultimate lateral capacity.

Recent studies by Mayne, et al. (1991) and Agaiby, et al. (1991) have shown that the hyperbolic asymptote (H_h) is the most reasonable criterion for describing an ultimate lateral capacity for free-head shafts. The value of H_h is always greater than any applied load level, and therefore, represents an upper bound value. Since a free-head shaft rotates about a point of equilibrium, full mobilization of the passive soil resistance cannot occur, unless the shaft is rotated a complete $\Theta = 90^\circ$. This explains the observed continued increase in H - δ data with no apparent peak "failure" load. Extensive experimental studies have shown that the Lateral or Moment Limit (H_L) criterion is approximately 64% of H_h . Also, the criterion for 2° rotation (H_{2°) has been shown to provide a reasonable safe limit to maintain loads to within the elastic behavior range

Table 1.2. Various Ultimate Load Criteria for Lateral Loading
(Modified after Hirany and Kulhawy, 1988)

<u>Source</u>	<u>Ultimate Load Criterion</u>
Walker and Cox (1966)	0.5 inch
New York City (1981)	1.0 inch
Pyke (1984)	Load at $\delta = 0.05 d$
Briaud (1984)	Load at $\delta = 0.10 d$
Broms (1964)	Load at $\delta = 0.20 d$
Davidson, et al. (1982)	Load at $\Theta = 2^\circ$
Ivey and Dunlap (1970)	Load at $\Theta = 5^\circ$
Slack and Walker (1970)	Load at breakpoint for $\log H : \log \delta$
Kulhawy (1988)	Lateral or Moment Limit*
Manoliu, et al. (1985)	Hyperbolic Asymptote**

Notes:

H = lateral load

δ = horizontal groundline deflection

Θ = shaft rotation

d = shaft diameter

*Defined as breakpoint in depth of rotation vs. H or M plot.

**Projected value H_b assuming $H = \delta / (1/K_i + \delta/H_b)$

K_i = initial stiffness = H/δ

(Davidson, et al. 1982). The $H_{2\sigma}$ criterion has been used extensively by the Electric Power Research Institute (EPRI) for evaluation and load testing of drilled shaft foundations with $2 \leq L/d \leq 10$. Experimental tests by Mayne et al. (1991) and Agaiby et al. (1991) have found that $H_L \approx H_{2\sigma}$. Therefore, an inherent FS = $1/(0.64) = 1.56$ already exists for most interpretations of lateral capacities.

Loading levels less than H_L or $H_{2\sigma}$ may be considered to be within tolerable ranges of horizontal deflection. For the adopted maximum allowable lateral deflection criterion of $\delta = 0.5$ inch, the LLWAS meets or exceeds each of the capacity criteria given in Table 1.2. For the Walker and Cox (1966) and NYC (1981) criteria that were developed primarily for small diameter pile foundations, the calculated FS = 1 and 2, respectively. For large diameter drilled shafts, however, these deflection-based criteria seem unduly

conservative and unwarranted. If the ratio of δ/d is expressed in terms of the allowable deflection ($\delta = 0.5$ in) to the design 4-foot diameter of the LLWAS shaft, the lateral load $H = 0.01 d$ provides calculated $FS = 5, 10, \text{ and } 20$ for the ultimate capacity interpretations given by Pyke (1984), Briaud (1984), and Broms (1964), respectively. For the $H_{2\sigma}$ criterion, a 20-foot long shaft under high moment loading would permit a horizontal deflection at groundline equal to $0.5 L \tan(\Theta = 2^\circ) = 4.2$ inches. This implies a $FS \approx 8$ on displacements for the adopted maximum deflection criterion.

1.5 SCOPE OF STUDY

The Geotechnical Division of the School of Civil Engineering at Georgia Institute of Technology was contracted by the Federal Aviation Administration Southern Region to provide an engineering evaluation of the existing foundation system used by the LLWAS program. This study includes an evaluation of the load-deflection-capacity of the drilled shaft foundations under lateral and moment loading and general design recommendations for future LLWAS sites underlain by marginal soils or shallow bedrock conditions. The conclusions and recommendations are based on the results of a compiled database of similar-type foundations under similar loading conditions, computer simulation studies, and available analytical methods. This research study performed no full-scale field testing program or specific in-situ or laboratory testing program at any of the LLWAS tower foundation locations. Therefore, the study has actually been performed as an analytical exercise in the numerical evaluation of possible worst to best scenarios that might be encountered at a given site. If specific sites of interest are cited by FAA or if detailed information is required at existing or future LLWAS tower locations, then additional geotechnical testing and analysis may be warranted. These additional studies can be performed and completed by the Georgia Institute of Technology under an extended scope of services contract.

To complete the study, load test data on laterally-loaded and moment-loaded drilled shaft foundations were compiled from the open literature and published reports. These drilled shafts had low slenderness ratios ($2 \leq L/d \leq 12$) and were therefore similar in geometry to those used by the FAA on LLWAS projects. A simple hyperbolic model based on

elastic continuum analysis was utilized to analyze these data in a rational framework. The results are presented in Section 2 of this report. Section 3 reviews four commercial programs developed for investigating the behavior of deep foundations under lateral and moment loading. Finally, Section 4 addresses the problem of minimum required socket lengths for shafts installed at sites with shallow bedrock conditions.

1.6 REFERENCES

- Agaiby, S.W., Kulhawy, F.H., and Trautmann, C.H. (1991), "An Experimental Study of the Drained Behavior of Drilled Shaft Foundations Subjected to Static and Repeated Lateral and Moment Loading", Report TR-100223, Electric Power Research Institute, Palo Alto, 320 p.
- Briaud, J.L. (1984), discussion in Laterally-Loaded Deep Foundations (STP 835), ASTM, Philadelphia, pp. 239-243.
- Broms, B.B. (1964), "Lateral Resistance of Piles in Cohesive Soils", Journal of the Soil Mechanics and Foundations Division, ASCE, Vol. 90, No. SM2, pp. 27-63.
- Davidson, H.L., Cass, P.G., Khilji, K.H., and McQuade, P.V. (1982), "Laterally-Loaded Drilled Pier Research", Report EL-2197, Electric Power Research Institute, Palo Alto, 324 p.
- DiGioia, A.M., Davidson, H.L., and Donovan, T.D. (1981), "Laterally-Loaded Drilled Piers - A Design Model", Drilled Piers and Caissons, ASCE, New York, 132-149.
- Hirany, A. and Kulhawy, F.H. (1988), "Conduct and Interpretation of Load Tests on Drilled Shaft Foundations", Report EL-5915, Electric Power Research Institute, Palo Alto, CA, 374 p.
- Ivey, D.L. and Dunlap, W.A. (1970), "Design Procedure Compared to Full-Scale Tests of Drilled Shaft Footings", Research Report 105-3, University of Texas, Austin, 59 p.
- Manoliu, I., Dimitriu, D.V., Radulescu, N., and Dobrescu, G. (1985), "Load-Deformation Characteristics of Drilled Shafts", Proceedings, 11th International Conference on Soil Mechanics and Foundation Engineering, Vol. 3, San Francisco, pp. 1553-1558.
- Mayne, P.W., Kulhawy, F.H., and Trautmann, C.H. (1991), "An Experimental Study of the Behavior of Drilled Shafts in Clay Under Static and Cyclic Lateral and Moment Loading", Report TR-100221, Electric Power Research Institute, Palo Alto, 344 p.
- New York City (1981), Building Code of the City of New York, Gould Publications, Binghamton, NY, 481 p.

Poulos, H.G. and Davis, E.H. (1980), Pile Foundation Analysis and Design, John Wiley and Sons, New York, 397 p.

Pyke, R. (1984), discussion in Laterally-Loaded Deep Foundations (STP 835), ASTM, Philadelphia, pp. 239-243.

Slack, D.C. and Walker, J.N. (1970), "Deflections of Shallow Pier Foundations", Journal of the Soil Mechanics and Foundations Division, ASCE, Vol. 96, No. SM4, pp. 1143-1157.

Walker, J.N. and Cox, E.H. (1966), "Design of Pier Foundations for Lateral Loads", Transactions, American Society of Agricultural Engineers, Vol. 9, No. 3, pp. 417-420.

Section 2

BEHAVIOR OF Laterally-Loaded Drilled Shafts

The nonlinear load-deflection behavior of rigid drilled shafts subjected to lateral and moment loads can be simulated by using a mathematical hyperbolic model. Two parameters, the hyperbolic ultimate capacity (H_u) and initial stiffness (K_i), are derived from actual load test data collected from the published literature. Limit equilibrium analysis and elastic continuum theory are used to formulate H_u and K_i in terms of shear strength and initial tangent modulus of cohesive and cohesionless soils. Where available, in-situ soil properties at test sites are examined and correlated with values of backcalculated shear strength and elastic modulus, which are then compared with some published and unpublished correlations. For practical use, it is possible to predict the load-deflection behavior of rigid drilled shafts, as well as determine their allowable lateral and moment capacity, by conducting in-situ tests at the particular site.

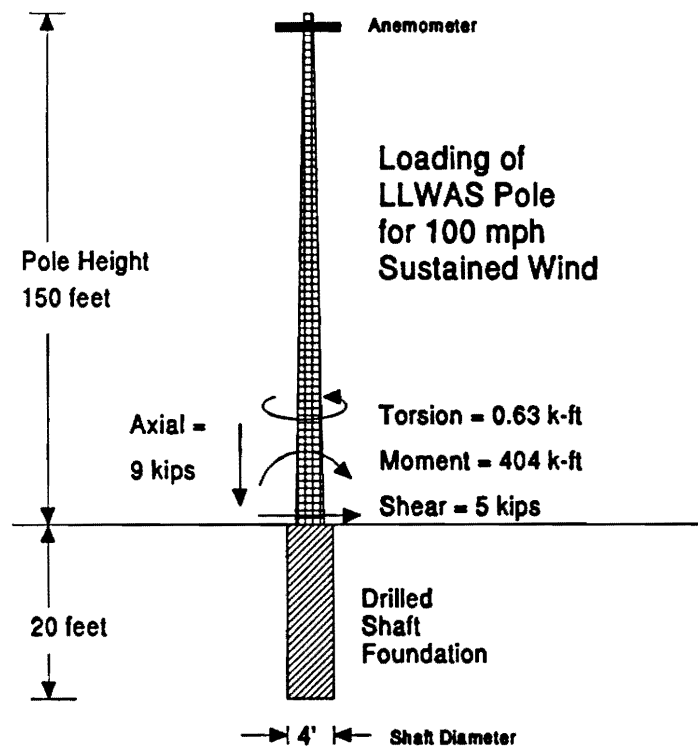


Figure 2.1. Structural Loads on the LLWAS Tower Foundations

2.1. LLWAS FOUNDATIONS

The typical structure of LLWAS system includes a 150 ft hollow steel pole supported by a 20-foot long drilled shaft foundation with a 4-foot diameter, as shown in Figure 2.1. Several important characteristics of the drilled shaft foundation system are highlighted to provide guidelines during the entire program of study relevant to the FAA LLWAS program. These include various criteria for consideration, including: (1) the allowable lateral capacity of the foundation system, (2) rigid behavior, and (3) relevant soil shearing mode.

2.1.1. Lateral Capacity Criteria

The nonlinear load-deflection curves of laterally-loaded drilled shafts show no apparent peak values, and therefore, no clearly defined ultimate load at failure. In many cases, the definition of lateral capacity is more serviceability-oriented than its actual peak capacity. More often, the lateral capacity of rigid drilled shafts is governed by the maximum amount of deflection or angle of rotation which the supported structure or equipment can tolerate. Hirany and Kulhawy (1988) distinguished twelve different criteria being used to determine the lateral capacity, as indicated in Figure 2.2.

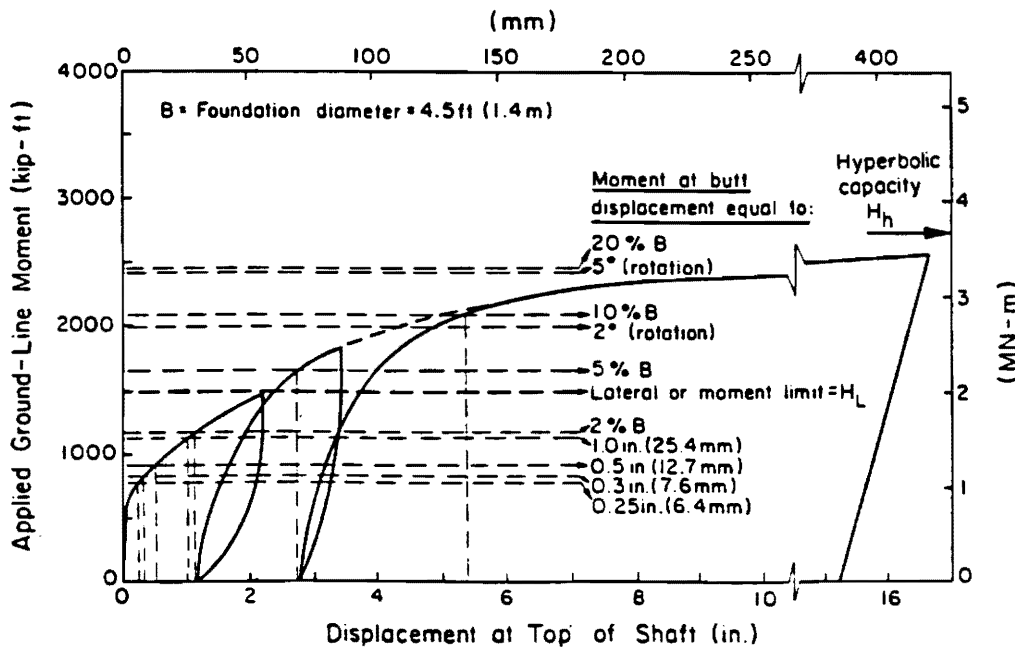


Figure 2.2. Comparison of Lateral Load Interpretation Criteria
(Source: Hirany and Kulhawy, 1988)

These criteria differ in emphasis and range from definitions focusing on the yield region of the curve to those attempting to predict an ultimate value for the curve. Most of these criteria are based on the allowable deflection or angle of rotation. For this particular project, the allowable groundline deflection (i.e. at top of drilled shaft) has been established as approximately 0.5 inch, as discussed previously in Section 1 of this report.

2.1.2. Rigidity Criteria

Due to the type of drilled shafts used by FAA for LLWAS tower foundations, the scope of interest in this study is limited to those that behave rigidly when subjected to lateral loads and moments. The general behavior of a laterally-loaded drilled shaft or pile was described by Broms (1964) and may be categorized as either flexible or rigid behavior, as indicated by Figure 2.3. For free-headed short rigid shafts, the shaft is assumed to rotate about a point of equilibrium at depth without significant deformation along the shaft, as indicated in Figure 2.3(a). For free-headed long flexible shafts, the shaft is assumed to bend and deform from the top of shaft to a point of critical depth, as indicated in Figure 2.3(b). Well-established criteria for determining the rigidity of shaft have been reported by Broms (1964), Poulos and Davis (1980), Bierschwale et al. (1981), Carter and Kulhawy (1988), and Poulos and Hull (1989).

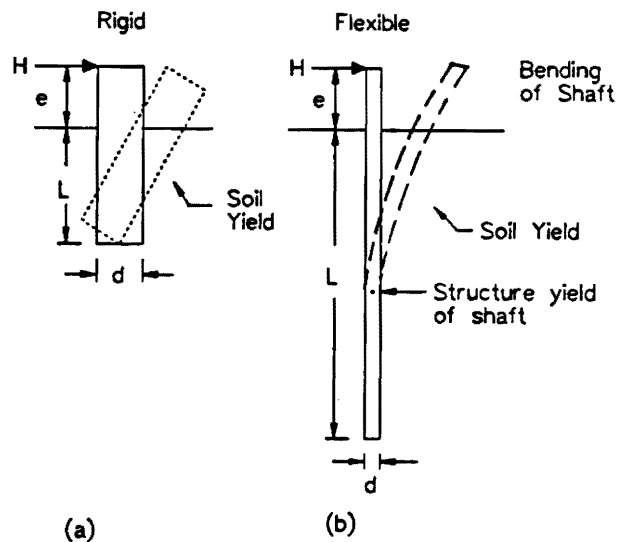


Figure 2.3. Concept of Rigid versus Flexible Shaft Behavior
(Modified after Broms, 1964)

The most straightforward or simplest definition of rigid or flexible behavior of drilled shafts is probably the length to diameter ratio or slenderness ratio (L/d). The shaft may be considered to be rigid when $L/d < 6$, or it may be considered to be flexible when $L/d > 20$ (Bierschwale et al., 1981). LLWAS foundations are constructed with $L/d = 5$, and would therefore be categorized as rigid.

The subgrade reaction method (Broms, 1964) separates the rigid-flexible categories according to the parameter:

$$\beta L = \left(\frac{k_h d}{4 E_p I_p} \right)^{1/4} L \quad [2.1]$$

in which βL = dimensionless length, k_h = coefficient of subgrade reaction, L = embedded length of shaft, d = diameter of shaft, E_p = Young's modulus of shaft and I_p = moment of inertia of shaft ($I_p = \pi d^4/64$ for circular shaft). The shaft is considered to be rigid if $\beta L < 1.5$. On the other hand, the shaft is considered to be flexible if $\beta L > 2.5$. An intermediate classification occurs with $1.5 \leq \beta L \leq 2.5$.

Alternatively, elastic continuum theory solved using the boundary element formulation (Poulos and Davis, 1980) utilizes the parameter:

$$K_r = \frac{E_p I_p}{E_s L^4} \quad [2.2]$$

in which K_r = flexibility factor, E_s = Young's modulus of soil. The shaft is considered to be rigid if $K_r > 10^{-2}$. On the other hand, the shaft is considered to be flexible if $K_r < 10^{-5}$.

The finite element solution to the elastic continuum approach (Carter and Kulhawy, 1988) uses the ratio of pier modulus (E_p) to modified soil shear modulus (G^*):

$$E_p/G^* \quad [2.3]$$

in which $G^* = G(1+3\nu/4)$, $G = E_s/[2(1+\nu)]$ = shear modulus of soil, and ν = Poisson's ratio of soil. If $L/d < 0.05 (E_p/G^*)^{1/4}$, the shaft is considered to behave rigidly. Conversely, the shaft is considered to be flexible if $L/d > (E_p/G^*)^{1/4}$.

A recent approach (Poulos and Hull, 1989) defines rigidity according to the calculated value of critical length (L_c):

uniform soil:

$$L_c = 4.44 \left(\frac{E_p I_p}{E_s} \right)^{1/4} \quad [2.4a]$$

Gibson soil:

$$L_c = 3.30 \left(\frac{E_p I_p}{N_h} \right)^{1/5} \quad [2.4b]$$

in which E_s = elastic modulus for uniform soil and N_h = rate of increase of E_s with depth for Gibson soil (i.e. $E_s = N_h z$). For pier shaft lengths longer than this value, no apparent effect on laterally loaded deflection response occurs. The shaft is considered to be rigid when $L < L_c/3$ and flexible when $L > L_c$.

The criteria based upon the above definitions are summarized in Table 2.1. It is noted that there is a transitional zone between completely "rigid" and completely "flexible". Cross referencing among these criteria may be necessary to identify the "rigid" or "nearly rigid" behavior of shafts in this study. Since the LLWAS foundations are rather rigid and since the rigidity criteria vary, it is important to verify that every drilled shaft in the load test database is defined as either "rigid" or at least "nearly rigid".

2.1.3. Soil Shearing Mode

Civil engineering structures impart their loads to the ground through stress attenuation from the foundation system. Stress rotation and boundary effects result in a propagation of stresses in three orthogonal directions. There are various loading modes for different engineering problems, which can be simplified in terms of testing type. Figure 2.4 illustrates the application of different shearing modes in geotechnical problems and

Table 2.1 Alternative Criteria of Foundation Rigidity

Source	Rigid Behavior	Flexible Behavior
Broms (1964)	$\beta L < 1.5^{(a)}$	$\beta L > 2.5^{(a)}$
Bierschwale, et al. (1981)	$L/d < 6$	$L/d > 20$
Poulos and Davis (1980)	$K_r > 10^{-2}^{(c)}$	$K_r < 10^{-5}^{(c)}$
Carter and Kulhawy (1988)	$L/d < (L/d)_{\text{rigid}}^{(d)}$	$L/d > (L/d)_{\text{flexible}}^{(e)}$
Poulos and Hull (1989)	$L < L_c/3^{(g)}$	$L > L_c^{(g)}$

Notes:

(a) $\beta = (k_h d / 4 E_p I_p)^{1/4}^{(b)}$

(b) k_h = Coefficient of Subgrade Reaction

(c) $K_r = E_p I_p / E_s L^4$ = Flexibility Factor

(d) $(L/d)_{\text{rigid}} = 0.05(E_p/G^*)^{1/2}^{(f)}$

(e) $(L/d)_{\text{flexible}} = (E_p/G^*)^{2/7}^{(f)}$

(f) $G^* = G(1+3\nu/4)$ = Modified Soil Shear Modulus

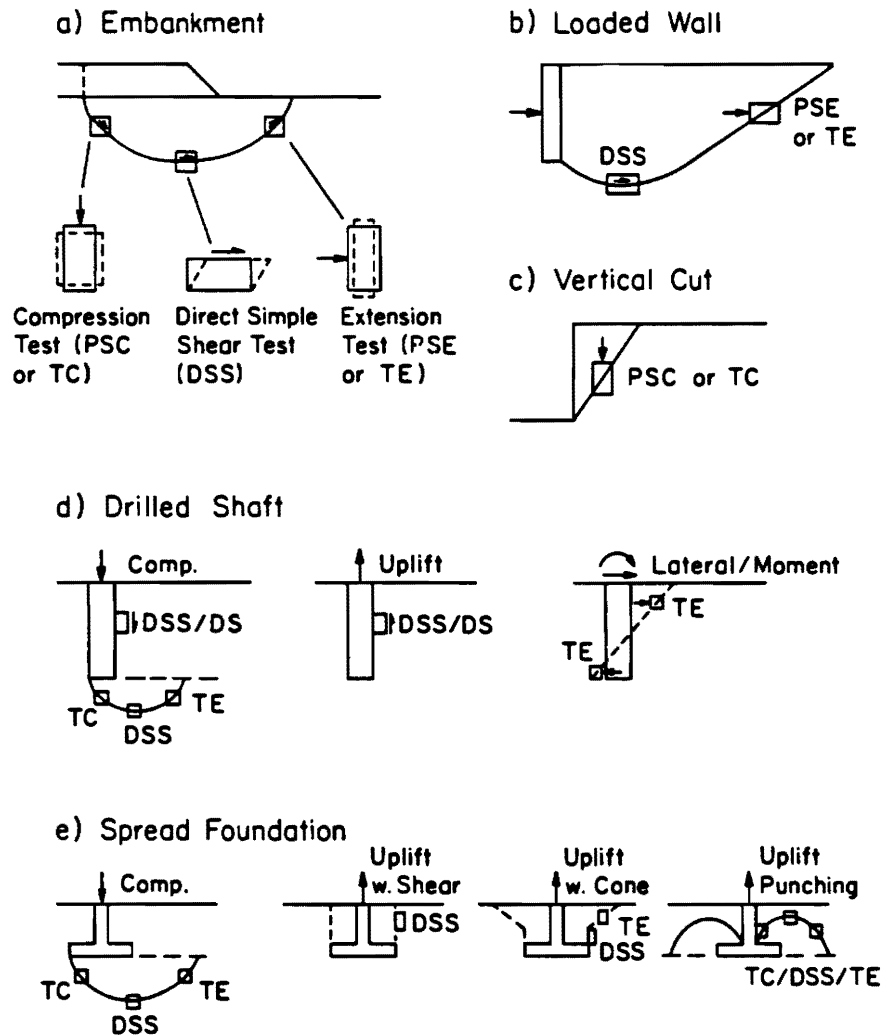
(g) $L_c = 4.44(E_p I_p / E_s)^{1/4}$ = Critical Length of Pier in Uniform Soil

$L_c = 3.30(E_p I_p / N_h)^{1/5}$ = Critical Length of Pier in Gibson Soil ^(h)

(h) $N_h = E_s / z$ = Rate of Increase of E_s

includes: plane strain compression (PSC), plane strain extension (PSE), triaxial compression (TC), triaxial extension(TE), direct shear (DS), and direct simple shear (DSS). The laterally-loaded drilled shaft problem involves a horizontal loading of soil in front of the shaft, and therefore, a passive or extension mode of shearing is appropriate. The loading of soil elements adjacent to the shaft is such that a three-dimensional problem truly exists. The most appropriate test type might actually be a cubical or true triaxial test, in which the lateral stress in the direction of loading is the major principal stress. The true stress path is unknown but involves changes in all three principal stress directions, as well as stress rotation considerations. Instead of

performing the complicated true triaxial test, the more common triaxial extension (TE) test provides a stress path that approximates the problem. Therefore, the triaxial extension test should be adopted as the relevant shearing mode of soil for the particular case of drilled shafts subjected to lateral and moment loading. (Mayne, 1991).



Note: Plane strain tests (PSC/PSE) used for long features
 Triaxial tests (TC/TE) used for near symmetrical features
 Direct shear (DS) normally substituted for DSS to evaluate ϕ

Figure 2.4. Relevance of Laboratory Strength Tests to Field Conditions
 (Source: Kulhawy and Mayne, 1990)

2.2. LOAD TEST DATABASE

A load test database of rigid drilled shafts subjected to lateral and moment loads has been compiled during this study. The database has served to: (1) verify the applicability of the hyperbolic model for predicting the load-deflection behavior, (2) backcalculate the shear strength and soil modulus from hyperbolic parameters, (3) provide correlations between backcalculated soil parameters and in-situ test results, and finally, (4) predict the load-deflection behavior and allowable lateral capacity corresponding to certain design criteria.

More than 100 individual load test data were collected from the published literature, however, only 54 sets of data have been selected to satisfy the requirements for rigid, drilled, and reinforced concrete shafts. The test sites for drilled shafts in cohesive and cohesionless soils are summarized in Tables 2.2 and 2.3, respectively. It is easy to identify the material and construction method of the shafts, while the rigidity of the shafts requires in-depth examination. Instead of using the Bierschwale et al. (1981) rigidity criteria of $L/d < 6$ for strict rigid behavior, the criteria of $L/d < 12$ is used to allow more data to be used for this study. However, other criteria described in previous section are applied subsequently to evaluate the degree of rigidity of these shafts. From stress-strain data, the soil modulus (E_s) can be defined as the initial tangent modulus (E_t), which provides the maximum modulus value and consequently gives the most conservative results in identifying "rigid" behavior.

Results of the rigidity classification are summarized for cohesive soils in Table 2.4 and indicate that load test Nos. 22, 23, 24, and 86 not only violate the "rigid" criteria but also are categorized as "flexible" shafts and are therefore discarded from further study. Test Nos. 14, 21, and 38 also have K_r smaller than 0.01 and their L/d ratio are very close to $(E_p/G)^{2/3}$, which also suggests "non-rigid" behavior. Results of the rigidity evaluation for drilled shafts in cohesionless soils are given in Table 2.5 and also indicate that several load tests (Nos. 42, 48, 87, and 88) severely violate the "rigid" assumptions and are therefore discarded. Besides these tests, most of the data satisfy the Poulos and Davis (1980) criteria of $K_r > 0.01$, but do not always satisfy other criteria. They are

Table 2.2. Load Test Database on Laterally-Loaded Drilled Shafts in Cohesive Soils

File	e(ft)	L(ft)	d(ft)	L/d	Site	Reference	Remark
01	2.6	20.0	3.0	6.7	TX	Bierschwale et al, 1981	
02	2.6	15.0	3.0	5.0	TX	Bierschwale et al, 1981	
03	2.6	15.0	2.5	6.0	TX	Bierschwale et al, 1981	
07	1.0	15.0	4.0	3.8	CA	Bhushan et al, 1979	
08	1.0	15.0	4.0	3.8	CA	Bhushan et al, 1979	
09	1.0	12.5	4.0	3.1	CA	Bhushan et al, 1979	
10	1.0	12.5	4.0	3.1	CA	Bhushan et al, 1979	
11	1.0	15.5	4.0	3.9	CA	Bhushan et al, 1979	
12	1.0	15.5	4.0	3.9	CA	Bhushan et al, 1979	
13	1.0	9.0	2.0	4.5	CA	Bhushan et al, 1979	
14	1.0	15.5	2.0	7.8	CA	Bhushan et al, 1979	
15	1.0	17.0	4.0	4.3	CA	Bhushan et al, 1979	Slope(2.8:1)
16	1.0	17.0	4.0	4.3	CA	Bhushan et al, 1979	Slope(1.4:1)
17	1.0	17.0	4.0	4.3	CA	Bhushan et al, 1979	Slope(1.4:1)
18	1.0	22.0	4.0	5.5	CA	Bhushan et al, 1979	Slope(1.4:1)
20	1.0	17.0	5.0	3.4	Canada	Ismael et al, 1978	
21	1.0	38.0	5.0	7.6	Canada	Ismael et al, 1978	
22	1.6	36.0	3.4	10.6	China	Lu, 1981	
23	1.6	36.0	3.4	10.6	China	Lu, 1981	Battered(1:5)
24	1.6	36.0	3.4	10.6	China	Lu, 1981	Battered(1:5)
29	2.5	20.0	3.0	6.7	TX	Briaud et al, 1984	
34	0.9	37.4	6.0	6.2	TX	Dunnivant et al, 1989	
35	0.1	5.0	0.5	10.0	NY	Huang et al, 1989	
37	0.1	5.0	1.0	5.0	NY	Huang et al, 1989	
38	0.1	10.0	1.0	10.0	NY	Huang et al, 1989	
43	80.0	20.0	3.0	6.7	Canada	Adams et al, 1973	
49	24.4	8.2	2.7	3.1	OH	Behn, 1960	
50	24.4	12.0	2.7	4.5	OH	Behn, 1960	
53	24.1	7.9	2.7	3.0	OH	Behn, 1960	
54	24.2	12.0	2.7	4.5	OH	Behn, 1960	
56	80.0	11.7	4.5	2.6	VA	EPRI, 1982	
61	80.0	12.5	5.0	2.5	OK	EPRI, 1982	
67	80.0	17.5	4.5	3.9	OR	EPRI, 1982	
68	80.0	15.0	4.5	3.3	NB	EPRI, 1982	
83	0.1	10.0	2.2	4.5	CA	Briaud et al, 1984	
84	0.1	15.0	2.2	6.8	CA	Briaud et al, 1984	
85	0.1	10.0	2.1	4.8	CA	Briaud et al, 1984	
86	0.1	15.0	2.1	7.1	CA	Briaud et al, 1984	

Notes: e = eccentricity, L = length, d = diameter

Table 2.3. Load Test Database on Laterally-Loaded Drilled Shafts in Cohesionless Soils

File	e(ft)	L(ft)	d(ft)	L/d	Site	Reference	Remark
39	30.0	7.0	2.5	2.8	NC	Gabr et al, 1988	Slope(3.5:1)
40	32.0	5.0	2.5	2.0	NC	Gabr et al, 1988	Slope(3.5:1)
41	30.0	7.0	2.5	2.8	NC	Gabr et al, 1988	Slope(3.5:1)
42	80.0	20.0	3.0	6.7	Canada	Adams et al, 1973	
48	4.8	28.0	3.3	8.5	Japan	Kishida et al, 1985	
51	24.4	8.0	2.7	3.0	OH	Behn, 1960	
52	24.3	12.3	2.7	4.6	OH	Behn, 1960	
57	80.0	16.0	4.5	3.6	PA	EPRI, 1982	
58	80.0	21.0	5.0	4.2	NJ	EPRI, 1982	
59	80.0	15.8	5.0	3.2	MD	EPRI, 1982	
62	80.0	16.8	5.3	3.2	MO	EPRI, 1982	
64	80.0	16.0	4.8	3.3	AZ	EPRI, 1982	
65	80.0	20.3	5.0	4.1	CA	EPRI, 1982	
87	0.1	10	2.4	4.2	CA	Briaud et al, 1984	
88	0.1	15	2.4	6.3	CA	Briaud et al, 1984	

Notes: e = eccentricity, L = length, d = diameter

considered to be either "rigid" or in-between "rigid" and "flexible" behavior, and nevertheless, have been included in this study. Some observed scatter in subsequent correlations may be due in part to this "imperfection" in rigidity classification.

Sources of the load test database were examined to collect all available geotechnical information. This included the geometry of the drilled shafts, eccentricity of loading, groundwater level, soil classification and index properties, and laboratory/field test results. In-situ field tests included: field vane test (FV), standard penetration test (SPT), cone penetration test (CPT), piezocone penetration test (CPTU), pressuremeter test (PMT) and dilatometer test (DMT). Few laboratory test results have been reported, in general, and these typically include: unconfined compression test (UC), unconsolidated-undrained test (UU), consolidated-undrained test (CU), miniature vane test (MV), and torvane test (TV). Tables 2.6 and 2.7 summarize all the available laboratory and in-situ test information for cohesive and cohesionless soils, respectively. Both ranges and "weighted" average values are provided, based on the layering of soil profiles. It is indicated in some tests that the soil properties vary significantly along the profiles and this created some difficulties in attempting to obtain the reasonable average values. It

Table 2.4. Rigidity of Drilled Shafts in Cohesive Soils

File	L(ft)	L/d	Ep(ksf)	Ip(ft ⁴)	Ei(ksf)	Kr	Lc/L	(L/d)r	(L/d)f
01	20.0	6.7	449571	3.98	340	0.033	1.89	2.69	9.74
02	15.0	5.0	527488	3.98	481	0.086	2.41	2.45	9.23
03	15.0	6.0	591887	1.92	249	0.090	2.43	3.60	11.52
07	15.0	3.8	485592	12.57	963	0.125	2.64	1.66	7.40
08	15.0	3.8	485592	12.57	982	0.123	2.63	1.64	7.35
09	12.5	3.1	485592	12.57	1117	0.224	3.05	1.54	7.09
10	12.5	3.1	485592	12.57	975	0.256	3.16	1.65	7.37
11	15.5	3.9	485592	12.57	907	0.117	2.59	1.71	7.52
12	15.5	3.9	485592	12.57	1114	0.095	2.46	1.54	7.09
13	9.0	4.5	485592	0.79	1231	0.047	2.07	1.47	6.89
14	15.5	7.8	485592	0.79	707	0.009	1.38	1.94	8.08
15	17.0	4.3	485592	12.57	1187	0.062	2.21	1.49	6.97
16	17.0	4.3	485592	12.57	419	0.174	2.87	2.51	9.38
17	17.0	4.3	485592	12.57	647	0.113	2.57	2.02	8.29
18	22.0	5.5	485592	12.57	663	0.039	1.98	2.00	8.23
20	17.0	3.4	485592	30.68	995	0.179	2.89	1.63	7.33
21	38.0	7.6	485592	30.68	856	0.008	1.34	1.76	7.65
22	36.0	10.6	485592	6.56	947	0.002	0.94	1.67	7.43
23	36.0	10.6	485592	6.56	909	0.002	0.95	1.71	7.52
24	36.0	10.6	485592	6.56	1017	0.002	0.92	1.61	7.28
29	20.0	6.7	485592	3.98	456	0.026	1.79	2.41	9.16
34	37.4	6.2	485592	63.62	1089	0.014	1.54	1.56	7.14
35	5.0	10.0	485592	0.00	218	0.011	1.44	3.49	11.31
37	5.0	5.0	485592	0.05	475	0.080	2.36	2.36	9.05
38	10.0	10.0	485592	0.05	266	0.009	1.37	3.16	10.68
43	20.0	6.7	485592	3.98	428	0.028	1.82	2.49	9.32
49	8.2	3.1	485592	2.49	1070	0.250	3.14	1.57	7.18
50	12.0	4.5	485592	2.49	1396	0.042	2.01	1.38	6.65
53	7.9	3.0	485592	2.49	680	0.457	3.65	1.97	8.17
54	12.0	4.5	485592	2.49	452	0.129	2.66	2.42	9.18
56	11.7	2.6	485592	20.13	909	0.574	3.86	1.71	7.52
61	12.5	2.5	485592	30.68	573	1.065	4.51	2.15	8.58
67	17.5	3.9	485592	20.13	554	0.188	2.92	2.19	8.66
68	15.0	3.3	485592	20.13	844	0.229	3.07	1.77	7.68
83	10.0	4.5	485592	1.15	1286	0.043	2.03	1.44	6.81
84	15.0	6.8	485592	1.15	1073	0.010	1.41	1.57	7.17
85	10.0	4.8	485592	0.95	1675	0.028	1.81	1.26	6.31
86	15.0	7.1	485592	0.95	1714	0.005	1.20	1.24	6.27

Notes: See Table 2.1 for rigidity criteria

(L/d)r = (L/d)rigid, (L/d)f = (L/d)flexible

Table 2.5. Rigidity of Drilled Shafts in Cohesionless Soils

File	L(ft)	L/d	Ep(ksf)	Ip(ft ^ 4)	Ei(ksf)	Kr	Lc/L	(L/d)r	(L/d)f
39	7.0	2.8	485592	1.92	1447	0.268	3.19	1.35	6.58
40	5.0	2.0	485592	1.92	110	13.544	8.52	4.91	13.75
41	7.0	2.8	485592	1.92	796	0.487	3.71	1.82	7.81
42	20.0	6.7	485592	3.98	1730	0.007	1.28	1.24	6.26
48	28.0	8.5	485592	5.68	3136	0.001	0.86	0.92	5.28
51	8.0	3.0	485592	2.49	4590	0.064	2.24	0.76	4.73
52	12.3	4.6	485592	2.49	3785	0.014	1.53	0.84	5.00
57	16.0	3.6	485592	30.68	2001	0.114	2.58	1.15	6.00
58	21.0	4.2	485592	30.68	1638	0.047	2.06	1.27	6.35
59	15.8	3.2	485592	30.68	2666	0.090	2.43	1.00	5.53
62	16.8	3.2	485592	37.29	1540	0.148	2.75	1.31	6.47
64	16.0	3.3	485592	26.06	2850	0.068	2.27	0.96	5.42
65	20.3	4.1	485592	30.68	1102	0.080	2.36	1.55	7.12
87	10.0	4.2	485592	1.63	7831	0.010	1.41	0.58	4.06
88	15.0	6.3	485592	1.63	4677	0.003	1.07	0.75	4.71

Notes: See Table 2.1 for rigidity criteria

(L/d)r = (L/d)rigid, (L/d)f = (L/d)flexible

must also be pointed out that the soil shearing mode for all these tests, with the exception of pressuremeter test (PMT) and dilatometer test (DMT), are approximated by triaxial compression tests (TC), rather than the more suitable triaxial extension test mode (TE) for the laterally-loaded drilled shaft problem. The comparison of various shearing modes under drained and undrained conditions have been reviewed and discussed by Kulhawy and Mayne (1990).

2.3. FOUNDATION LOAD-DEFLECTION RESPONSE

2.3.1. Hyperbolic Load-Deflection Model

Kondner (1963) proposed a hyperbolic model to describe the nonlinear stress-strain behavior of soils. This model has been adapted for many applications, for example, to express the variation of shear modulus and damping ratio with respect to strain amplitude (Hardin and Drnevich, 1972) and to simulate the load-deflection behavior of laterally loaded drilled shafts (Manoliu et al., 1985; Mayne and Kulhawy, 1991). The basic hyperbolic equation used in this study is given as:

$$H = \frac{\delta}{a+b\delta} \quad [2.5]$$

Table 2.6. Summary of Laboratory and Field Tests from Load Test Sites in Clays

(Unit: ksf)																												
File	L (ft)	d (ft)	L/d	cwl (ft)	PI (%)	Su(ksf)						SPT-N			CPT			PMT			DMT							
						UC	UU	MV	FV	TV	CIU	Range	Avg.	(N1)60	qc	qt	Su	PL	Su	Em	Po	P1	Ed					
01	20.0	3.0	6.7	16	44	2.2	NA	2.5	NA	NA	NA	14-20	18	20	NA	NA	NA	NA	NA	NA	NA	NA	NA	NA	NA	NA	NA	NA
02	15.0	3.0	5.0	16	43	2.2	NA	2.5	NA	NA	NA	14-20	18	19	NA	NA	NA	NA	NA	NA	NA	NA	NA	NA	NA	NA	NA	NA
03	15.0	2.5	6.0	16	43	2.2	NA	2.5	NA	NA	NA	14-20	18	19	NA	NA	NA	NA	NA	NA	NA	NA	NA	NA	NA	NA	NA	NA
07	15.0	4.0	3.8	NE	28	3.1	5.5	NA	NA	NA	NA	19-44	29	34	NA	NA	NA	NA	NA	NA	NA	NA	NA	NA	NA	NA	NA	NA
08	15.0	4.0	3.8	NE	28	3.1	5.5	NA	NA	NA	NA	19-44	29	34	NA	NA	NA	NA	NA	NA	NA	NA	NA	NA	NA	NA	NA	NA
09	12.5	4.0	3.1	NE	26	3.7	3.6	NA	NA	NA	NA	19-43	31	37	NA	NA	NA	NA	NA	NA	NA	NA	NA	NA	NA	NA	NA	NA
10	12.5	4.0	3.1	NE	26	3.7	3.6	NA	NA	NA	NA	19-43	31	37	NA	NA	NA	NA	NA	NA	NA	NA	NA	NA	NA	NA	NA	NA
11	15.5	4.0	3.9	NE	24	3.5	3.6	NA	NA	NA	NA	19-43	31	35	NA	NA	NA	NA	NA	NA	NA	NA	NA	NA	NA	NA	NA	NA
12	15.5	4.0	3.9	NE	24	3.5	3.6	NA	NA	NA	NA	19-43	31	35	NA	NA	NA	NA	NA	NA	NA	NA	NA	NA	NA	NA	NA	NA
13	9.0	2.0	4.5	NE	26	4.4	3.6	NA	NA	NA	NA	19-43	32	40	NA	NA	NA	NA	NA	NA	NA	NA	NA	NA	NA	NA	NA	NA
14	15.5	2.0	7.8	NE	24	3.5	3.6	NA	NA	NA	NA	19-43	31	35	NA	NA	NA	NA	NA	NA	NA	NA	NA	NA	NA	NA	NA	NA
15	17.0	4.0	4.3	NE	30	4.2	NA	NA	NA	NA	NA	19-120	48	51	NA	NA	NA	NA	NA	NA	NA	NA	NA	NA	NA	NA	NA	NA
16	17.0	4.0	4.3	NE	13	3.8	4.6	NA	NA	NA	NA	18-64	37	38	NA	NA	NA	NA	NA	NA	NA	NA	NA	NA	NA	NA	NA	NA
17	17.0	4.0	4.3	NE	13	3.8	4.6	NA	NA	NA	NA	18-64	37	38	NA	NA	NA	NA	NA	NA	NA	NA	NA	NA	NA	NA	NA	NA
18	22.0	4.0	5.5	NE	NA	5.6	3.6	NA	NA	NA	NA	70-200	120	115	NA	NA	NA	NA	NA	NA	NA	NA	NA	NA	NA	NA	NA	NA
20	17.0	5.0	3.4	0	12	1.2	0.6	NA	NA	NA	0.9	NA	NA	NA	NA	NA	NA	NA	1.2	NA	NA	NA	NA	NA	NA	NA	NA	NA
21	38.0	5.0	7.6	0	14	1.2	0.7	NA	NA	NA	1.3	NA	NA	NA	NA	NA	NA	NA	1.4	NA	NA	NA	NA	NA	NA	NA	NA	NA
22	36.0	3.4	10.6	NA	16	NA	NA	NA	NA	NA	NA	12-30	19	17	NA	NA	NA	NA	NA	NA	NA	NA	NA	NA	NA	NA	NA	NA
23	36.0	3.4	10.6	NA	16	NA	NA	NA	NA	NA	NA	12-30	19	17	NA	NA	NA	NA	NA	NA	NA	NA	NA	NA	NA	NA	NA	NA
24	36.0	3.4	10.6	NA	16	NA	NA	NA	NA	NA	NA	12-30	19	17	NA	NA	NA	NA	NA	NA	NA	NA	NA	NA	NA	NA	NA	NA
29	20.0	3.0	6.7	15	30	2.0	NA	2.0	NA	NA	NA	NA	NA	NA	NA	NA	NA	NA	NA	NA	NA	NA	NA	NA	NA	NA	NA	NA
34	37.4	6.0	6.2	0	NA	NA	1.6	NA	1.8	NA	1.5	NA	16	15	NA	NA	NA	NA	NA	NA	NA	NA	NA	NA	NA	NA	NA	NA
35	5.0	0.5	10.0	1.1	10	NA	0.7	NA	1.3	0.6	NA	6	6	14	NA	34	NA	8.0	NA	70	3.6	8.8	170	NA	NA	NA	NA	NA
37	5.0	1.0	5.0	1.1	10	NA	0.7	NA	1.3	0.6	NA	6	6	14	NA	34	NA	8.0	NA	70	3.6	8.8	170	NA	NA	NA	NA	NA
38	10.0	1.0	10.0	1.1	14	NA	0.7	NA	1.3	0.6	NA	4-6	5	9	NA	22	NA	8.0	NA	65	3.9	7.0	110	NA	NA	NA	NA	NA
43	20.0	3.0	6.7	NA	NA	8.0	NA	NA	NA	NA	NA	20-150	105	112	NA	NA	NA	117	NA	NA	NA	NA	NA	NA	NA	NA	NA	NA
49	8.2	2.7	3.1	NA	10	1.7	NA	NA	NA	NA	NA	21-132	82	88	NA	NA	NA	NA	NA	NA	NA	NA	NA	NA	NA	NA	NA	NA
50	12.0	2.7	4.5	NA	7	NA	NA	NA	NA	NA	NA	14-37	25	24	NA	NA	NA	NA	NA	NA	NA	NA	NA	NA	NA	NA	NA	NA
53	7.9	2.7	3.0	NA	31	NA	NA	NA	NA	NA	NA	1-4	3	3	NA	NA	NA	NA	NA	NA	NA	NA	NA	NA	NA	NA	NA	NA
54	12.0	2.7	4.5	NA	30	NA	NA	NA	NA	NA	NA	NA	NA	NA	NA	NA	NA	NA	NA	NA	NA	NA	NA	NA	NA	NA	NA	NA
56	11.7	4.5	2.6	NE	NA	NA	3.5	NA	NA	NA	NA	3-80	25	26	NA	NA	NA	NA	NA	NA	521	NA	NA	NA	NA	NA	NA	NA
61	12.5	5.0	2.5	NE	NA	NA	3.6	NA	NA	NA	NA	14-80	22	23	NA	NA	NA	NA	NA	393	NA	NA	NA	NA	NA	NA	NA	NA
67	17.5	4.5	3.9	9.5	NA	NA	1.7	NA	NA	NA	NA	8-25	14	13	NA	NA	NA	NA	NA	183	NA	NA	NA	NA	NA	NA	NA	NA
68	15.0	4.5	3.3	NE	NA	NA	1.8	NA	NA	NA	NA	8-25	15	14	NA	NA	NA	NA	NA	421	NA	NA	NA	NA	NA	NA	NA	NA
83	10.0	2.2	4.5	NE	17	NA	NA	NA	NA	NA	NA	NA	NA	NA	80	NA	4.0	60	NA	1340	NA	NA	NA	NA	NA	NA	NA	NA
84	15.0	2.2	6.8	NE	17	NA	NA	NA	NA	NA	NA	NA	NA	NA	110	NA	5.5	70	NA	1340	NA	NA	NA	NA	NA	NA	NA	NA
85	10.0	2.1	4.8	NE	22	NA	NA	NA	NA	NA	NA	NA	NA	NA	460	NA	23	10	NA	215	NA	NA	NA	NA	NA	NA	NA	NA
86	15.0	2.1	7.1	NE	22	NA	NA	NA	NA	NA	NA	NA	NA	NA	540	NA	27	16	NA	280	NA	NA	NA	NA	NA	NA	NA	NA

Notes: NA - Not Available MV - Mini. Vane CPT: qc - Tip Resistance PMT: PL - Limit Pressure DMT: Po - Contact Pressure
 NE - Not Encountered FV - Field Vane qt - Corrected qc Em - PMT Modulus P1 - Expansion Pressure
 UC - Unconfined Comp. TV - Torvane Ed - DMT Modulus
 UU - UU Triaxial Test

Table 2.7. Summary of Laboratory and Field Tests from Load Test Sites in Sands

File	L (ft)	d (ft)	L/d -	GWL (ft)	ϕtc'(deg)		SPT-N			CP T		PMT		DMT		
					DS	TX	Range	Avg.	(N1)60	qc	qt	PL	Em	Po	P1	Ed
39	7.0	2.5	2.8	NA	NA	NA	NA	NA	NA	140	NA	NA	NA	NA	NA	230
40	5.0	2.5	2.0	NA	NA	NA	NA	NA	NA	110	NA	NA	NA	NA	NA	76
41	7.0	2.5	2.8	NA	NA	NA	NA	NA	NA	400	NA	NA	NA	NA	NA	260
42	20.0	3.0	6.7	NA	NA	NA	5-30	17	18	NA	NA	22	NA	NA	NA	NA
48	28.0	3.3	8.5	0	NA	NA	5-50+	50	50	NA	NA	NA	NA	NA	NA	NA
51	8.0	2.7	3.0	NA	NA	NA	17-70	38	36	NA	NA	NA	NA	NA	NA	NA
52	12.3	2.7	4.6	NA	NA	NA	16-56	30	29	NA	NA	NA	NA	NA	NA	NA
57	16.0	4.5	3.6	11	NA	29.2	3-13	7	8	NA	NA	NA	98	NA	NA	NA
58	21.0	5.0	4.2	12.5	NA	43.2	25-50+	50	50	NA	NA	NA	668	NA	NA	NA
59	15.8	5.0	3.2	12.5	NA	43.2	25-50+	50	50	NA	NA	NA	668	NA	NA	NA
62	16.8	5.3	3.2	7.5	NA	38.1	8-42	15	17	NA	NA	NA	215	NA	NA	NA
64	16.0	4.8	3.3	16	NA	38.8	8-50+	50	50	NA	NA	NA	1915	NA	NA	NA
65	20.3	5.0	4.1	10	NA	33.8	3-12	9	10	NA	NA	NA	73	NA	NA	NA
87	10.0	2.4	4.2	NE	48	NA	NA	NA	NA	600	NA	44	280	NA	NA	NA
88	20.0	2.4	8.3	NE	48	NA	NA	NA	NA	700	NA	44	280	NA	NA	NA

Notes: NA - Not Available
NE - Not Encountered
DS - Direct Shear Test
TX - Triaxial Test

CPT: qc - Tip Resistance
qt - Corrected qc
PMT: PL - Limit Pressure
Em - PMT Modulus

DMT: Po - Contact Pressure
P1 - Expansion Pressure
Ed - DMT Modulus

in which H = lateral load, δ = groundline deflection of shaft, and a and b are hyperbolic parameters related to ultimate capacity and stiffness. This expression can be rearranged to provide a linear fit for load-deflection data using transformed axes, whereby:

$$\frac{\delta}{H} = a + b\delta \quad [2.6]$$

Regression analysis can be used in the transformed axes to obtain the parameters a (intercept) and b (slope). The ultimate lateral capacity (H_u) and initial stiffness (K_i) of the load-deflection response can then be determined as the inverse of slope ($H_u = 1/b$) and inverse of intercept ($K_i = 1/a$), respectively. Once the hyperbolic model and parameters are established, the magnitude of lateral load at various deflection levels can be calculated by:

$$H = \frac{\delta}{\frac{1}{K_i} + \frac{\delta}{H_u}} \quad [2.7]$$

Alternatively, the horizontal deflection can be expressed in terms of lateral load by:

$$\delta = \frac{H_u}{K_i} \frac{H}{(H_u - H)} \quad [2.8]$$

The basic procedure is illustrated with actual load test data in Figures 2.5 and 2.6. This load test was performed at College Station, Texas, and was documented by Bierschwale et al. (1981). The drilled shaft is 15 ft long, 2.5 ft in diameter, and has an eccentricity of 2.6 ft for the applied lateral load.

This methodology has been verified by Mayne et al. (1991) and Agaiby et al. (1991) and proven to be capable of providing a good agreement between hyperbolic fit and measured data. The hyperbolic ultimate lateral capacity (H_u) is always higher than the measured maximum lateral force (as shown in Figure 2.5) because free-headed rigid drilled shafts can never fully mobilize the available soil resistance.

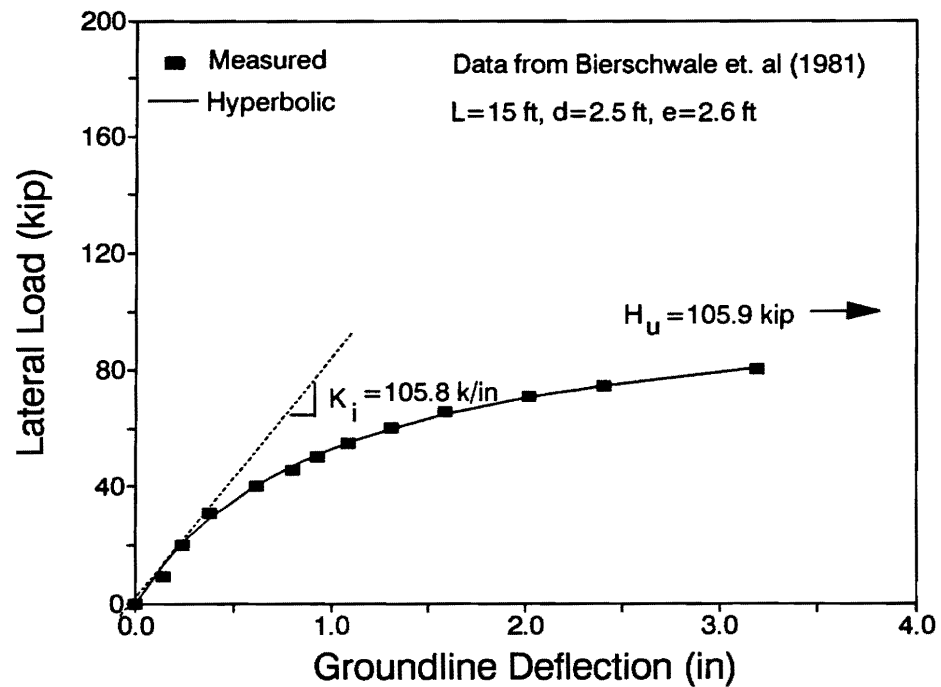


Figure 2.5. Hyperbolic Fit of Load-Deflection Curve

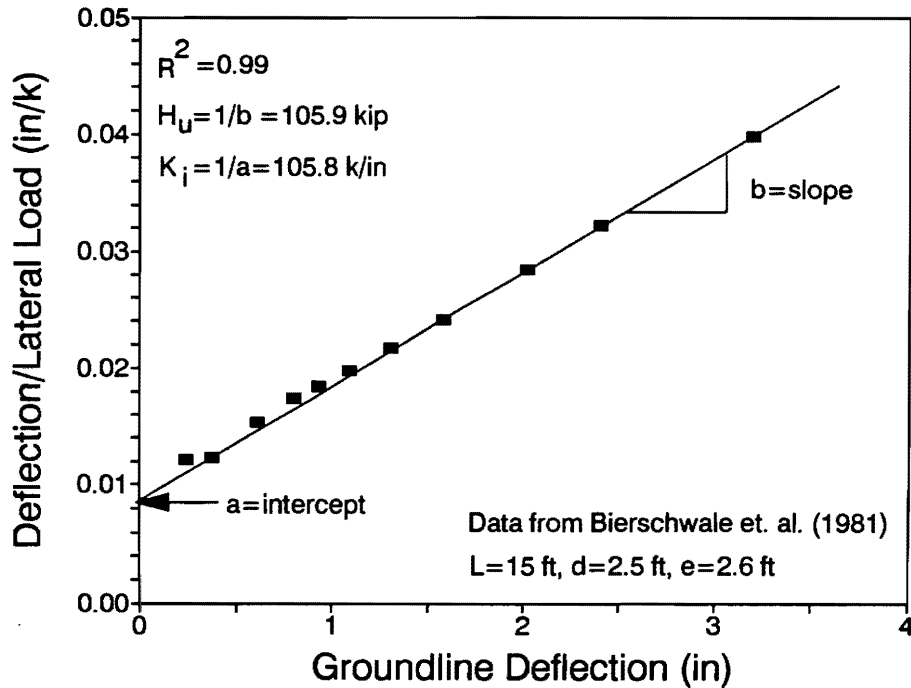


Figure 2.6. Derivation of Hyperbolic Parameters

The hyperbolic parameters H_u and K_i can be theoretically related directly to the pier geometry, soil shear strength, and relevant soil modulus. These stress-strain-strength characteristics are usually defined in terms of the undrained shear strength (s_u) and initial tangent modulus (E_t) for cohesive soils; and drained friction angle (ϕ') and initial tangent modulus for cohesionless soils. The manipulation involves the application of limit equilibrium analysis (Poulos and Davis, 1980; Randolph and Houlsby, 1984) and elastic continuum theory (Poulos and Hull, 1989). Some fundamental assumptions are made to simplify the problem and to obtain satisfactory closed-form solutions.

2.3.2. Limit Equilibrium Analysis

The conventional approach for analyzing the ultimate lateral capacity is to use limit equilibrium analysis which accounts for the balance of forces and moments. An equilibrium condition is evaluated from the applied lateral load at the top of the drilled shaft and the passive soil resistance along the shaft. As shown in Figure 2.7(a), the depth to the point of rotation (z_r) is determined by summing the moments taken at the top

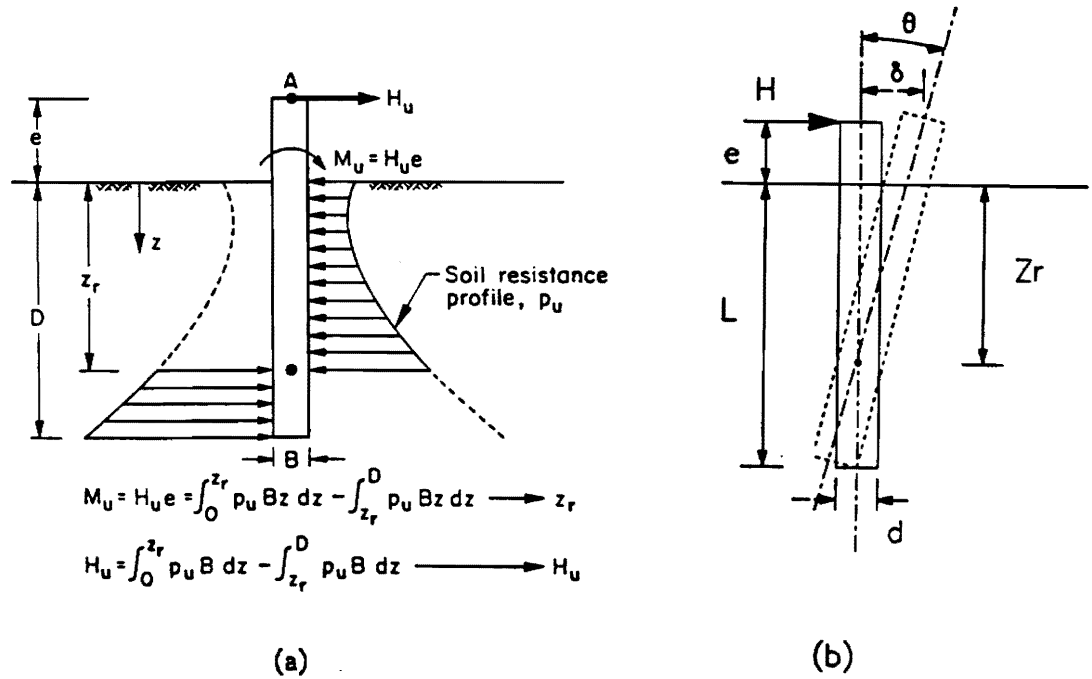


Figure 2.7. Rigorous Method of Limit Equilibrium Analysis
(Modified after Poulos and Davis, 1980)

of the foundations, such that $\Sigma M_A = 0$. Then, the ultimate lateral load is derived by summing forces horizontally ($\Sigma F_h = 0$). The distribution of soil resistance plays an important role in the analysis, which is assumed either to be uniform along the shaft or varying with depth. In the case of undrained loading, the lateral soil resistance (p_u) is commonly expressed in terms of a bearing factor (N_p), defined as:

$$N_p = \frac{P_u}{s_u} \quad [2.9]$$

Figure 2.8 shows different profiles for N_p in cohesive soils suggested by Broms (1964), Randolph and Houlsby (1984), Hansen (1961), Reese (1958), and Stevens & Audibert (1979). Formulations of N_p were discussed in detail by Randolph and Houlsby (1984) and Reese (1958).

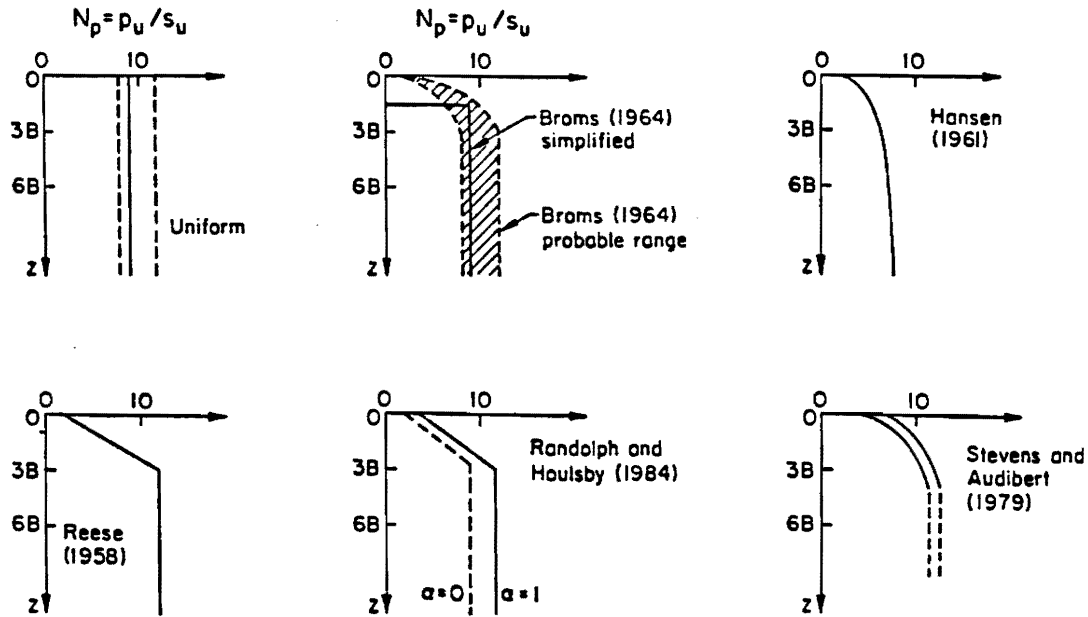


Figure 2.8. Recommended Profiles of Lateral Soil Resistance
(Compiled by Mayne, 1991)

Assuming a simple uniformly distributed soil resistance (p_u) with depth, the depth to the point of rotation (z_r) and the ultimate lateral capacity (H_u) can be determined as follows:

$$z_r = \left(\frac{L}{2} \right) \left[\left(1 + \frac{2e}{L} \right) + 1 \right]^{1/2} - e \quad [2.10]$$

$$\frac{H_u}{p_u L d} = \left[\left(1 + \frac{2e}{L} \right)^2 + 1 \right]^{1/2} - \left(1 + \frac{2e}{L} \right) \quad [2.11]$$

where e = eccentricity of loading, d = shaft diameter and L = embedded length.

The limit equilibrium analysis for free-headed shaft foundations under lateral and moment loading has an inherent shortcoming since the soil resistance can never be fully mobilized (to reach plastic state) unless the rigid shaft is rotated 90° . Therefore, this study combines the elastic continuum theory to evaluate the ultimate lateral capacity. In clays,

the approach considers both a uniform distribution of soil resistance, and a varying soil resistance distribution with reduced lateral soil resistance near the ground surface based on the combined wedge/plasticity model. In sands, a Gibson model is used with E_s increasing with depth. The depth to the point of rotation z_r is evaluated by both limit equilibrium analysis and elastic continuum theory. That is, three different approaches are utilized: (1) elastic continuum theory for both z_r and H_u , assuming uniform distribution of lateral soil resistance; (2) limit equilibrium analysis for z_r and elastic continuum theory for H_u , assuming uniform distribution of lateral soil resistance; and (3) limit equilibrium analysis for z_r and elastic continuum theory for H_u , assuming reduced soil resistance distribution. The maximum shear stress backcalculated from the load test results (i.e. undrained shear strength in the case of cohesive soils and indirectly obtained as drained friction angle in the case of cohesionless soils) is actually derived from elastic continuum theory discussed in the following section.

2.3.3. Elastic Continuum Theory

Poulos and Hull (1989) developed a series of approximate closed-form solutions for the ultimate lateral load and load-deflection relationships of laterally loaded drilled shafts, assuming the soil is an elastic, homogeneous and isotropic medium. The horizontal groundline deflection (δ) and the rotation angle (θ) are determined as follows (see Figure 2.7(b)):

$$\delta = \frac{HI_{12}}{E_s L} \quad [2.12]$$

$$\theta = \frac{HI_{23}}{E_s L^2} \quad [2.13]$$

where $I_{12} = I_1 + I_2(e/d)$ and $I_{23} = I_2 + I_3(e/d)$. The parameters I_1 , I_2 and I_3 are influence factors which are derived from the approximation of boundary element analysis by Poulos and Hull (1989) and which are supported by finite element analysis conducted independently by Kuhlemeyer (1979) and Randolph (1981). The soil modulus (E_s) is assumed to either be (1) a constant value along the shaft for cohesive soils or (2) the value at the bottom of shaft along which the soil modulus is assumed to be linearly

increasing for cohesionless soils (Gibson soil). The influence factors vary with soil type and the rigidity of drilled shafts. For rigid drilled shafts,

$$\text{Cohesive Soils:} \quad I_1 = 0.976 + 2.196 \log(L/d) \quad [2.14]$$

$$I_2 = 0.701 + 3.225 \log(L/d) \quad [2.15]$$

$$I_3 = 1.086 + 6.292 \log(L/d) \quad [2.16]$$

$$\text{Cohesionless Soils:} \quad I_1 = 3.181 + 9.701 \log(L/d) \quad [2.17]$$

$$I_2 = 2.409 + 12.71 \log(L/d) \quad [2.18]$$

$$I_3 = 1.844 + 18.65 \log(L/d) \quad [2.19]$$

The unrestrained rigid drilled shaft rotates when subjected to lateral load (Figure 2.7(b)). Since only small strains are expected to be developed in elastic theory, it is appropriate to express the shear strain (γ) in terms of the ratio of groundline deflection (δ) to the depth to the point of rotation (z_r), i.e.

$$\gamma = \frac{\delta}{z_r} \quad [2.20]$$

That is, for small angles of rotation, $\tan \theta \approx \theta \approx \gamma_{\text{average}}$. Based on the theory of elasticity, the shear modulus can be expressed as:

$$G = \frac{\tau}{\gamma} \quad [2.21]$$

For undrained loading, the (maximum) shear stress (τ) becomes the undrained shear strength (s_u) and G is directly related to the Young's modulus of soil (E) by adopting a Poisson's ratio (ν) of 0.5, such that:

$$G = \frac{E_s}{2(1+\nu)} = \frac{E_s}{3} \quad [2.22]$$

By rearranging equations [2.20], [2.21], and [2.22], the following expression can be derived :

$$\delta = \gamma z_r = \left(\frac{\tau}{G} \right) z_r = \left(\frac{s_u}{G} \right) z_r = \frac{3 s_u z_r}{E_s} \quad [2.23]$$

The ultimate lateral capacity (H_u) can now be derived by combining equation [2.12] and [2.23], given as follow:

$$H_u = \frac{3 s_u z_r L}{I_{12}} \quad [2.24]$$

The depth to the point of rotation (z_r) can be assessed in several ways. Considering small strain elastic behavior of drilled shafts, $z_r = \delta/\theta$ is appropriate for small strain assumption. In lieu of the aforementioned limit equilibrium approach given by equation [2.10], z_r can alternatively be expressed in terms of I_{12} and I_{23} by combining equations [2.12] and [2.13]:

$$z_r = \frac{\delta}{\theta} = \frac{I_{12} L}{I_{23}} \quad [2.25]$$

Equation [2.24] is valid only for a uniformly distributed profile of soil resistance along shaft. To account for varying distributions of lateral soil resistance, H_u can be calculated assuming a wedge reduction at shallow depths for the lateral soil resistance (Reese, 1958; Randolph and Houlsby, 1984). The reduced lateral resistance (p_u) near the ground surface can be approximated to an equivalent uniform distribution by introducing the reduction factor $(1-d/L)$. The resulting expression is given as:

$$H_u = \left(\frac{3 s_u z_r L}{I_{12}} \right) \left(1 - \frac{d}{L} \right) \quad [2.26]$$

In the case of drained response, the value of s_u is replaced with maximum shear stress (τ_{max}). To study the deformability of the laterally loaded drilled shaft, the initial stiffness (K_i) of the load-deflection curve can be expressed in terms of the initial tangent modulus (E_i) from the stress-strain relationship by substituting $H/\delta = K_i$ into equation [2.12]:

$$K_i = \frac{E_i L}{I_{12}} \quad [2.27]$$

Thus, the ultimate capacity and stiffness from the hyperbolic model have been related to shaft geometry, soil modulus, and shear strength.

2.3.4. Interpretation of Undrained Strength and Soil Modulus

The three approaches used to calculate the ultimate lateral capacity H_u may also be used to backfigure the relevant undrained shear strength (s_u) for cohesive soils and the maximum shear stress (τ_{max}) for cohesionless soil. The point of equilibrium z_r may be assessed using elastic continuum theory (equation [2.25]) or limit equilibrium analysis (equation [2.10]). The maximum shear strength may be backcalculated using elastic continuum theory and assuming uniform distribution of lateral soil resistance:

$$s_u = \frac{H_u I_{12}}{3 z_r L} \quad [2.28]$$

Or, using elastic continuum theory and assuming reduced lateral soil resistance distribution:

$$s_u = \frac{H_u I_{12}}{3 z_r L} \frac{1}{(1 - \frac{d}{L})} \quad [2.29]$$

In summary, three approaches are utilized: (1) elastic continuum theory for both z_r and H_u , assuming uniform distribution of lateral soil resistance (equations [2.25] and [2.28]); (2) limit equilibrium analysis for z_r and elastic continuum theory for H_u , assuming uniform distribution of lateral soil resistance (equation [2.10] and [2.28]); and (3) limit equilibrium analysis for z_r and elastic continuum theory for H_u , assuming reduced soil resistance distribution (equation [2.10] and [2.29]). Among these approaches, the elastic continuum theory gives the smallest s_u while the limit equilibrium approach with wedge soil resistance distribution gives the largest. The differences between them will be examined later using the compiled load test database. Equation [2.27] may also be rearranged to backfigure the initial tangent modulus E_t of soils using load test data:

$$E_t = \frac{K_t I_{12}}{L} \quad [2.30]$$

Table 2.8. Relative Values of Effective Stress Friction Angle

Test Type	Friction Angle (°)
<u>Cohesive Soils</u>	
Triaxial Compression ¹ (TC)	1.00 ϕ_{tc}'
Triaxial Extension (TE)	1.22 ϕ_{tc}'
Plane Strain Compression (PSC)	1.10 ϕ_{tc}'
Plane Strain Extension (PSE)	1.34 ϕ_{tc}' (= 1.10 x 1.22)
Direct Shear ² (DS)	$\tan^{-1} [\tan \phi_{psc}' \cos \phi_{cv}']$
<u>Cohesionless Soils</u>	
Triaxial Compression ¹ (TC)	1.00 ϕ_{tc}'
Triaxial Extension (TE)	1.12 ϕ_{tc}'
Plane Strain Compression (PSC)	1.12 ϕ_{tc}'
Plane Strain Extension (PSE)	1.25 ϕ_{tc}' (= 1.12 x 1.12)
Direct Shear (DS)	$\tan^{-1} [\tan \phi_{psc}' \cos \phi_{cv}']$

Notes:

(1) CIUC, CK₀UC, or CAUC

(2) Based on results from sand

2.3.5. Interpretation of Drained Strength

Cohesionless soils are usually associated with drained loading conditions. In these cases, the maximum shear stress (τ_{max}) interpreted from hyperbolic parameters is often expressed in terms of a drained friction angle (ϕ'). For laterally-loaded drilled shafts, this friction angle is determined under triaxial extension loading conditions rather than the more common triaxial compression mode which is more appropriate for vertically loaded foundations.

Direct relationships between the drained friction angle under triaxial extension (ϕ_{te}') and drained friction angle under triaxial compression (ϕ_{tc}') is readily available from procedures given by Kulhawy and Mayne (1990) and summarized in Table 2.8. Agaiby, Kulhawy and Trautmann (1991) developed the relationship between ϕ_{te}' and normalized maximum shear stress (τ_{max}/σ_{vo}'), given as:

$$\frac{\tau_{\max}}{\sigma'_{vo}} = \frac{\sin \phi'_{te}}{1 - \sin \phi'_{te}} \quad [2.31]$$

in which σ'_{vo} = vertical effective overburden stress. Rearranging equation [2.31]:

$$\phi'_{te} = \sin^{-1} \left[\frac{\tau_{\max}}{\sigma'_{vo} + \tau_{\max}} \right] \quad [2.32]$$

since $\phi'_{te} = 1.12 \phi'_{tc}$ for triaxial test results, the drained friction angle corresponding to the triaxial compression mode (ϕ'_{tc}) can be derived using laterally-loaded drilled shaft test data:

$$\phi'_{tc} = 0.89 \sin^{-1} \left[\frac{\tau_{\max}}{\sigma'_{vo} + \tau_{\max}} \right] \quad [2.33]$$

2.4. UTILIZATION OF LOAD TEST DATABASE

Load-deflection data were digitized from selected load tests in the database. Only data from rigid shafts ($2 < L/d < 12$) were considered because LLWAS foundations have low slenderness ratios ($L/d = 5$). The load test measurements have been expressed in terms of lateral load (H), moment (M) induced by lateral load and eccentricity (e), groundline deflection of the shaft head (δ), and rotation angle (Θ). For consistency and because of limited availability of test results, lateral load (H) and groundline deflection (δ) are used throughout the study, even though the rotation angle might be a better parameter for evaluating the behavior of rigid shafts. Due to the large eccentricity of loading ($e/L = 3$ to 5) of the LLWAS system, the moment applied at the top of shafts is more critical than the lateral load. In the final presentation of the design charts, all lateral loads have been converted to moments by multiplying by a specific eccentricity ($M = H e$).

Each data set was evaluated in a spreadsheet format as shown in Figure 2.9. Using equation [2.7] described in the preceding sections, the ultimate lateral capacity (H_u) and initial stiffness (K_i) were derived by substituting lateral loads (H) and corresponding deflections (δ) into the hyperbolic model. The undrained shear strength (s_u) and initial

tangent modulus (E_t) for cohesive soils were backcalculated from hyperbolic parameters H_u and K_t . The drained friction angle (ϕ_{tc}') and initial tangent modulus (E_t) for cohesionless soils were backcalculated from the same parameters. Three different approaches were evaluated to derive s_u and ϕ' . These approaches have different theoretical bases and assumptions, with which the elastic theory gives the smallest s_u and ϕ_{tc}' while limit equilibrium analysis with wedge-reduction soil resistance distribution gives the largest s_u and ϕ_{tc}' . Summaries of backcalculated results for cohesive and cohesionless soils are listed in Tables 2.9 and 2.10, respectively. The τ_{max} in Table 2.10 is equivalent to the s_u in Table 2.9 for all calculations.

When compared with laboratory or field test results, the backcalculated parameters should be more related to the triaxial extension mode (TE) rather than common triaxial compression test (TC). Kulhawy and Mayne (1990) reported relative values of drained friction angle (ϕ') with respect to various shearing modes for normally consolidated cohesive and cohesionless soils (Table 2.8). They also reported the normalized undrained shear strength (s_u/σ_{vo}') for cohesive soils as a function of shearing mode (Figure 2.10). It is observed that the drained friction angle for sands under TE loading (ϕ_{tc}') is approximately 1.12 times the angle under TC loading (ϕ_{tc}'), and s_u/σ_{vo}' for clays under TE loading is approximately one-half as s_u/σ_{vo}' under TC loading. Therefore, it is not surprising that most of the backcalculated values of s_u are lower than the measured values and most of the backcalculated ϕ_{tc}' are higher than the measured values of ϕ_{tc}' .

Eccentricity (e) also has significant effect on the results. Eccentricities in the load tests varied from several inches by applying lateral loads almost directly to the top of shaft to more than 100 ft by attaching segments of pole and applying loads at the top of pole in several large scale field tests. In this study, the LLWAS system installs poles with the length up to 150 ft to be supported by the drilled shafts. A concentrated load of 5 kip applied at about 80 ft above the ground surface has been assumed to simulate the resultant of distributed wind loads, resulting in an applied groundline moment of 404 k-ft (see Figure 2.1).

Another limitation for the aforementioned approach is the assumption of uniformity of soil properties along the lengths of the drilled shafts. Since the methodology cited herein is essentially a one-layer approach, the results might not work out very well if the soil properties vary significantly along the shafts.

BACKCALCULATION OF Su, Es, AND Kh FOR RIGID DRILLED SHAFTS																											
GIVEN INFORMATION SITE = SHAFT III, COLLEGE STATION, TX REFERENCE = BIRSCHWALE ET AL. 1981 L(ft) = 15.00 d(ft) = 2.50 e(ft) = 2.60								Regression Output:																			
								Constant		0.0094																	
								Std Err of Y Est		0.0004																	
								R Squared		0.9984																	
								No. of Observations		11																	
								Degrees of Freedom		9																	
								X Coefficient(s)		0.0094																	
								Std Err of Coef.		0.0001																	
CALCULATED PARAMETERS																											
L/d Ratio		=		6.00		I1		=		2.68		AVG. Su(ksf)		=		0.667											
e/d Ratio		=		1.04		I2		=		3.21		Hu/(PuLd)		=		0.331											
e/L Ratio		=		0.17		I3		=		5.98		AVG. Pu(ksf)		=		8.542											
Estimated zr(ft)		=		11.45		I12		=		3.24		Ei/Su		=		412											
Hu(kips)		=		105.93		I23		=		4.25		Gi/Su		=		137											
Ki(k/in)		=		105.83		Ip(ft4)		=		1.92																	
Ei(ksf)		=		274.43		fc(psi)		=		5200																	
Gi(ksf)		=		91.48		Ep(ksf)		=		591887																	
						Ep Ip		=		1134930																	
														Poulos		Brom											
Meas. Defl.		Meas. Force		Normal Strain		Shear Strain		Secant Modulus		Shear Modulus		Shear Stress		Poulos Calc.		Poulos Crit. Length		Brom Calc.		Brom Dimen. Length		Modu. Ratio		Rigidity Index			
δ		H		δ/H		ε		γ		Es		G		τ		Kr		Lc		kh		μL		Es/Su		G/Su	
(in.)		(kips)		(in/k)		(in/in)		(in/in)		(ksf)		(ksf)		(ksf)		-		(ft)		(k/ft3)		(ft)					
0.000		0.00		0.000		0.000		0.000		274.43		91.48		0.000		0.082		35.6		0.0		0.00		412		137	
0.143		9.43		0.015		0.005		0.001		170.49		56.83		0.059		0.131		40.1		106.0		1.31		256		85	
0.243		19.95		0.012		0.008		0.002		213.08		71.03		0.126		0.105		37.9		132.5		1.39		320		107	
0.379		30.77		0.012		0.013		0.003		210.83		70.28		0.194		0.106		38.0		131.1		1.38		316		105	
0.615		40.14		0.015		0.021		0.004		169.17		56.39		0.253		0.133		40.2		105.2		1.31		254		85	
0.799		45.91		0.017		0.027		0.006		148.93		49.64		0.289		0.151		41.5		92.6		1.27		223		74	
0.927		50.33		0.018		0.031		0.007		140.72		46.91		0.317		0.159		42.1		87.5		1.25		211		70	
1.089		55.08		0.020		0.036		0.008		131.19		43.73		0.347		0.171		42.8		81.6		1.23		197		66	
1.307		60.29		0.022		0.044		0.010		119.60		39.87		0.379		0.187		43.8		74.4		1.20		179		60	
1.583		65.96		0.024		0.053		0.012		108.03		36.01		0.415		0.208		45.0		67.2		1.17		162		54	
2.021		71.24		0.028		0.067		0.015		91.42		30.47		0.448		0.245		46.9		56.9		1.12		137		46	
2.404		74.70		0.032		0.080		0.018		80.56		26.85		0.470		0.278		48.4		50.1		1.09		121		40	
3.193		80.31		0.040		0.106		0.023		65.22		21.74		0.505		0.344		51.0		40.6		1.03		98		33	

Figure 2.9. Example of Spreadsheet Used to Evaluate Load Test Data

Table 2.9. Backcalculated Hyperbolic Parameters and Soil Properties for Clay Sites

										(1)		(2)		(3)	
	e	L	d	L/d	I12	I23	Ki	Hu	Ei	Su	Ir	Su	Ir	Su	Ir
File	(ft)	(ft)	(ft)	-	-	-	(k/in)	(kip)	(ksf)	(ksf)	-	(ksf)	-	(ksf)	-
01	2.6	20.0	3.0	6.7	3.222	4.173	176	237	340	0.824	138	0.944	120	1.110	102
02	2.6	15.0	3.0	5.0	3.023	3.906	199	154	481	0.891	180	1.037	155	1.296	124
03	2.6	15.0	2.5	6.0	3.241	4.247	96	112	249	0.705	118	0.808	103	0.970	86
07	1.0	15.0	4.0	3.8	2.407	2.865	500	600	963	2.547	126	3.105	103	4.234	76
08	1.0	15.0	4.0	3.8	2.407	2.865	510	633	982	2.687	122	3.275	100	4.467	73
09	1.0	12.5	4.0	3.1	2.246	2.633	518	500	1117	2.808	133	3.494	107	5.139	72
10	1.0	12.5	4.0	3.1	2.246	2.633	452	480	975	2.696	121	3.354	97	4.933	66
11	1.0	15.5	4.0	3.9	2.435	2.907	481	553	907	2.230	136	2.710	112	3.652	83
12	1.0	15.5	4.0	3.9	2.435	2.907	591	633	1114	2.553	145	3.102	120	4.181	89
13	1.0	9.0	2.0	4.5	2.722	3.385	339	213	1231	2.967	138	3.517	117	4.522	91
14	1.0	15.5	2.0	7.8	3.159	4.000	289	535	707	2.969	79	3.401	69	3.904	60
15	1.0	17.0	4.0	4.3	2.516	3.024	668	326	1187	1.137	348	1.369	289	1.791	221
16	1.0	17.0	4.0	4.3	2.516	3.024	236	163	419	0.569	246	0.685	204	0.895	156
17	1.0	17.0	4.0	4.3	2.516	3.024	364	102	647	0.356	606	0.428	503	0.560	385
18	1.0	22.0	4.0	5.5	2.742	3.350	443	1061	663	2.448	90	2.885	77	3.526	63
20	1.0	17.0	5.0	3.4	2.285	2.676	617	184	995	0.568	584	0.702	473	0.994	334
21	1.0	38.0	5.0	7.6	3.003	3.716	902	270	856	0.232	1231	0.268	1066	0.308	926
22	1.6	36.0	3.4	10.6	3.409	4.349	833	174	947	0.195	1621	0.220	1436	0.243	1301
23	1.6	36.0	3.4	10.6	3.409	4.349	800	147	909	0.164	1843	0.186	1633	0.205	1479
24	1.6	36.0	3.4	10.6	3.409	4.349	895	130	1017	0.145	2331	0.164	2065	0.181	1870
29	2.5	20.0	3.0	6.7	3.205	4.142	237	210	456	0.725	210	0.830	183	0.977	155
34	0.9	37.4	6.0	6.2	2.801	3.414	1211	466	1089	0.379	957	0.444	817	0.529	686
35	0.1	5.0	0.5	10.0	3.251	4.074	28	3	218	0.163	447	0.185	393	0.206	353
37	0.1	5.0	1.0	5.0	2.570	3.065	77	6	475	0.245	646	0.293	540	0.366	432
38	0.1	10.0	1.0	10.0	3.211	4.000	69	6	266	0.080	1108	0.091	972	0.101	875
43	80.0	20.0	3.0	6.7	16.218	28.438	44	119	428	2.820	51	3.048	47	3.586	40
49	24.4	8.2	2.7	3.1	8.808	14.628	83	20	1070	1.450	246	1.630	219	2.417	148
50	24.4	12.0	2.7	4.5	8.115	13.364	172	18	1396	0.557	835	0.616	755	0.792	587
53	24.1	7.9	2.7	3.0	8.784	14.576	51	3	680	0.234	971	0.263	862	0.397	571
54	24.2	12.0	2.7	4.5	8.068	13.278	56	7	452	0.215	700	0.238	633	0.306	492
56	80.0	11.7	4.5	2.6	15.831	27.318	56	24	909	1.596	190	1.789	169	2.908	104
61	80.0	12.5	5.0	2.5	14.550	24.959	41	38	573	2.023	94	2.277	84	3.794	50
67	80.0	17.5	4.5	3.9	14.172	24.533	57	29	554	0.774	238	0.853	217	1.148	161
68	80.0	15.0	4.5	3.3	14.856	25.726	71	33	844	1.258	224	1.393	202	1.990	141
83	0.1	9.4	2.2	4.4	2.408	2.815	419	67	1286	0.716	599	0.870	493	1.130	379
84	0.1	14.4	2.2	6.7	2.809	3.402	459	80	1073	0.440	814	0.515	695	0.606	591
85	0.1	8.9	2.1	4.2	2.370	2.760	524	102	1675	1.183	472	1.444	387	1.898	294
86	0.1	13.9	2.1	6.5	2.789	3.373	712	99	1714	0.578	989	0.677	843	0.800	714

(1) z_r estimated by elastic theory, assuming uniform soil resistance.

(2) z_r estimated by limit equilibrium, assuming uniform soil resistance.

(3) z_r estimated by limit equilibrium, assuming reduced soil resistance distribution.

* $Ir = Ei/Su =$ Rigidity Index

Table 2.10. Backcalculated Hyperbolic Parameters and Soil Properties for Sand Sites

File	e	L	d	L/d	I12	I23	σ_{vo}'	Ki	Hu	Eid	(1)		(2)		(3)	
											γ_{max}	ϕ_{te}'	γ_{max}	ϕ_{te}'	γ_{max}	ϕ_{te}'
	(ft)	(ft)	(ft)	-	-	-	(ksf)	(k/in)	(kip)	(ksf)	(ksf)	(deg)	(ksf)	(deg)	(ksf)	(deg)
39	30.0	7.0	2.5	2.8	42.201	51.736	-	20	2	1447	0.704	-	1.091	-	1.698	-
40	32.0	5.0	2.5	2.0	46.006	53.968	-	1	1	110	0.720	-	1.184	-	2.368	-
41	30.0	7.0	2.5	2.8	42.201	51.736	-	11	2	796	0.704	-	1.091	-	1.698	-
42	80.0	20.0	3.0	6.7	62.697	81.720	-	46	33	1730	2.247	-	3.267	-	3.844	-
48	4.8	28.0	3.3	8.5	14.636	17.511	1.75	500	128	3136	0.953	20.6	1.197	24.0	1.357	25.9
51	24.4	8.0	2.7	3.0	33.627	41.200	-	91	15	4590	3.219	-	4.910	-	7.370	-
52	24.3	12.3	2.7	4.6	31.034	38.927	-	125	21	3785	1.801	-	2.611	-	3.335	-
57	80.0	16.0	4.5	3.6	55.581	70.003	2.00	48	40	2001	3.646	40.2	5.538	47.3	7.706	52.6
58	80.0	21.0	5.0	4.2	48.581	61.636	1.77	59	54	1638	2.516	35.9	3.749	42.8	4.921	47.3
59	80.0	15.8	5.0	3.2	52.383	65.282	1.77	67	75	2666	6.538	51.9	10.041	58.2	14.690	63.2
62	80.0	16.8	5.3	3.2	50.126	62.473	1.52	43	58	1540	4.279	47.6	6.556	54.3	9.537	59.6
64	80.0	16.0	4.8	3.3	53.527	67.033	2.00	71	63	2850	5.499	47.2	8.401	53.9	12.001	59.0
65	80.0	20.3	5.0	4.1	49.058	62.136	1.89	38	48	1102	2.413	34.1	3.607	41.0	4.786	45.8
87	0.1	10.0	2.4	4.2	9.296	10.421	-	702	134	7831	4.648	-	5.888	-	7.747	-
88	0.1	15.0	2.4	6.3	10.985	12.636	-	532.2	149	4677	2.798	-	3.450	-	4.107	-

(1) γ_{te} estimated by elastic theory, assuming uniform soil resistance.

(2) γ_{te} estimated by limit equilibrium, assuming uniform soil resistance.

(3) γ_{te} estimated by limit equilibrium, assuming reduced soil resistance distribution.

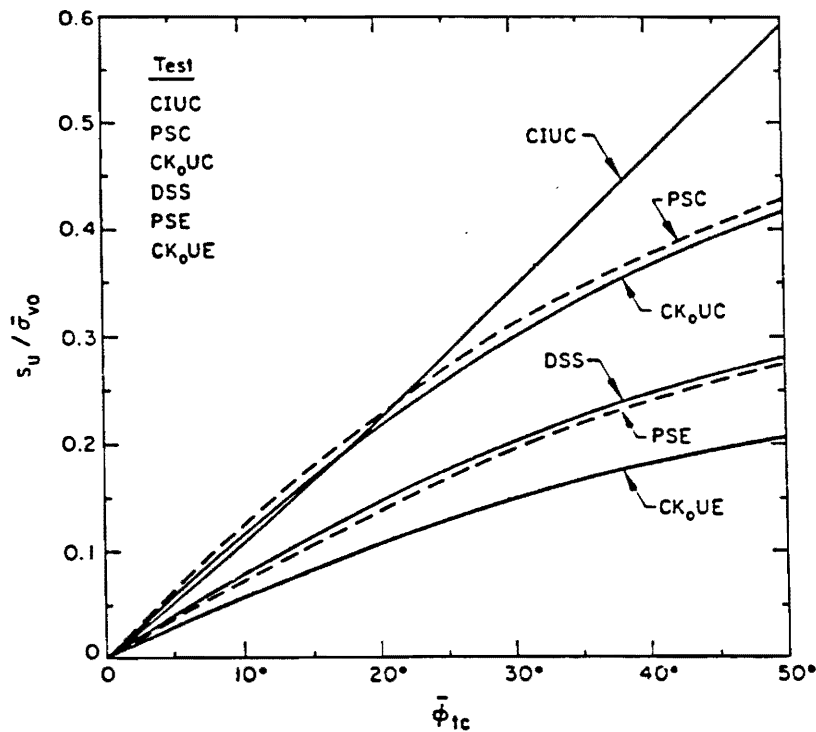


Figure 2.10. Undrained Strength Ratio as a Function of Test Type

(Source: Kulhawy and Mayne, 1990)

To calculate ϕ_{e}' using equation [2.32], the effective overburden stress (σ_{vo}') must be determined. This requires groundwater and unit weight information at each of the test sites. Unfortunately, not every source of load test data reported the groundwater level (GWL) at test sites, which limits the efficient use of data since GWL affects the magnitude of σ_{vo}' tremendously.

2.4.1. Standard Penetration Test Correlations

Since the backcalculated shear strength (s_u) and initial tangent modulus (E_t) of the soils at each of the test sites are obtained using the hyperbolic model and aforementioned theories, it is of interest to correlate the results with in-situ testing results. If relevant correlations can be established with certain degree of confidence, the load-deflection behavior of laterally loaded rigid drilled shafts may be predicted by proper evaluation of parameters obtained from in-situ tests. It is realized that this approach may have the shortcoming of oversimplifying the complicated load-deflection behavior, however, the study attempts to provide a guideline to first approximate the problem with a reasonable factor of safety.

As indicated in Tables 2.6 and 2.7, the standard penetration test (SPT) is the most popular field test available. Cone or piezocone penetration test (CPT or CPTU), vane shear tests (VST), pressuremeter test (PMT), and dilatometer test (DMT) data are available at some test sites, however, the incomplete presentation of these test results or lack thereof limits the reliability of a statistical study using these other tests.

The standard penetration test (SPT) has been the most widely-used field test in the United States for many decades. Many researchers have attempted to overcome some of the inherent shortcomings of this test. Skempton (1986) proposed corrections for energy ratio (hammer type), borehole diameter, sampling method and rod length (similar to the overburden pressure correction) to obtain more consistent SPT results, as listed in Table 2.11. In this study, only energy ratio and overburden pressure have been taken into account since much of the other information is unavailable.

Figures 2.11, 2.12, and 2.13 indicate the regression analysis results of backcalculated undrained shear strength (s_u) versus SPT-N values for cohesive soils, in which s_u has been determined by three different approaches mentioned in the previous section. Figure 2.14 indicates the regression analysis results of initial tangent modulus (E_i) versus SPT-N values for cohesive soils.

Table 2.11 SPT Correction Factors for Field Procedures

Factor	Equipment Variables	Value
Energy Ratio	Safety Hammer	0.90
	Donut Hammer	0.75
Borehole Diameter	2.5 to 4.5 in	1.00
	6.0 in	1.05
	8.0 in	1.15
Sampling Method	Standard Sampler	1.00
	Sampler without Liner	1.20
Rod Length	Rods > 30 ft	1.00
	20 to 30 ft	0.95
	13 to 20 ft	0.85
	10 to 13 ft	0.75

Source: Skempton (1986)

Since the maximum shear stress (τ_{max}) is more readily usable than the drained friction angle (ϕ_w') for backcalculating hyperbolic parameters, Figures 2.15 , 2.16 and 2.17 indicate the regression analysis results of τ_{max} versus corrected SPT-N values for cohesionless soils. Corrections were made for the effects of overburden pressure and energy ratios as appropriate. Figure 2.18 indicates the regression analysis results of initial tangent modulus (E_i) versus corrected SPT-N values for cohesionless soils. The E_i for cohesionless soils is the value at the tip of shafts. The distribution of soil modulus is assumed to be linearly increasing with depth.

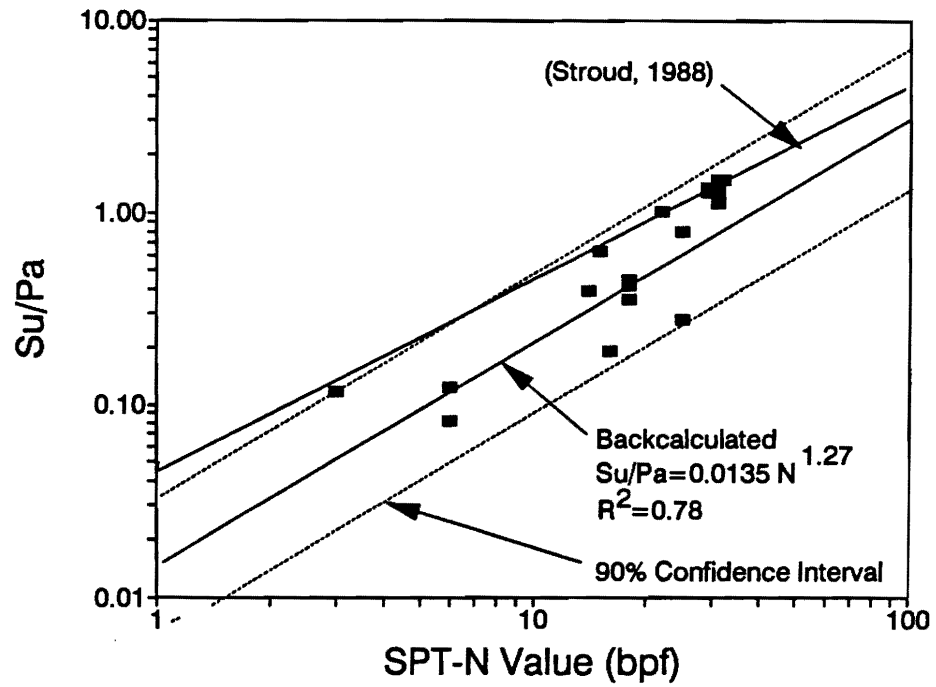


Figure 2.11. Correlation between s_u and SPT-N Value for Cohesive Soils - Method 1.

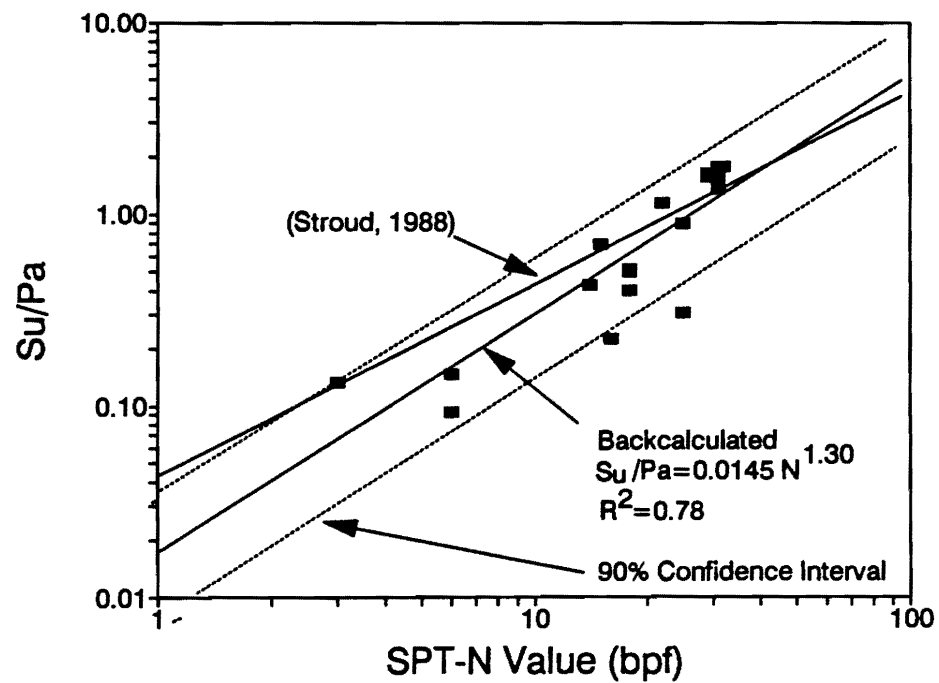


Figure 2.12. Correlation between s_u and SPT-N Value for Cohesive Soils - Method 2.

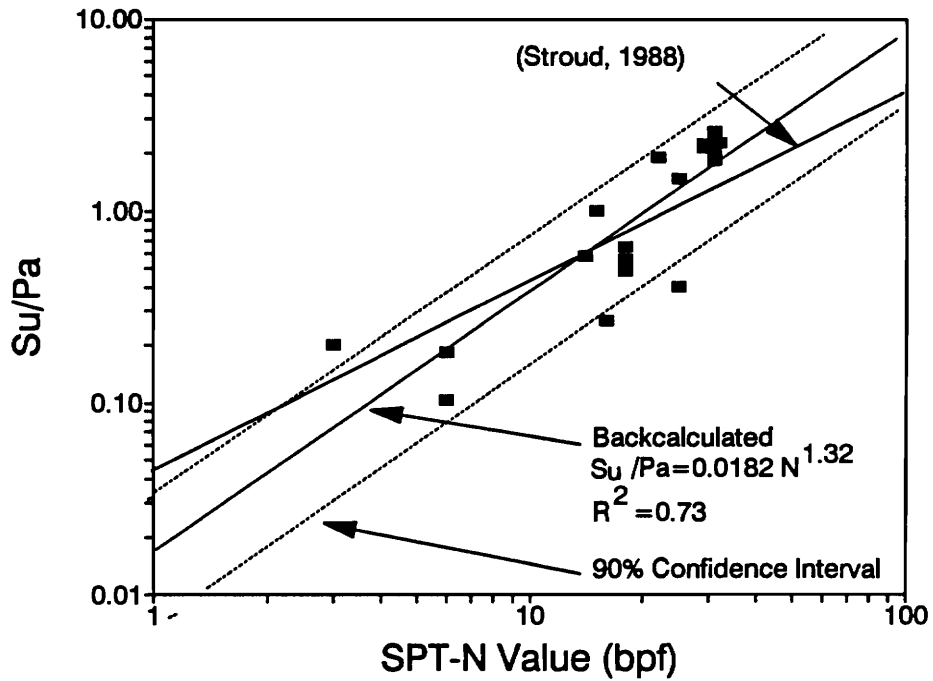


Figure 2.13. Correlation between s_u and SPT-N Value for Cohesive Soils - Method 3.

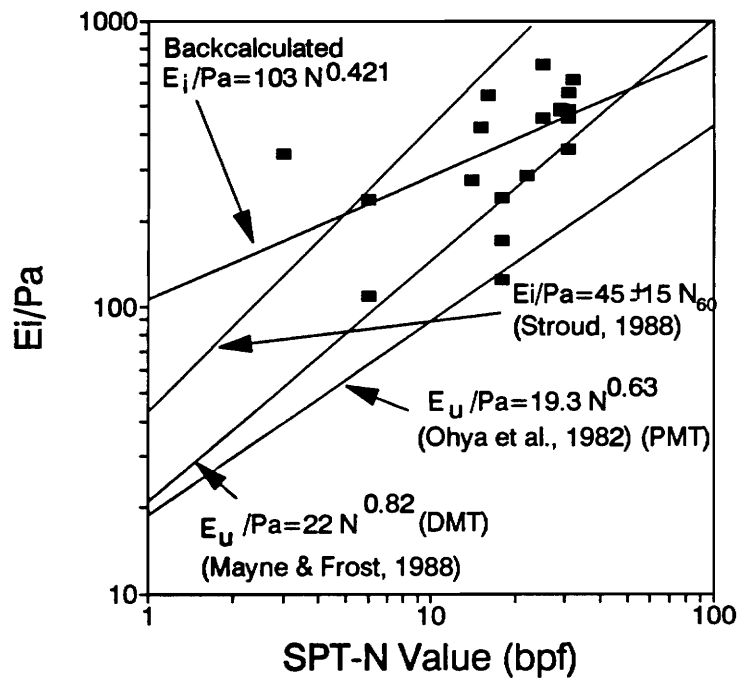


Figure 2.14. Correlation Between Soil Modulus E_i and SPT-N Value for Cohesive Soils

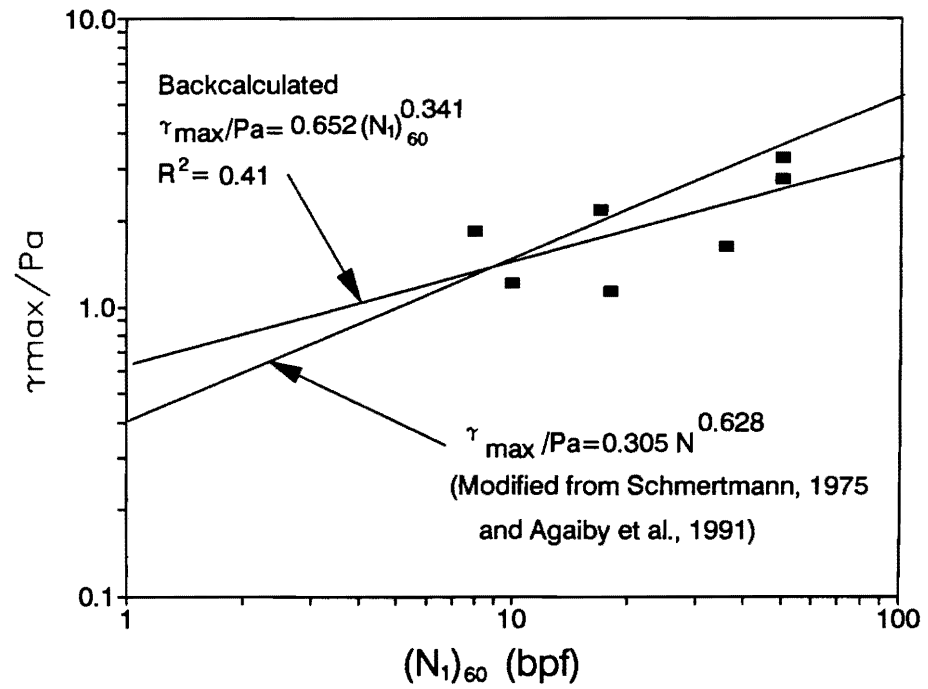


Figure 2.15. Correlation between Sand Strength and SPT-N Value - Method 1.

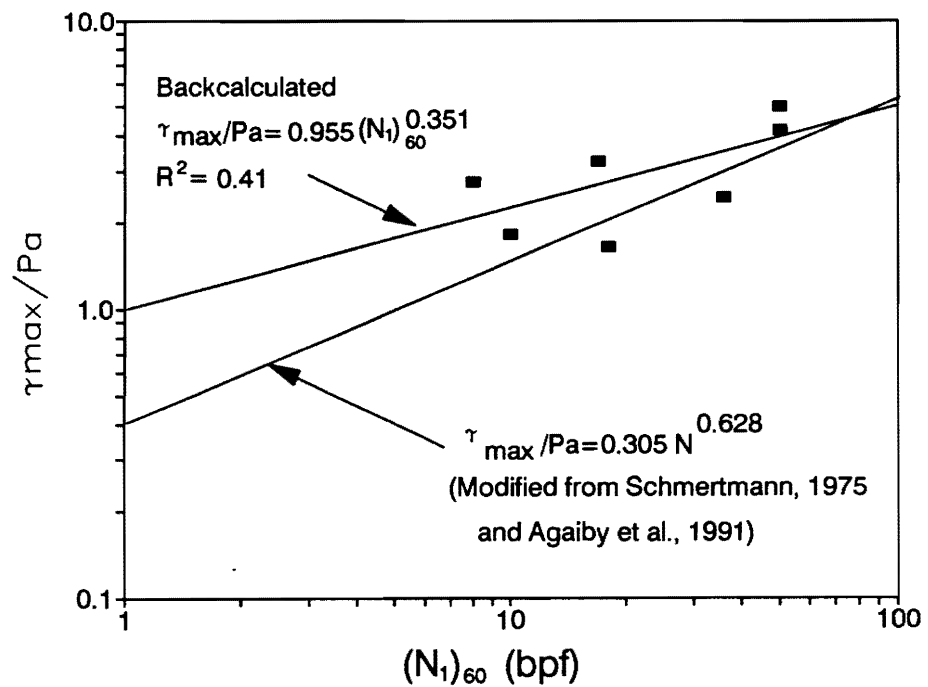


Figure 2.16. Correlation between Sand Strength and SPT-N Value - Method 2.

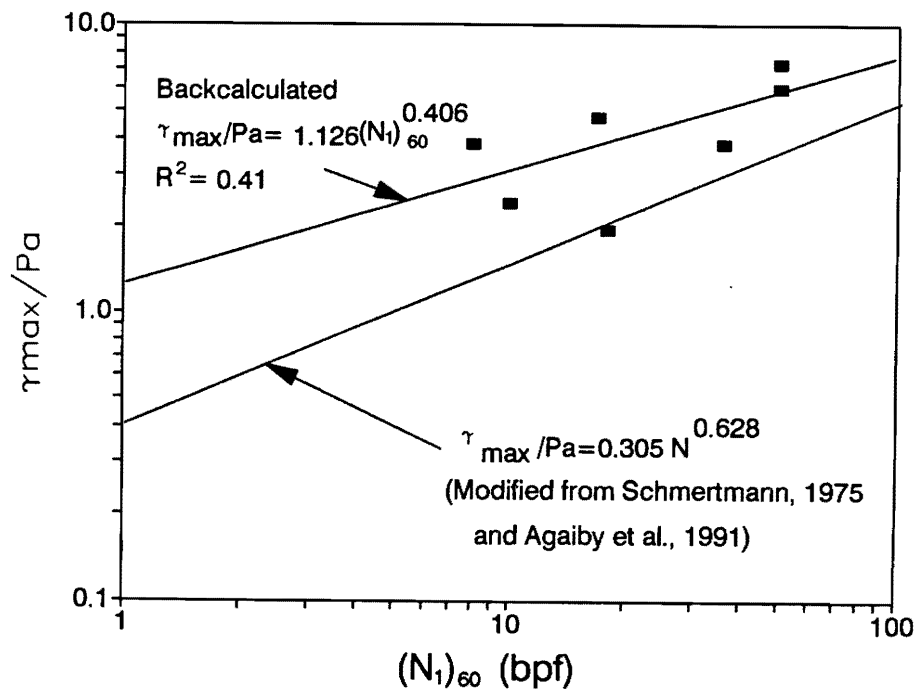


Figure 2.17. Correlation between Sand Strength and SPT-N Value - Method 3.

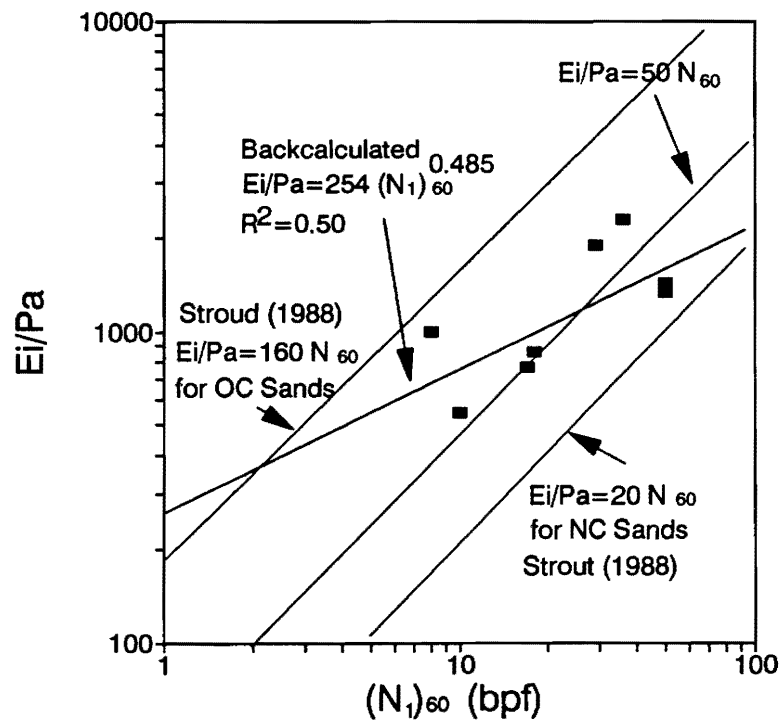


Figure 2.18. Correlation between E_i and SPT-N Value for Sands

It is not surprising that some scatter are observed in the trends since the actual behavior of laterally-loaded drilled shafts is more complicated than fully considered herein. Stress history, shearing mode, rate of loading and anisotropy are some important factors affecting s_u which are not taken into consideration in the SPT results. Stroud (1988) reported correlations between the undrained shear strength and SPT-N value for overconsolidated clays. Stroud (1988) also reported relationships between drained soil modulus (E') backfigured from the performance of shallow foundations and SPT-N value for both fissured overconsolidated clays and cohesionless soils. Several other similar correlations reported by Mayne and Frost (1988), and Ohya et al. (1982) also compare favorably with the derived trends.

Schmertmann (1975) presented an empirical relationship between the drained friction angle under compression mode (ϕ_{tc}') for sands and SPT-N value as a function of effective overburden stress (σ_{vo}'). Consequently, the drained shear strength (τ_{max}) can be expressed in terms of the SPT-N value using equation [2.31], provided that the effective overburden pressure (σ_{vo}') is also considered. The ϕ_{tc}' in equation [2.31] is assumed to be equivalent to $1.12 \phi_{tc}'$. The result can be approximated by:

$$\tau_{max}/P_A = 0.305 N^{0.628} \quad [2.34]$$

In order to compare this relationship with existing correlations, it is reiterated that the relevant shearing mode for laterally-loaded drilled shafts is approximated by the triaxial extension (TE) mode rather than triaxial compression (TC). The modification can be accomplished by utilizing conversion factors adopted from Table 2.8 and Figure 2.10. In addition, the soil modulus used in the hyperbolic model is the corresponding value of initial tangent modulus. This initial tangent modulus is higher than secant values of modulus measured at larger strain levels.

For the preliminary analysis of laterally-loaded rigid drilled shafts, the aforementioned correlations for estimating soil strength and initial modulus from the results of SPT-N values are summarized as follows:

Cohesive Soils:

$$\text{Method 1: } s_u/p_a = 0.0135 N^{1.27} \quad [2.35]$$

$$\text{Method 2: } s_u/p_a = 0.0145 N^{1.30} \quad [2.36]$$

$$\text{Method 3: } s_u/p_a = 0.0182 N^{1.32} \quad [2.37]$$

$$E_i/p_a = 103 N^{0.42} \quad [2.38]$$

Cohesionless Soils:

$$\text{Method 1: } \tau_{\max}/p_a = 0.652 (N_1)_{60}^{0.341} \quad [2.39]$$

$$\text{Method 2: } \tau_{\max}/p_a = 0.955 (N_1)_{60}^{0.351} \quad [2.40]$$

$$\text{Method 3: } \tau_{\max}/p_a = 1.126 (N_1)_{60}^{0.406} \quad [2.41]$$

$$E_i/p_a = 254 (N_1)_{60}^{0.485} \quad [2.42]$$

in which N = measured SPT resistance in clays and $(N_1)_{60}$ = the corrected SPT-N value in sands. As noted previously, the relationships derived from three different approaches are presented.

2.4.2. Prediction of Load-Deflection Curves

For this particular project, it is very possible that SPT-N values might be the only field test data available to the design engineer unless otherwise requested. This section of the report attempts to provide a reasonable prediction for load-deflection curves of various shaft geometries using SPT-N values. Ideally, equations [2.35] to [2.42] can be used to estimate s_u , τ_{\max} and E_i . This is followed by using equations [2.24] and [2.27] to derive the hyperbolic values of lateral capacity (H_u) and stiffness (K_s).

$$H_u = \frac{3 s_u z_r L}{I_{12}} \quad [2.24]$$

$$K_1 = \frac{E_1 L}{I_{12}} \quad [2.27]$$

Finally, equation [2.7] is used with respect to various deflection levels to formulate the load-deflection relationship. This is accomplished by substituting equations [2.24] and [2.27] into equation [2.7].

$$H = \frac{\delta}{\frac{1}{K_1} + \frac{\delta}{H_u}} \quad [2.7]$$

$$H = \frac{L}{\left[\frac{1}{E_1 \delta} + \frac{1}{3 z_r s_u} \right] I_{12}} \quad [2.43]$$

After examining Figures 2.11 to 2.18, modified relationships for sandy and cohesionless soils were adopted to generate the load-deflection curves. In lieu of the backcalculated equations [2.39] to [2.42], the modified relationship of equation [2.34] was selected to calculate τ_{\max} and the expression of $E_t/P_s = 50$ N in Figure 2.18 selected to calculate E_t . Predicted H- δ curves for cohesive and cohesionless soils with a standard LLWAS shaft geometry of 4' ϕ x 20' are shown in Figure 2.19 and 2.20, respectively. These graphs present the moment loading applied at the top of shafts, which is equivalent to a lateral load acting with an eccentricity of 80.8 feet (i.e., $M = H e$). The curves have been developed using the lower bound of the correlation relationships in Equations [2.35] and [2.38] in order to produce conservative predictions.

The FAA Technical Officer has indicated that the LLWAS system allows up to 4 ft of lateral movement without jeopardizing the normal operation of the alarm device. With the geometry and anticipated rigidity of the 150-foot long hollow steel pole, the lateral deflection at the top of drilled shaft should not exceed 0.5 inch to satisfy this requirement. This should provide an adequate criterion for determining the allowable lateral capacity of the LLWAS drilled shafts.

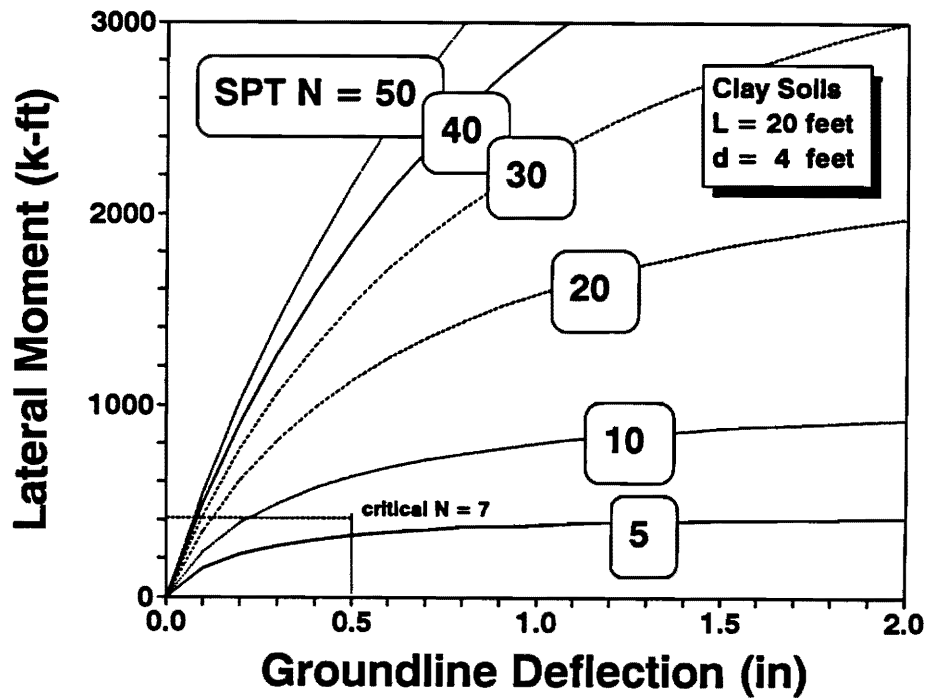


Figure 2.19. Predicted Load-Deflection Curves for Cohesive Soils

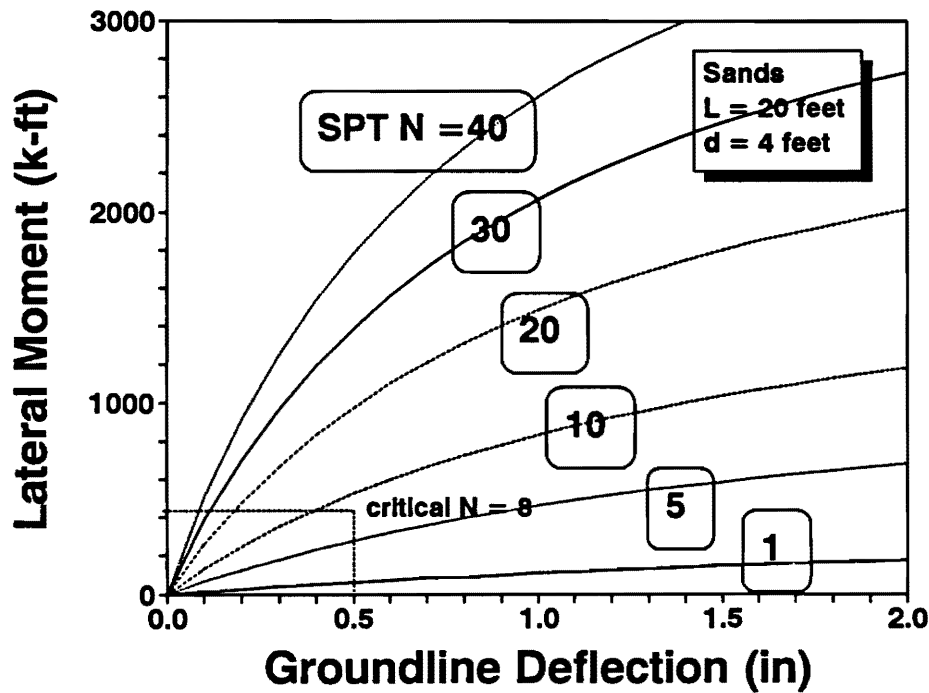


Figure 2.20. Predicted Load-Deflection Curves for Cohesionless Soils

2.5. CONCLUSIONS

A review and analysis of available load test data on rigid drilled shaft performance under lateral and moment loading indicates the following conclusions:

1. A simple hyperbolic model can effectively be used to describe the nonlinear load-deflection behavior of rigid drilled shaft foundations, provided that the profile of soil properties adjacent to the shaft do not vary significantly with depth. Limit equilibrium analysis and elastic continuum theory provide a rational basis for evaluating the lateral behavior of shafts in this perspective.

2. The shear strength (undrained shear strength for cohesive soils and drained friction angle for cohesionless soils) and initial elastic modulus of soils can be backcalculated using the load-deflection curves obtained from actual load tests. Observed differences between the backcalculated parameters and the properties measured by laboratory or field tests are likely due to the several reasons, including:

- a. The true rigidity of the shafts in some cases is not perfect, and only a partial rigid behavior occurs during loading.
- b. Except for PMT and DMT tests, the majority of available laboratory and field tests on soil are performed under compression loading conditions, whereas the relevant mode of directional loading for laterally-loaded drilled shafts is better simulated by an extension mode.
- c. The theoretical derivation used in this methodology simplifies the true three-dimensional and complicated load-deflection behavior.
- d. Testing errors and disturbance of soil incurred in the test programs.

3. The backcalculated parameters and in-situ test parameters were studied using only the standard penetration test (SPT) results since limited data types of other field data

were available. The statistically best-fit correlations have been established, though some of these results may still not be totally satisfactory from a reliability viewpoint. The trends compare favorably with previously developed correlations.

4. Charts have been developed to predict the lateral-load deflection and capacity for the standard LLWAS shaft geometry in terms of the soil type and average SPT-N value. For SPT-N values lower than 7 in clays and SPT-N value lower than 8 in sands, the standard 4' ϕ x 20' drilled shaft does not appear to provide sufficient load-deflection response. In the event that such soft soils are encountered in practice, more sophisticated analyses, such as the computer programs MFAD or LTBASE, are recommended to determine the adequacy of the standard LLWAS foundation. Pending the results of those analyses, it may be necessary to extend the length of the foundation (i.e., $L = 30$ feet), in order to achieve the desired foundation stiffness. Alternatively, an increase in the shaft diameter (d) is also feasible, but likely less practical.

2.6. REFERENCES

Agaiby, S.W., Kulhawy, F.H., and Trautmann, C.H. (1991), "Experimental Study of Drained Lateral and Moment Behavior of Drilled Shafts During Static and Repeated Loading", Report TR-100223, Electric Power Research Institute, Palo Alto, Dec. 1991.

Bierschwale, M.W., Coyle, H.M., and Bartoskewitz, R.E. (1981), "Lateral Load Tests on Drilled Shafts", Drilled Piers and Caissons, ASCE, New York, pp. 98-113.

Broms, B.B. (1964), "Lateral Resistance of Piles in Cohesive Soils", Journal of the Soil Mechanics and Foundations Division, ASCE, Vol. 90, No. SM2, pp. 27-63.

Carter J.P. and Kulhawy, F.H. (1988), "Analysis and Design of Drilled Shaft Foundations Socketed into Rock", Report EL-5918, Electric Power Research Institute, Palo Alto, 188 p.

Hansen, J.B. (1961), "The Ultimate Resistance of Rigid Piles Against Transversal Forces", Bulletin 12, Danish Geotechnical Institute, Copenhagen, pp. 5-9.

Hardin, B.O. and Drnevich, V.P. (1972), "Shear Modulus and Damping in Soils", Journal of the Soil Mechanics and Foundations Division, Vol. 98, SM7, pp. 667-692.

Hirany, A. and Kulhawy, F.H. (1988), "Conduct and Interpretation of Load Tests on Drilled Shaft Foundations", Report EL-5915, Vol. 1, Electric Power Research Institute, Palo Alto, 374 p.

Kondner, R. L. (1963), "Hyperbolic Stress-Strain Response: Cohesive Soils", Journal of Soil Mechanics and Foundations Division, ASCE, Vol. 89, SM1, pp.115-143.

Kulhawy, F.H. and Mayne, P.W. (1990), "Manual on Estimating Soil Properties for Foundation Design", Report EL-6800, Electric Power Research Inst., Palo Alto, 360 p.

Kuhlemeyer, R. L. (1979), "Static and Dynamic Laterally Loaded Floating Piles", Journal of the Geotechnical Engineering Division, ASCE, Vol. 105, GT2, pp. 289-304.

Manoliu, I., Dimitriu, D.V., Radulescu, N., Dobrescu, G. (1985), "Load-Deformation Characteristics of Drilled Piers", Proceedings, 11th International Conference on Soil Mechanics and Foundation Engineering, Vol. 3, San Francisco, pp. 1553-1558.

Mayne, P.W. (1991), "Experimental Study of Undrained Lateral and Moment Behavior of Drilled Shafts during Static and Cyclic Loading", Ph.D. Thesis, Cornell University, School of Civil and Environmental Engineering, Ithaca, NY, January, 448 p.

Mayne, P.W. and Kulhawy, F.H. (1991), "Load-Displacement Behavior of Laterally Loaded Rigid Drilled Shafts in Clay", Proceedings, 4th International Conference on Piling and Deep Foundations, Stresa, Italy, pp. 409-413.

Mayne, P.W., Kulhawy, F.H., and Trautmann, C.H. (1991), "Static and Cyclic Lateral and Moment Behavior of Drilled Shafts in Clays", Report TR-100221, Electric Power Research Institute, Palo Alto, CA.

Mayne, P.W. and Frost, D.D. (1988), "Dilatometer Experience in Washington, D.C., and Vicinity", Transportation Research Record, No. 1169, Washington, D.C., pp. 16-23.

Ohya, S., Imai, T., and Matsubara, M. (1982), "Relationships Between N Value by SPT and LLT Pressuremeter Results", Proceedings, 2nd European Symposium on Penetration Testing, Vol. 1, Amsterdam, pp. 125-130.

Poulos, H.G. and Davis, E.H. (1980), Pile Foundation Analysis and Design, John Wiley and Sons, New York, 397 p.

Poulos, H.G. and Hull, T.S. (1989), "The Role of Analytical Geomechanics in Foundation Engineering", Foundation Engineering: Current Principles and Practices (GSP 22), Vol. 2, ASCE, New York, pp. 1578-1606.

Randolph, M.F. (1981), "The Response of Flexible Piles to Lateral Loadings", Geotechnique, Vol. 31, No. 2, pp. 247-259.

Randolph, M.F. and Houlsby, G.T. (1984), "The Limiting Pressure on a Circular Pile Loaded Laterally in Cohesive Soils", Geotechnique, Vol. 34, No. 4, pp. 613-623.

Reese, L.C. (1958), Discussion of "Soil Modulus for Laterally Loaded Piles", Transactions, ASCE, Vol. 123, pp. 1071-1074.

Schmertmann, J.H. (1975), "Measurement of In-Situ Shear Strength", Proceedings, In-Situ Measurement of Soil Properties, Vol. 2, ASCE, Raleigh, NC, pp. 57-138.

Skempton, A.W. (1986), "SPT Procedures and the Effects in Sands of Overburden Pressure, Relative Density, Particle Size, Aging, and Overconsolidation", Geotechnique, 2Vol. 36, No. 3, pp. 425-447.

Stevens, J.B. and Audibert, J.M.E. (1979), "Re-examination of p-y Curve Formulations", Proceedings, 11th Offshore Technology Conference, Vol. 1, Houston, pp. 397-403.

Stroud, M. A. (1988), "The Standard Penetration Test - Its Application and Interpretation, Part 2", Penetration Testing in UK, Thomas Telford, London, pp. 29-49.

SECTION 3

COMPUTER MODELLING OF Laterally-Loaded Drilled Shafts

For the analysis of drilled shafts which are subjected to lateral and moment loading, four commercial computer programs: COM624 (Reese, 1977), LTBASE (Borden and Gabr, 1987), PIGLET (Randolph, 1989), and MFAD (Davidson, et al., 1990) have been utilized to evaluate the LLWAS tower foundations. Both MFAD and LTBASE programs have been specifically developed for rigid drilled shafts. Therefore, the two methods have been employed to examine available actual load test data in several case studies to check their validity. The results of in-situ pressuremeter testing (PMT) and/or dilatometer testing (DMT) are used to determine the soil shear strength and soil modulus.

3.1. ANALYTICAL METHODOLOGIES FOR LATERAL PILE PROBLEM

A variety of methods have been developed for analyzing laterally-loaded pile behavior. Pile foundations include driven steel, timber, and concrete members, as well as augered and bored piles, such as the drilled shaft. Basically, the analytical approaches can be divided into linear and nonlinear analysis. The linear analysis methods fall into three main categories (Poulos, 1982). The simplest one is the subgrade reaction method, in which the soil is represented by a set of closely spaced, discrete, and independent linear springs. The second method uses the boundary element analysis to model the soil as an elastic continuum. The third method utilizes the finite element technique. In the finite element analysis, Desai and Appel (1976) used three dimensional elements for both pile and soil, while Randolph (1981) used a Fourier series to express the displacement field.

There are essentially four approaches for the nonlinear method. The first one is to model the soil as a set of discrete and independent nonlinear springs, known as the nonlinear subgrade reaction or p-y method. The second method is the modified boundary element analysis, in which an elastic-plastic soil model is incorporated. The third method is the nonlinear finite element analysis, in which a semi-empirical formulation is developed to account for the soil nonlinearity and a pseudo-visco-plastic finite element algorithm is

used. Finally, the fourth nonlinear method used to model the soil behavior is semi-empirical and utilizes a hyperbola to represent the stress-strain behavior of soil, and the degradation of soil modulus with strain. This method has been discussed in Section 2.

The linear methods are based either upon the concept of subgrade reaction theory or purely elastic continuum considerations. It is obvious that the linear methods do not take into account the nonlinearity of the soil response, and therefore, lead to unconservative predictions in variance with actual behavior (Ismael, 1978). In the application of linear methods, the value of soil modulus must be adjusted for different stress levels in order to obtain a more representative prediction.

These current state-of-the-art analysis methods used in laterally loaded pile analysis are summarized in Table 3.1. More detailed discussions can be found in Poulos (1982) and Poulos and Hull (1989). Four different computer programs have been developed according to these different approaches and these will be discussed in more detail in the following section. A detailed parametric study can be found in Fang (1991).

Table 3.1. Different Approaches for the Analysis of Laterally-Loaded Piles

	Subgrade Reaction	Boundary Element	Finite Element	Semi-Empirical
Linear Analysis	soil is modeled as linear springs	soil is modeled as an elastic continuum	either using 3-D soil and pile elements or expressing the displacement field in terms of a Fourier Series	
Nonlinear Analysis	soil is modeled as nonlinear springs	soil is modeled as an elastic-plastic material	a semi-analytic formulation is used and a pseudo-visco-plastic finite element algorithm is employed	hyperbolic model

3.2. COMPARISON OF PROGRAMS: COM624, LTBASE, PIGLET, and MFAD

For laterally-loaded pile analysis in soil profiles, several computer programs have been developed according to the different theoretical approaches. Four commercially available computer programs have been reviewed for this study. These include: COM624,

PIGLET, LTBASE, and MFAD. A fifth computer method (DEFPIG) is discussed and utilized later in Section 4 of this report for application with rock-socketed shafts.

The basic theories and mathematical techniques for each of the four computer programs are summarized in Table 3.2. Figure 3.1 illustrates the different theory models for the four computer programs.

Table 3.2. Theoretical and Mathematical Basis for Each of the Four Computer Programs

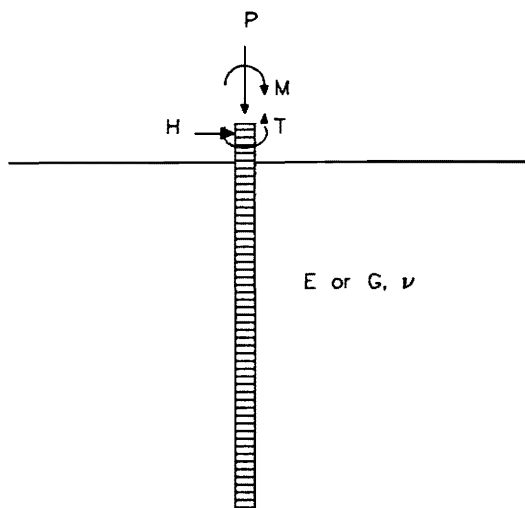
PROGRAM	SOLUTION FOR	THEORY	NUMERICAL
COM624	single pile (flexible)	nonlinear subgrade reaction	F.D.M.
PIGLET	pile group (flexible)	linear elastic theory	F.E.M.
MFAD	single pile (rigid)	nonlinear subgrade reaction plus empirical four-spring model	F.E.M.
LTBASE	single pile (rigid)	nonlinear subgrade reaction	F.D.M.

Note: F.D.M. = Finite Difference Method; F.E.M. = Finite Element Method

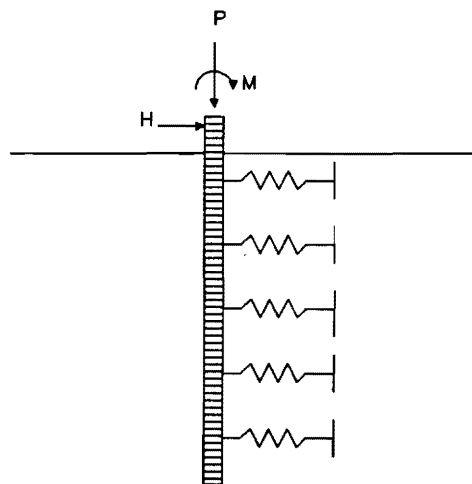
The following sections give a brief summary concerning the basis of analysis for each of the four programs.

3.2.1 COM624

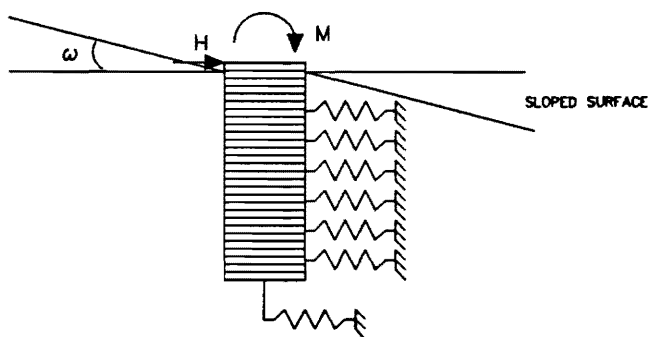
COM624, developed by Reese, Cooley, and Radhakrishnan (1984), has been widely used in pile analysis. The method which is utilized in the laterally-loaded pile analysis is based on the theory of subgrade reaction. The fourth-order governing differential



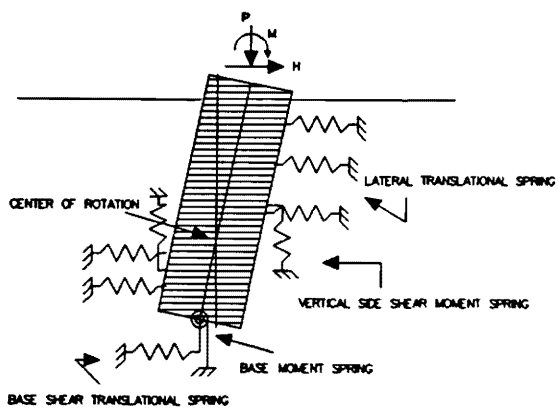
(a) PIGLET



(b) COM624



(c) LTBASE



(d) MFAD

Figure 3.1. Theoretical Basis for Soil Stiffness of the Computer Programs

equation is solved using the finite difference technique. COM624 has been developed for long, flexible piles, whose length to diameter (L/d) ratios are typically greater than about 20.

3.2.2. LTBASE

LTBASE, LaTeral pier analysis including Base And Slope Effect, has been developed by Borden and Gabr (1987). This program also utilizes the finite difference technique to solve the non-linear simulation model formulated using the subgrade reaction method. A procedure to account for the influence of the mobilized resistance at the base of the rigid drilled shafts on the predicted lateral response is incorporated in the program. Shafts which have been constructed on sloping hillside also can be analyzed.

3.2.3. PIGLET

PIGLET is a computer program developed by Randolph (1989) for the analysis and design of pile groups under general loading conditions. It is presented in terms of a number of approximate and yet compact solutions for the response of single piles or piers subjected to different loading modes, i.e. axial, torsional, and lateral loadings. It is also appropriately modified to account for interaction effects between piles in the pile group. The soil is modelled as an elastic continuum with a stiffness which either varies linearly with depth or is constant with depth. To predict the response of pile group under lateral loading, Randolph fitted the results of a parametric study using the finite element method to a set of simple algebraic expressions.

3.2.4. MFAD

MFAD (Moment Foundation Analysis and Design; Davidson, et al. 1990) is a revision of the earlier computer program "PADLL" (Pier Analysis and Design for Lateral Loads; Davidson, et al. 1982) prepared by GAI Consultants Inc. for the Electric Power Research Institute.

MFAD utilizes a semi-empirical, nonlinear four-spring load-deflection and ultimate capacity model developed in that project. The four-spring nonlinear subgrade reaction

model characterizes the soil-pier interaction through the use of four discrete sets of springs, as shown in Figure 3.1 (d) (Gonzalez and DiGioia, 1990). The four springs sets include: (1) lateral translational springs, (2) vertical side shear springs, (3) a base translational spring, and (4) a base moment spring. A theoretical linear four spring model was initially developed for an idealized problem of an elastic pier embedded in a linear elastic half space using dimensional analysis coupled with 3-D finite element parameter studies.

MFAD incorporates an ultimate lateral capacity model which is similar to Ivey's theory (1968) but uses the ultimate lateral pressure formulation developed by Hansen (1961) which is based on earth pressure theory. Thereafter, a nonlinear four-spring model which incorporates the above linear model and ultimate capacity model, as well as a variation of Reese and Welch's (1975) p-y curves, is modified to give a best fit to 14 prototype drilled piers field test data. MFAD can deal with rigid and nearly rigid piers with embedment length to diameter ratios (L/d) between two and ten ($2 \leq L/d \leq 10$). Analysis options include a nonlinear load-deflection prediction and an ultimate capacity analysis. It also has the ability to design a pier to satisfy one or more performance criteria.

3.3. CAPABILITIES AND LIMITATIONS

Since these programs are developed based upon different theories and mathematical techniques, it is important to know their abilities and potential limitations. Program COM624 has been originally designed for relatively long and flexible piles; program LTBASE was developed for rigid piers in level or sloping ground; MFAD is used for rigid piers; PIGLET is a linear analysis for single pile and pile group analysis. Program PIGLET is based upon elastic theory, while the other three are all based upon nonlinear subgrade reaction theory. MFAD estimates both groundline deflections and rotations, and has also been modified to fit field load test data on rigid shafts.

Different parameters are needed as input for the four computer programs. Generally, three categories of parameters need to be specified: (1) pier properties and geometry, (2)

Table 3.3. Capabilities and Limitations of the Computer Programs

	Feature	COM624	LTBASE	MFAD	PIGLET
soil	nonlinearity	nonlinear	nonlinear	nonlinear	linear elastic
	layers	yes	yes	Yes	idealized as $G = G_0 + mz$
	sloped surface	no	yes	no	no
pile	number	single	single	single	group
	rigidity	flexible	rigid	rigid; nearly rigid	flexible
	geometry	constant diameter along a segment	average diameter at midheight of a segment	constant diameter along a segment	all of the same length (idealized as cylindrical)
	flexural stiffness	input E_p , I_p	input $E_p I_p$	either calculated by the program or input by the user	input E_p
	head fixity	free or fixed head; lateral load & slope or lateral load & rotational restraint can be specified	free or fixed head	free head	pinned or fixed to pile cap (rigid cap, free to rotate)
	rake	no	no	no	yes
loading	vertical	yes	no	yes	yes
	horizontal	one direction	one direction	one direction	two perpendicular directions
	torsional	no	no	no	yes
	moment	yes	yes	yes	yes
	cyclic	yes	no	no	no
Design Option		no	no	yes	no
output	deflection	yes	yes	yes	yes
	moment distribution	yes	yes	yes	yes
	rotation	no	no	yes	no
	shear stress	yes	yes	yes	no

soil properties, and (3) applied loading conditions. The capabilities and limitations of the four programs related to these properties are summarized in Table 3.3. These include such variables as head fixity, pier flexibility, and nonlinearity.

The specific soil parameters needed for the four computers programs are listed in Table 3.4. Such parameters include undrained shear strength (s_u), soil modulus (E_s), shear modulus (G), unit weight (γ), effective stress friction angle (ϕ'), Poisson's ratio (ν), coefficient of subgrade reaction (k_h), and strain at 50% of ultimate strength ϵ_{50} .

Table 3.4. Input Soil Parameters for the Four Computer Programs

METHOD	γ	ϕ'	s_u	E_s	G	ν	k_h	ϵ_{50}
COM624	X	X	X				X	X
LTBASE	X	X	X				X	X
MFAD	X	X	X	X				
PIGLET					X *	X		

*Note: The value of shear modulus at the surface and the rate of increase of modulus with depth are specified.

The coefficient of subgrade reaction (k_h) is unfortunately not a basic soil parameter, but depends upon the soil stiffness and specific foundation geometry (Vesic, 1961; Pyke and Beikae, 1984). Consequently, guidance and judgement is required in the proper selection of k_h in analysis. Typical values of k_h for sand are given in Table 3.5 (Reese, et al., 1984). Reported values range from 20 to 225 pci. Values of k_h for clay are also given in Table 3.5 (Reese, et al., 1984), and reportedly range from 30 to 3000 pci. In the approach by DiGioia, et al. (1981), the following equation was developed for estimating k_h from shaft geometry (L , d) and soil modulus (E_s) in both clays and sands:

$$k_h = 4.6 \frac{E_s}{d} \left(\frac{L}{d} \right)^{-0.4} \quad [3.1]$$

The strain parameter (ϵ_{50}) used in subgrade reaction methods also requires discussion. The parameter is particularly important in clay soils, while not critical for sands. The

Table 3.5. Representative Values of k_h for Different Soils
(Adapted after Reese, et al., 1984)

Soil Type	Consistency	k_h (pci)	
		Above the Water Table	Below the Water Table
Sand	Loose	25	20
	Medium	90	60
	Dense	225	125
Clay	Very Soft	30	
	Soft	100	
	Medium to Stiff	300	
	Very Stiff to Hard	1000	
	Very Hard	3000	

recommended procedure is that the value of ϵ_{50} be obtained from triaxial tests on representative soil samples. When this is not feasible, suggested typical values of ϵ_{50} as a function of s_u for clays are shown in Table 3.6.

3.4. COMPARISONS OF PREDICTIONS FROM COMPUTER PROGRAMS

In order to examine the ability of the four programs to predict the lateral response of a rigid pier to lateral and moment loading, two hypothetical cases have been investigated to compare the load-deflection predictions. The pier geometry of the standard LLWAS foundation ($d = 4$ ft, $L = 20$ ft) is used in both cases. No eccentricity of loading was applied in these comparative studies. The scenario in case 1 consists of a laterally-loaded shaft in a uniform deposit of clay and subjected to an undrained loading condition. The

Table 3.6. Representative Values of ϵ_{50} for Clay Soils
(Source: Reese, et al., 1984)

Undrained Shear Strength s_u (ksf)	ϵ_{50} (%)
0.25 - 0.5	2
0.5 - 1.0	1
1.0 - 2.0	0.7
2.0 - 4.0	0.5
4.0 - 8.0	0.4

soil conditions in case 2 consist of uniform sand and represents a drained lateral loading condition. For MFAD and PIGLET, the soil modulus (E_s) is input directly into the programs. For the COM624 and LTBASE programs, Equation [3.1] has been used to convert E_s to an equivalent k_h for both cases.

3.4.1. Case 1 - Undrained Lateral Loading Condition

The properties of the idealized homogeneous clay layer and the drilled pier properties are given in Figure 3.2. The soil modulus to strength ratio is $E_s/s_u = 200$ and slenderness ratio of the drilled pier is $L/d = 5$.

Figure 3.3 presents the results of the predicted load-deflection curves from the four computer programs. It can be seen that the results from PIGLET (based on linear elastic theory) and MFAD (based on nonlinear, empirical method) are very consistent for low loading levels ($H < 100$ kips in this case), while COM624 and LTBASE tend to give significantly larger values of lateral deflection of a rigid pier at comparable loads. It is noted that COM624 presents a stiffer response in the load-deflection curve compared to LTBASE.

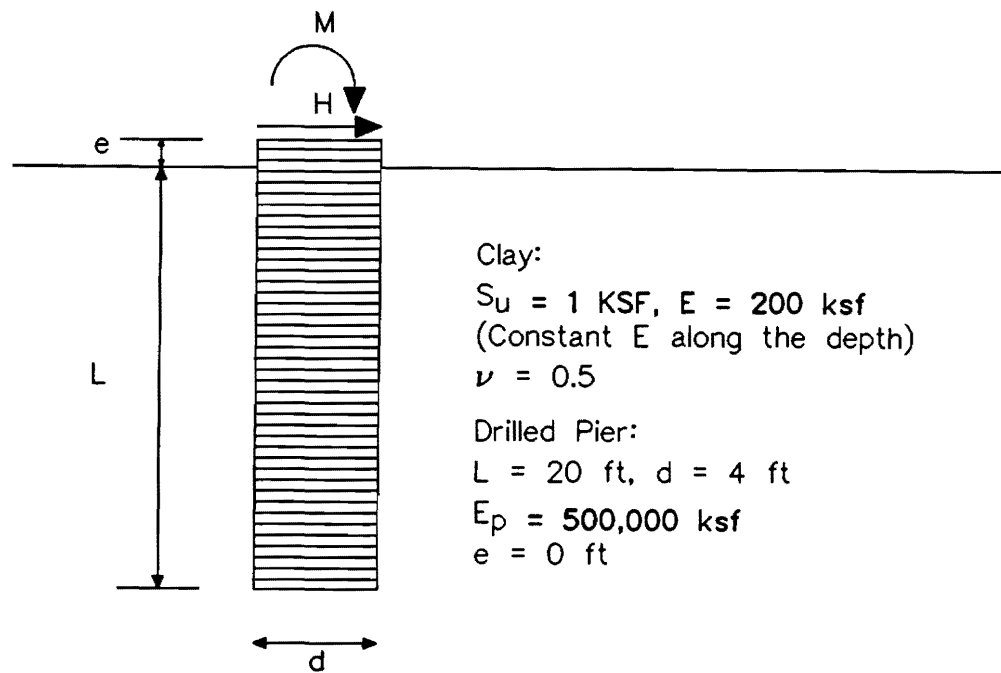


Figure 3.2. Shaft Geometry and Clay Properties for Case 1

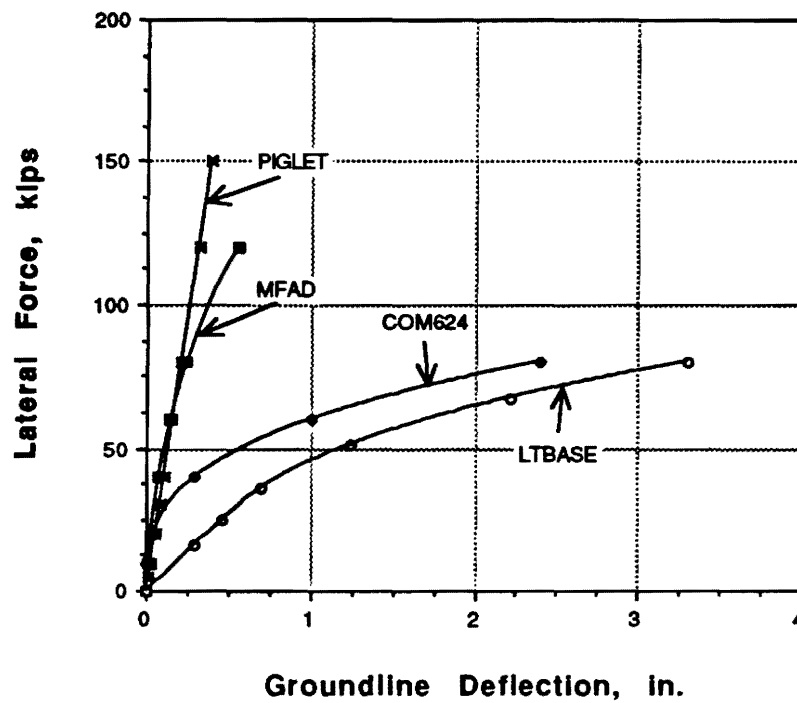


Figure 3.3. Results of Case 1 Analyses for Pier in Clay

3.4.2. Case 2 - Drained Lateral Loading Condition

For the example of drained load-deflection behavior of shafts, the properties of the idealized homogeneous sand layer, shaft geometry, and the shaft material properties are given in Figure 3.4. The soil modulus is assumed to increase linearly with depth, analogous to that for a Gibson-type soil (Poulos and Hull, 1989). This is also the typical assumption for analyses using the subgrade reaction model (Reese, et al. 1984).

The results of the predicted load-deflection curves from the four computer programs are presented in Figure 3.5. It is observed that MFAD and LTBASE yield similar results over the entire loading range. For very low loading level ($H < 50$ kips in this case), the results of PIGLET and MFAD are consistent. The program COM624 tends to give larger lateral deflections than the other three methods.

3.4.3. Discussion of Results

These parametric studies indicate that the nonlinear stress-strain characteristics of soil becomes more important as the applied load level increases. From the above results of case 1 and case 2, and since MFAD has been calibrated for rigid piers, it is reasonably regarded as an appropriate tool for predicting lateral response of drilled piers. LTBASE has also been designed for analyzing the behavior of rigid drilled piers. For the sand of case 2, it gives consistent result with MFAD; however, it gives much larger deflections for the clay of case 1.

Todate, LTBASE has not been calibrated as extensively as MFAD. Consequently, the latter might be considered to be more appropriate since EPRI has verified its use on a variety of projects throughout the U.S. The LTBASE is based on similar theoretical arguments, however, and should prove to provide relatively similar predictions. Both methods are therefore considered herein for possible use by FAA in the design and analysis of LLWAS tower foundations.

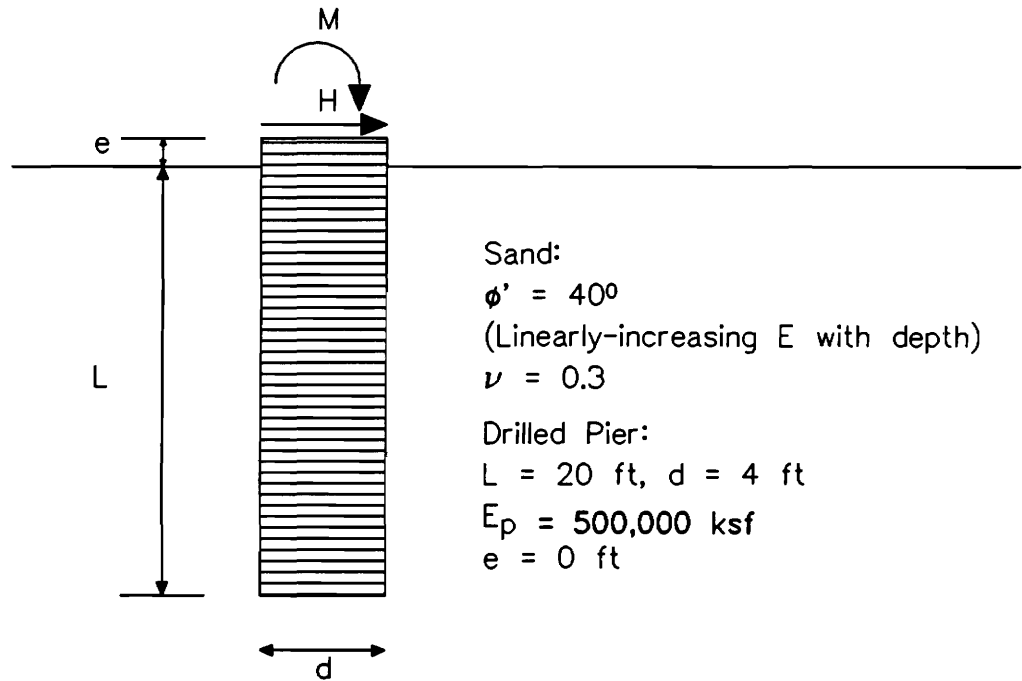


Figure 3.4. Shaft Geometry and Sand Properties for Case 2

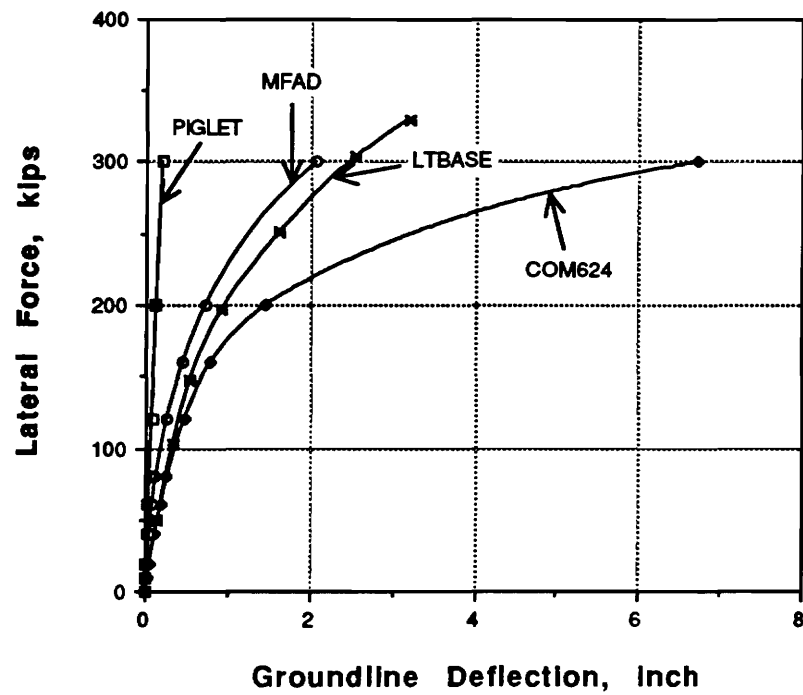


Figure 3.5. Results of Case 2 Analyses for Pier in Sand

3.5. CASE STUDIES

The predicted lateral deflections using the MFAD and LTBASE programs have been compared to the results of five lateral load tests reported in the open literatures. These case studies include: Texas A&M University campus site (Kasch, et al., 1977; Briaud, Smith, and Meyer, 1984), Barnhart Island site (Huang, et al., 1989), Delta site (Briaud, Pacal, and Shively, 1984), Alamo site (Briaud, Pacal, and Shively, 1984), and North Carolina Highway site (Gabr and Borden, 1988). Table 3.7 is a summary of the soil types, the pier geometries, and the soil test types performed for these five sites. In the first four cases, PMT was available for determinations of soil properties in-situ. For the Barnhart Island site and the North Carolina Highway site, DMT was available for determinations of soil properties in-situ. For convenience, the predicted methods are called MFAD-PMT approach, LTBASE-PMT approach, MFAD-DMT approach, and LTBASE-DMT approach. The first term denotes the computer program used, and the second term indicates the method in which the relevant soil parameters have been determined.

3.5.1. Texas A&M University Campus Site

Lateral pile load tests have been conducted on cast in-situ concrete piles at the campus of Texas A&M University in College Park, Texas (Kasch, et al., 1977; Briaud, Smith, and Meyer, 1984). The depth of the water table is between 14.8 and 18.0 feet depth. The drilled shaft is a cast in-situ concrete pile whose diameter = 3 ft, length = 20 ft, ($L/d = 6.6$), $e = 2.5$ ft and $EI = 1,046,393$ k-ft². The soils at this site consist of a firm to stiff clay in the upper 5 ft, and thereafter, stiff to very stiff clay within the depths of interest. The soil has been preconsolidated by desiccation above the water table. The average soil properties are given as follows: liquid limit = 50%, plastic limit = 20%, natural water content = 25%, and total unit weight = 128 pcf. Unconfined compression test values and miniature vane test values were averaged to provide the shear strength profile as shown in Figure 3.6. Pressuremeter test data are reported by Briaud, Smith, and Meyer (1984). The net limit pressure P_L^* and the pressuremeter modulus E_m are also shown in Figure 3.6. Note that $P_L^* = P_L - P_o$, where P_L is the limit pressure and P_o is the total horizontal earth pressure ($P_o = \sigma_{ho}$).

Table 3.7. Summary of the Case Studies and Load Test Data Reviewed

Site	Soil Type	e ft	L ft	d ft	L/d	Test Type	Reference
Texas A&M University Campus Site	stiff clay	2.5	20	3.0	6.6	UC MV PMT	Briaud, Smith, and Meyer, 1984
Barnhart Island Site	stiff clay	0	5	1	5	CPTU FV PMT DMT	Huang, et al., 1989
Delta Site	silty clay	0	10 15	2.2	4.6 7	CPT PMT	Briaud, Pacal, and Shively, 1984
Alamo Site	silty to sandy clay	0	10 15	2.1	4.7 7	CPT PMT	Briaud, Pacal, and Shively, 1984
North Carolina Highway Site	sand	30	7	2.5	2.8	DMT CPT	Gabr and Borden, 1988

Notes:

1. UC = unconfined compression test
2. MV = miniature field vane test
3. FV = field vane test
4. CPT = cone penetration test
5. CPTU = piezocone test
6. PMT = pressuremeter test
7. DMT = dilatometer test

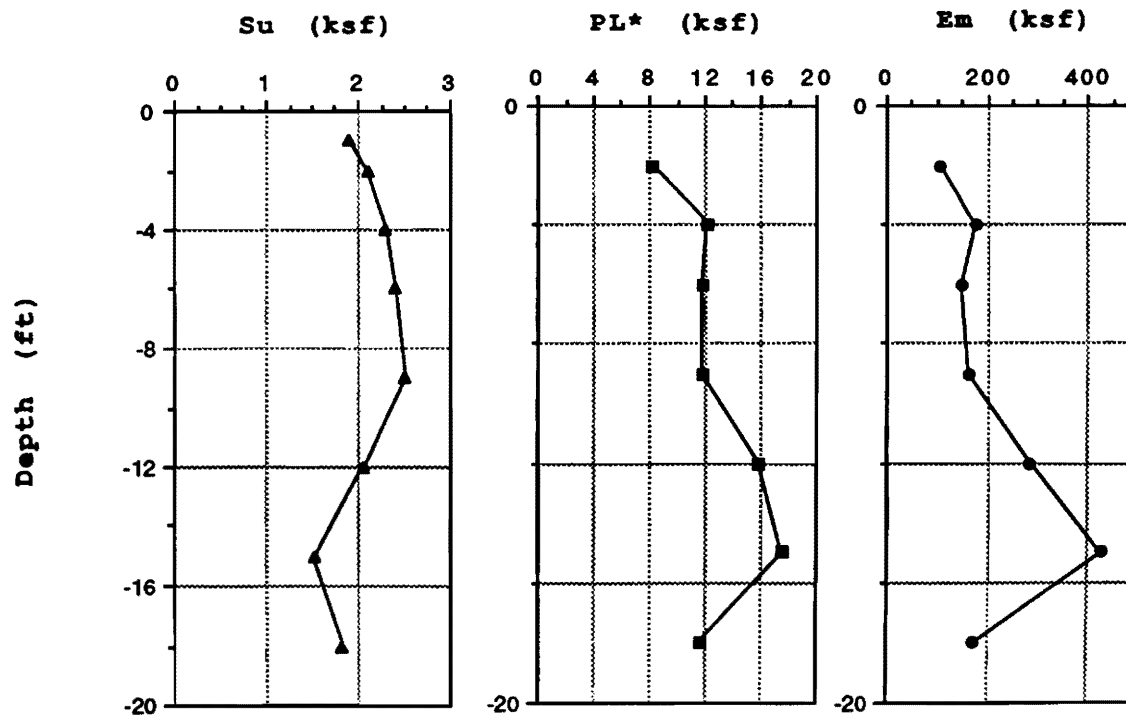


Figure 3.6. Results of In-Situ Testing at Texas A&M Campus Site.
(Source: Briaud, Smith, and Meyer, 1984)

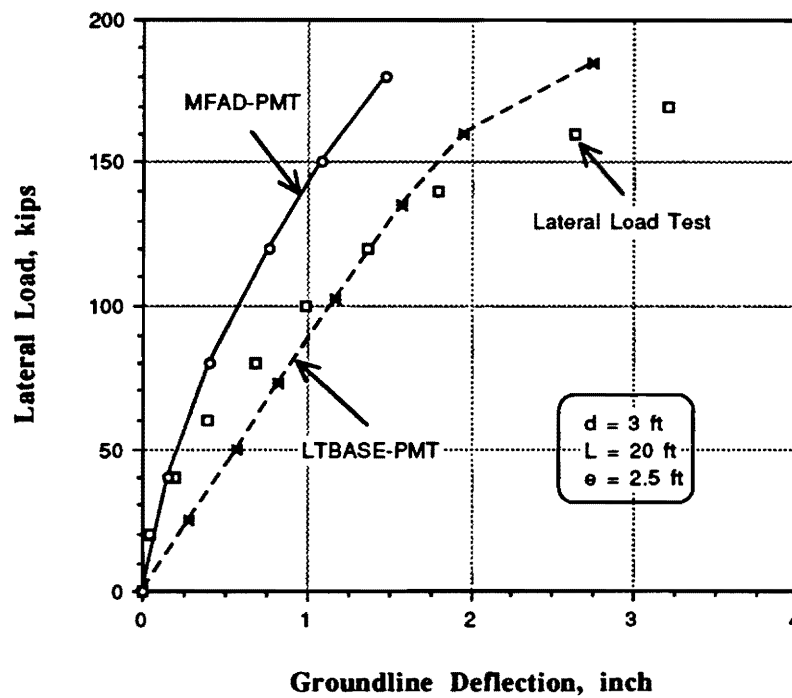


Figure 3.7. Measured and Predicted Deflections for Texas A&M Site

Table 3.8. Summary of the Soil Parameters from In-Situ PMT at the Four Sites

Depth ft	Em ksf	G ksf	PL-P0 ksf	Su ksf	Ir=G/Su	kh # pci	
Texas A&M Campus Site							
6.6	104	35	8.2	2.2	16	43	
13.1	176	59	12.2	3.1	19	73	
19.7	148	49	11.8	3.1	16	61	
29.5	162	54	11.8	3.0	18	67	
39.4	284	95	15.8	3.7	25	118	
49.2	426	142	17.6	3.8	37	177	
59.1	174	58	11.6	2.9	20	72	
Barnhart Island Site ##							
3.1	108	36	5.6	1.3	28	151	
4.0	45	15	9.7	4.3	4	63	
4.9	56	19	8.7	3.1	6	78	
5.9	62	21	10.0	3.7	6	87	
6.9	54	18	7.4	2.5	7	76	
7.9	102	34	5.5	1.3	26	143	
8.9	69	23	5.3	1.4	16	96	
9.8	71	24	6.3	1.7	14	99	
Delta Site						L=10 ft	L=15 ft
2.0	188	63	10.4	2.5	25	125	106
5.0	334	111	12.5	2.6	43	222	189
8.0	98	33	10.4	3.1	11	65	55
13.0	564	188	20.9	4.4	43	375	319
Alamo Site						L=10 ft	L=15 ft
2.0	460	153	39.7	10.9	14	310	264
5.0	2025	675	66.8	13.6	50	1365	1161
8.5	1460	487	94.0	23.2	21	984	837
13.0	1525	508	131.6	36.1	14	1028	874

kh is estimated from [3.1]

P0 is approximately equal to σ'_{h0} , which is estimated from DMT results

A summary of the calculated soil parameters from the PMT data is given in Table 3.8. Figure 3.7 presents the predicted load-deflection curve from the MFAD-PMT approach. The predicted response slightly underestimates the measured deflections. The LTBASE-PMT approach provides a better prediction in this case, as evident in Figure 3.7.

3.5.2 Barnhart Island Site

This test site is located on Barnhart Island, north of the village of Massena, New York (Huang, et al., 1989). Various in-situ tests have been performed at this site in order to predict the lateral response of small-diameter drilled shafts in desiccated clays. These tests include: piezocone (CPTU), flat dilatometer (DMT), field vane (FV), and prebored pressuremeter (PMT). Field and laboratory tests indicate that the upper 6 to 9 ft consists of highly overconsolidated and often fissured clays. The marine clays beneath this desiccated crust are softer, slightly overconsolidated, and often sensitive. The pressuremeter test results are shown in Figure 3.8. The diameter and the length of the drilled shaft are 1 ft and 10 feet ($L/d = 10$), respectively.

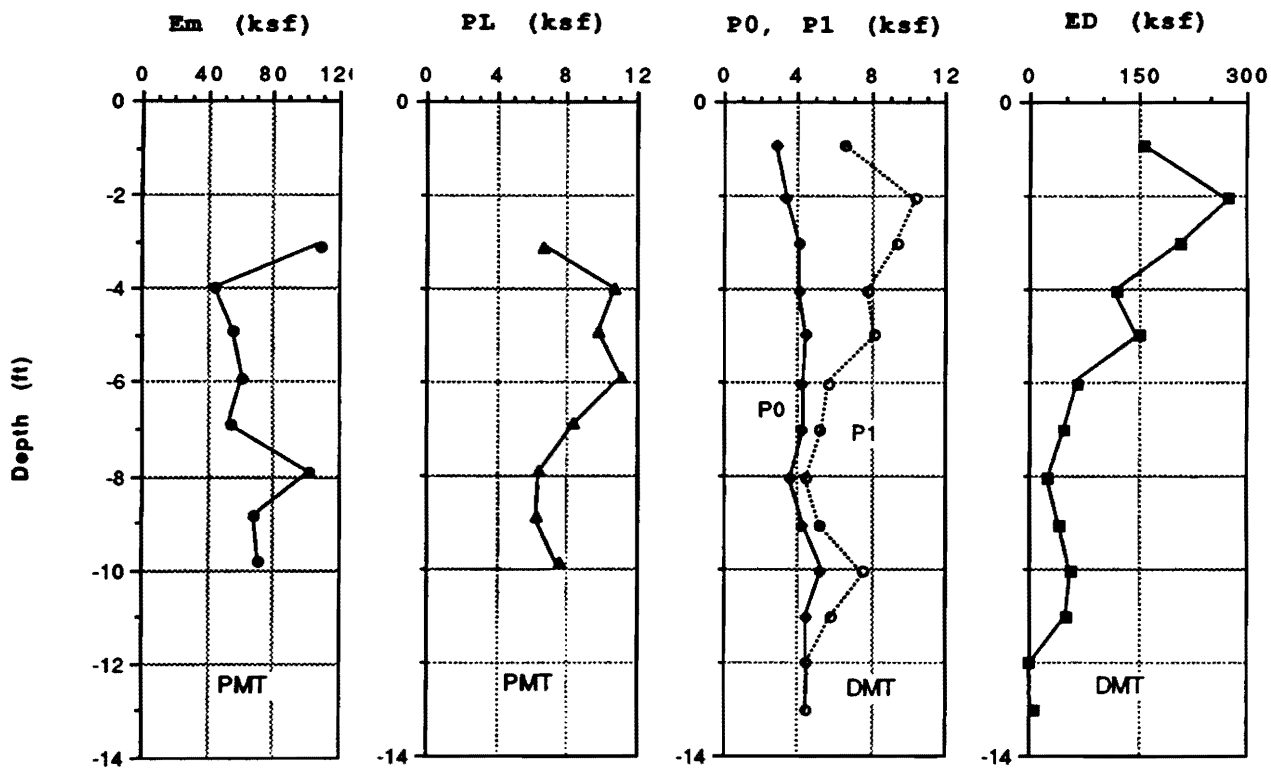


Figure 3.8. Summary of In-Situ PMT and DMT Results at Barnhart Site, Massena, NY.

(Source: Huang, et al., 1989)

The summary of the calculated soil parameters from the PMT at Massena, NY can be found in Table 3.8. Since the net limit pressure was not available, an estimation of the total horizontal stress (P_0) was obtained from the DMT data, also shown in Figure 3.8. Table 3.9 summarizes the soil parameters calculated from in-situ DMT at the site.

Figure 3.9 shows that both the MFAD-PMT and MFAD-DMT approaches underpredict the lateral load-deflection behavior of the drilled shaft at Massena. For the LTBASE program, the PMT data yield reasonable results, while the DMT data tends to overestimate deflections considerably. Also shown in the figure is the prediction using the simple hyperbolic model described in Section 2. In this case, the soil parameters determined from the DMT (Table 3.9) were utilized in the prediction. For this example, the hyperbolic model gave the best overall fit.

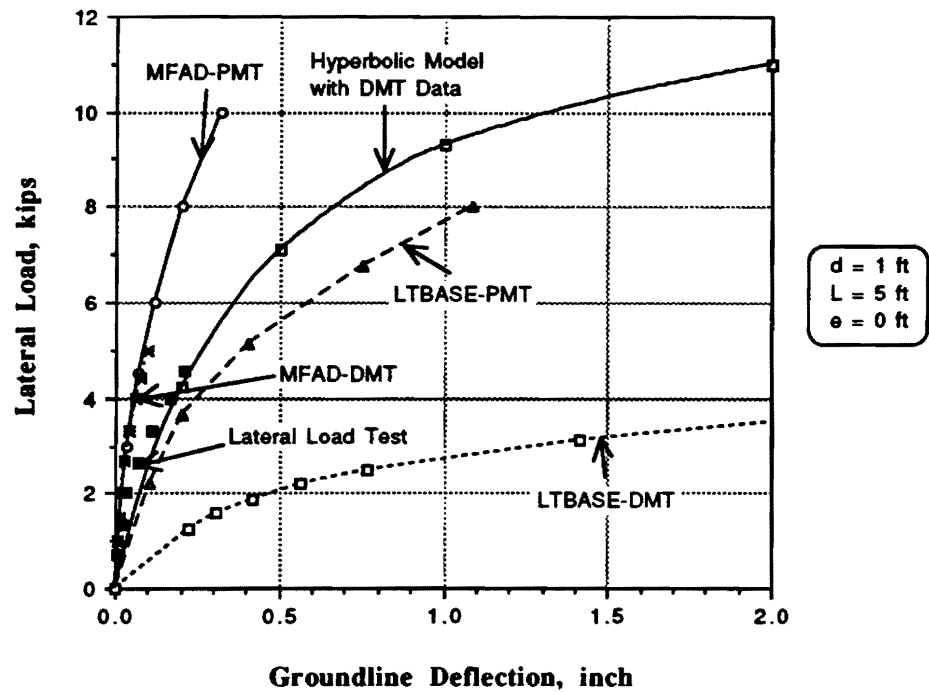


Figure 3.9. Measured and Predicted Response for Barnhart Island Site, Massena, NY.

**Table 3.9. Summary of Soil Parameters from In-Situ DMT at Barnhart
Island Site, Massena, New York (Huang, et al., 1989)**

Depth ft	PQ ksf	u_0 ksf	σ_{v0}' ksf	KD	S_u/σ_{v0}'	S_u ksf	ED ksf	r	kh # pci
0.95	2.84	0.00	0.10	27.18	5.74	0.60	159	88	222
2.07	3.38	0.05	0.18	18.88	3.64	0.64	276	143	386
3.02	4.05	0.11	0.22	17.78	3.38	0.75	209	93	292
4.04	4.03	0.17	0.27	14.27	2.57	0.69	119	57	166
4.99	4.41	0.23	0.32	13.24	2.34	0.74	150	68	210
6.04	4.26	0.30	0.37	10.84	1.82	0.66	66	33	92
7.02	4.26	0.36	0.41	9.47	1.54	0.63	47	25	66
8.07	3.61	0.43	0.46	6.89	1.03	0.48	26	18	36
9.06	4.26	0.49	0.51	7.41	1.13	0.58	42	24	59
10.04	5.24	0.55	0.56	8.44	1.33	0.74	57	26	80
11.02	4.51	0.61	0.60	6.47	0.96	0.58	51	30	71
12.01	4.47	0.67	0.65	5.85	0.84	0.55	0.2	0.1	0.3
13.02	4.45	0.73	0.70	5.33	0.75	0.52	5	3	7

kh is estimated from [3.1]

3.5.3 Delta Site

Drilled shafts have been used as the foundations for electric transmission line towers stretching 500 miles from Utah to California. For evaluating the behavior of drilled shafts, Briaud, Pacal, and Shively (1984) performed lateral load tests at three sites. One of these is the Delta site. The soil at this site consists of a lean silty clay, classified as CL. The average soil properties given by Briaud, Pacal, and Smith (1984) are as follows: undrained shear strength (s_u) = 3.8 ksf calculated as 1/20th of the cone penetrometer point resistance, dry unit weight = 98 lb/ft³, water content = 24.5 %, liquid limit = 34.8 %, plastic limit = 17.8 %. The water table was not encountered within the depth explored. Two lateral load tests have been performed at this site. The length of shaft no. 1 is about 10 feet and that of shaft no. 2 is 15 feet. The average diameters of both piers are 2.2 feet, such that $L/d = 4.6$ and 6.9, respectively.

A summary of given and calculated soil properties from the Delta site is given in Table 3.8. For the 10-foot pier ($L/d = 4.6$), the predicted load-deflection result is shown in Figure 3.10. The MFAD-PMT approach appears to overestimate the ultimate lateral capacity and underpredict the deflection. The LTBASE-PMT approach yields a relatively good prediction over the full range of applied loads.

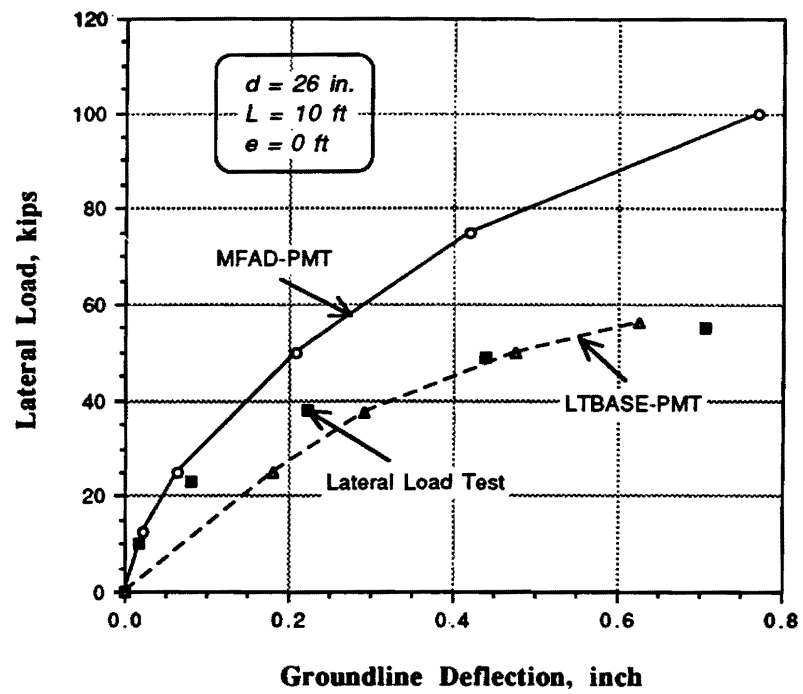


Figure 3.10. Measured and Predicted Response for Shaft 1 at Delta Site.

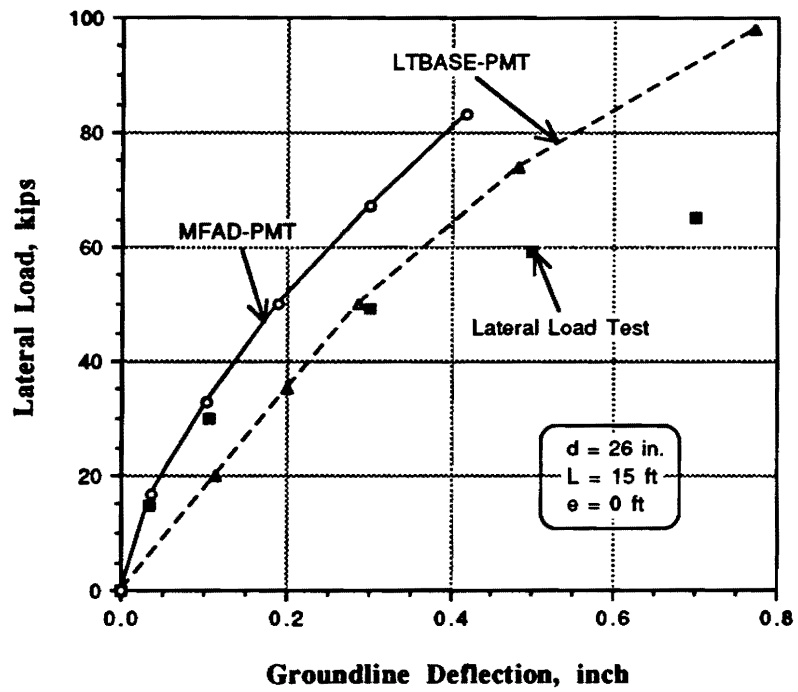


Figure 3.11. Measured and Predicted Response for Shaft 2 at Delta Site.

The second pier at the Delta site ($L/d \approx 7$), was also evaluated to yield the results shown in Figure 3.11. Similarly, the MFAD-PMT approach underpredicts the lateral deflection while the LTBASE-PMT approach gives a very reasonable estimate of groundline deflections for $H < 50$ kips. For loading $H > 50$ kips, LTBASE also underpredicts the magnitude of deflections.

3.5.4. Alamo Site

Load tests on rigid shafts have been performed at the Alamo site, a famous landmark in San Antonio, Texas. The soil at this site consists of a silty to sandy clay, classified as CL. Soil data at Alamo site have been reported by Briaud, Pacal, and Shively (1984). The average undrained shear strength (s_u) is 25.4 ksf, calculated as 1/20th of the cone penetrometer point resistance. The dry unit weight is 87.3 pcf. The natural water content = 15.5%. The liquid limit = 35.5% and the plastic limit = 13.5%. The water table was not encountered within the depth explored. Two lateral load tests have been performed on drilled shafts at the Alamo site. The length of one shaft is about 10 feet and the other is 15 feet. The average diameter of both piers is 2.1 feet ($L/d = 4.7$ and 7.1, respectively).

A summary of the reported and calculated soil properties for the Alamo Site is shown in Table 3.8. It is noted that the values of s_u from in-situ PMT are greater than 10 ksf. The MFAD program limits the maximum absolute value of s_u to 8 ksf. Therefore, $s_u = 8$ ksf was used as input values for the program MFAD.

The predicted results are shown in Figures 3.12 and 3.13. The results show that MFAD-PMT approach again underpredicts lateral deflections for both 10-ft and 15-ft long piers. The LTBASE-PMT approach gives relatively good predictions at low loading levels (i.e. $H < 50$ kips).

3.5.5. North Carolina Highway Site

Three rigid drilled shafts with diameters of 30 inches and lengths of 7 feet were constructed on a highway embankment in North Carolina (Gabr and Borden, 1988). The

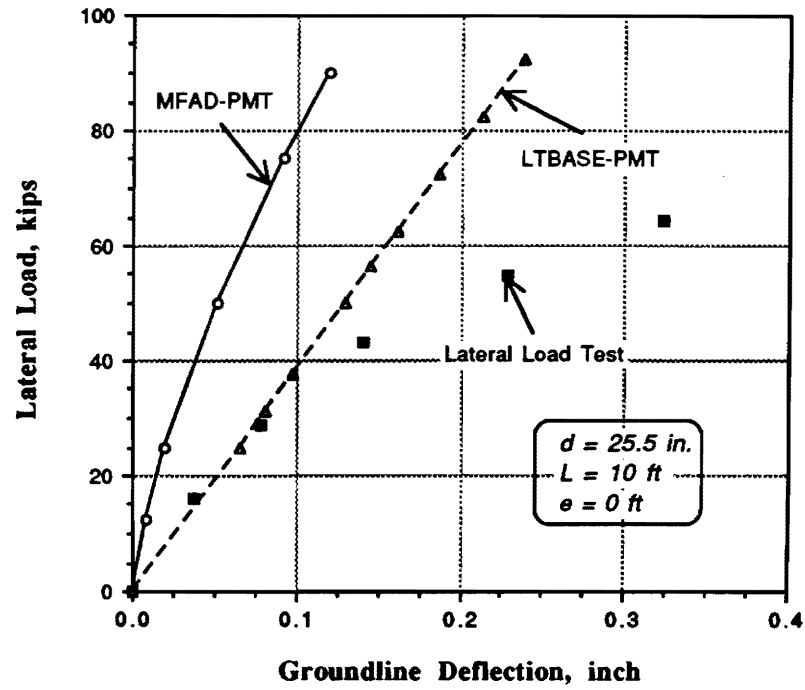


Figure 3.12. Measured and and Predicted Response for Pier 1 at Alamo Site.

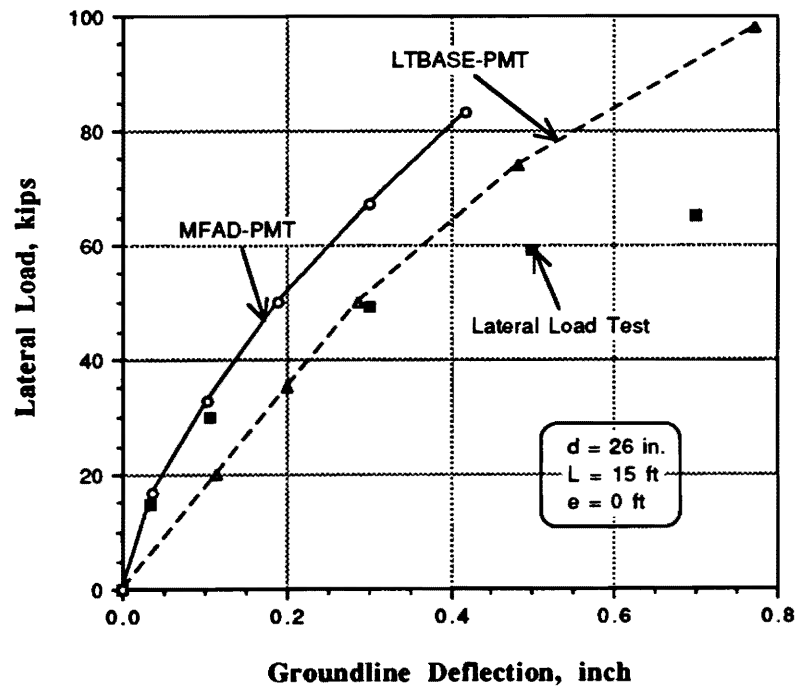


Figure 3.13. Measured and and Predicted Response for Pier 2 at Alamo Site.

results from tests on Pier#1 have been used in this study. This pier was constructed with dimensions of $d = 2.5$ feet and $L = 7$ feet. The loading was applied to the top of a 30-foot high column ($e = 30$ ft) supported by the pier, and consequently, a relatively high eccentricity of loading ($e/L \approx 4.3$) occurs, compared to the previous case studies reviewed. The soil profile at this site consists of sands with unit weights ranging from 92 to 106 pcf. Cone penetration test (CPT) and dilatometer tests (DMT) have been performed at this site. Soil parameters from the DMT data are given in Table 3.10.

The predicted lateral load-deflection relationships are shown in Figure 3.14. The MFAD-DMT approach tends to underpredict deflection while the LTBASE-DMT approach again yields reasonable predictions over the full range of loading.

Table 3.10. Summary of Soil Parameters from In-Situ DMT Soundings
at North Carolina Highway Site (Data from Gabr and Borden, 1988)

Depth feet	E_s ksf	k_h (Note*) pci	K_D	K_o	ϕ' degrees
1.31	1083	764	90	4.3	45.0
1.98	452	319	31	.56	47.0
2.64	302	213	12	.91	43.8
3.28	125	88	5	.47	41.3
3.94	50	35	2	.52	36.7
4.59	37	26	1	.43	32.8
5.25	17	12	1	.43	32.8
6.58	9	7	1	.43	32.8

*Note: k_h has been estimated using Equation [3.1]

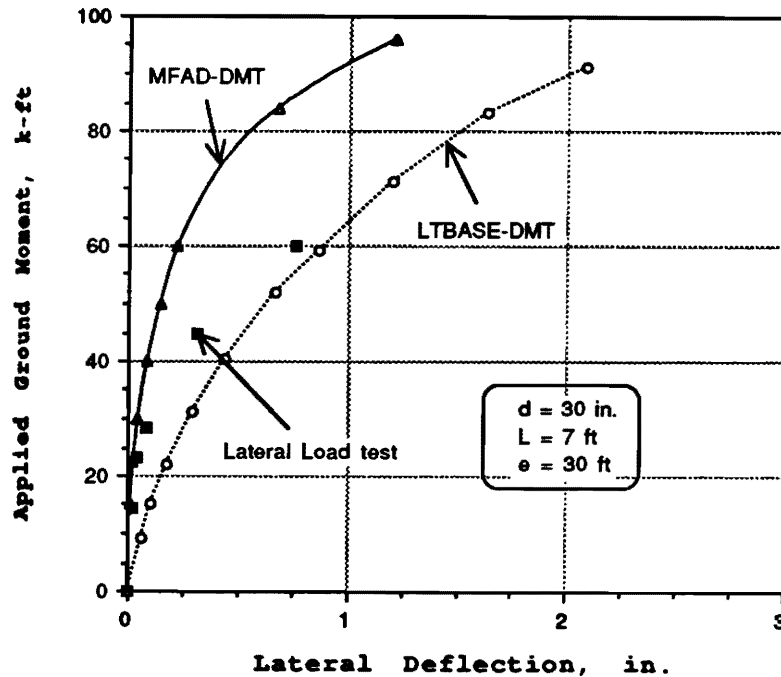


Figure 3.14. Measured and Predicted Response for Pier at North Carolina Highway Site

3.6. CONCLUSIONS

Programs MFAD and LTBASE are available for analyzing the response of laterally-loaded rigid drilled piers. Two other commercial programs (COM624 and PIGLET) were also reviewed, however, these primarily address the flexible response of long slender piles and piers. The LLWAS towers are supported by short and stubby shafts ($d = 4$ feet, $L = 20$ feet), and therefore classify as being relatively rigid. Consequently, Section 3 has focussed on the utilization of MFAD and LTBASE for evaluating the lateral-load behavior of drilled shafts.

Several case studies from the geotechnical literature have been collected and examined in terms of the predictive capabilities offered by MFAD and LTBASE. These case studies specifically addressed the behavior of rigid shafts ($2.8 \leq L/d \leq 7$) under lateral and moment loading ($0 \leq e/L \leq 4.3$). Also, at each of these sites, the results of high-quality in-situ pressuremeter tests (PMT) and dilatometer tests (DMT) have been used to determine the relevant shear strength and the modulus of the supporting soils. Based

upon five case studies (four consisting of clay deposits and one in sands), the LTBASE program consistently provided better predictions with the measured load test data than the MFAD analysis. In one selected example, the simple hyperbolic model and DMT results provided a superior prediction than either MFAD or LTBASE.

3.7. REFERENCES

Borden, R.H. and Gabr, M.A. (1987), "LTBASE: Computer Program for Laterally Loaded Pier Analysis Including Base and Slope Effects", Research No. HRP 86-5, North Carolina State University, Raleigh, 48 p.

Briaud, J.L., Pacal, A.J. and Shively, A.W. (1984), "Power Line Foundation Design Using the Pressuremeter", Proceedings, International Conference on Case Histories in Geotechnical Engineering, Vol. 1, University of Missouri, Rolla, pp.279-283.

Briaud, J.L., Smith, T. and Meyer, B. (1984), "Laterally-Loaded Piles and the Pressuremeter: Comparison of Existing Methods", Laterally Loaded Deep Foundations: Analysis and Performance, (STP 835), ASTM, Philadelphia, PA, pp. 97-111.

Davidson, H.L., Cass, P.G., Khilji, K., and McQuade, P. (1982), "Laterally Loaded Drilled Pier Research", Vol. 1: Design Methodology, Vol. 2: Research Documentation, EPRI Report EL-2197, Electric Power Research Institute, Palo Alto.

Davidson, H.L. (1990), "TL Workstation Code: Version 2.0; Volume 17: MFAD Manual", EPRI Report EL-6420, Vol. 17, Project 1493-7, Electric Power Research Institute, Palo Alto.

Desai, C.S. and Appel, G.C. (1976), "3-D Analysis of Laterally-Loaded Structures", Proceedings, 2nd International Conference of Numerical Methods in Geomechanics, Blacksburg, Vol. 1, pp. 405-418.

DiGioia, A.M., Davidson, H.L., and Donovan, T.D. (1981), "Laterally-Loaded Drilled Piers, A Design Model", Proceedings, Drilled Piers and Caissons Session, ASCE National Convention, St. Louis, Missouri, pp. 132-149.

Fang, J.S. (1991), "Comparison of Computer Methods for the Analysis of Lateral and Moment Behavior of Drilled Shaft Foundations", Special Research Project, School of Civil Engineering, Georgia Institute of Technology, Master of Science in Civil Engineering, Atlanta, GA, 142 p.

Gabr, M.A. and Borden, R.H. (1988), "Analysis of Load Deflection Response of Laterally-Loaded Piers Using DMT", Penetration Testing, Vol. 1, (Proc., ISOPT-1, Orlando), Balkema Publishers, Rotterdam, pp. 513-520.

- Hansen, B. (1961), "The Ultimate Resistance of Rigid Piles Against Transverse Forces", Bulletin, No. 12, The Danish Geotechnical Institute, Copenhagen, pp. 5-9.
- Huang, A.B., Lutenecker, A.J., Islam, M.Z., and Miller, G.A. (1989), "Analyses of Laterally-Loaded Drilled Shafts Using In-Situ Test Results", Research Record 1235, Transportation Research Board, Washington, pp. 60-67.
- Ismael, N.F. and Klym, T.W. (1978), "Behavior of Rigid Piers in Layered Cohesive Soils", Journal of Geotechnical Engineering, ASCE, Vol. 104, No. GT8, pp. 1061-1074.
- Ivey, D.L. (1968), "Theory of Resistance of a Drilled Shaft Footing to Overturning Loads", Research Report No. 105-1, Texas Transportation Institute, College Station, TX.
- Kasch, V.R., Coyle, H.M., Bartoskewitz, R.E., and Sarrer, W.G. (1977), "Lateral Load Test of a Drilled Shaft in Clay", Report No. TTI-211-1, Texas Transportation Institute, Texas A&M University, College Station, TX.
- Pyke, R. and Beikae, M. (1984), "A New Solution for the Resistance of Single Piles to Lateral Loading", Laterally-Loaded Deep Foundations (STP 835), ASTM, Philadelphia, PA, pp. 3-20.
- Poulos, H.G. (1982), "Developments in the Analysis of Static and Cyclic Lateral Response of Piles", Proceedings, Fourth International Conference on Numerical Methods in Geomechanics, Vol.3, Edmonton, Alberta, Canada, pp. 1117-1135.
- Poulos, H.G. and Hull, T.S. (1989), "The Role of Analytical Geomechanics in Foundation Engineering", Foundation Engineering: Current Principles and Practices, Vol. 2, ASCE, New York, pp. 1578-1606.
- Randolph, M.F. (1981), "The Response of Flexible Piles to Lateral Loading", Geotechnique, Vol. 31, No. 2, pp. 247-259.
- Randolph, M.F. (1989), "PIGLET: Analysis and Design of Pile Groups", Users Manual, University of West Australia, Nedlands, West Australia, pp. 26.
- Reese, L.C. and Welch, R. (1975), "Lateral Loading of Deep Foundations in Stiff Clay", Journal of Geotechnical Engineering, ASCE, Vol. 101, No. GT 7, pp. 633-649.
- Reese, L.C. (1977), "Laterally Loaded Piles: Program Documentation", Journal of the Geotechnical Engineering Division, ASCE, Vol. 103, No. GT 4, pp. 287-305.
- Reese, L.C., Cooley, L.A., and Radhakrishnan, N. (1984), "Laterally-Loaded Piles and Computer Program COM624", Technical Report K-84-2, Final Report, U.S. Army Engineering Division, Waterways Experiment Station, Vicksburg, MS, 91 p.
- Vesic, A.S. (1961), "Bending of Beam Resting on Isotropic Elastic Solid", Journal of the Engineering Mechanics Division, ASCE, Vol. 87, No. EM2, pp. 35-53.

SECTION 4

ELASTIC SOLUTIONS FOR ROCK-SOCKETED SHAFTS

4.1 METHODS OF ANALYSIS

Shafts which are rock-socketed and subjected to lateral-moment loading have been evaluated for the LLWAS project using three approaches, all of which utilize elastic continuum theory. The three methods include, boundary element analysis approach (Poulos 1972), finite element solutions (Carter and Kulhawy 1988), and a commercial computer program (DEFPIG). Details are given in the following sections of this report.

4.1.1. POULOS (1972) SOLUTION

In Poulos (1972) and Poulos and Davis (1980), elastic continuum theory is used to model drilled shaft behavior under conditions in which the foundation base (or tip) is either fixed or pinned. These conditions occur when the shaft tip is embedded fully or partially into rock. Solutions for the boundary conditions of fixed-head or free-head and pinned-tip or fixed-tip are included. See Figure 4.1 for an illustration of these boundary

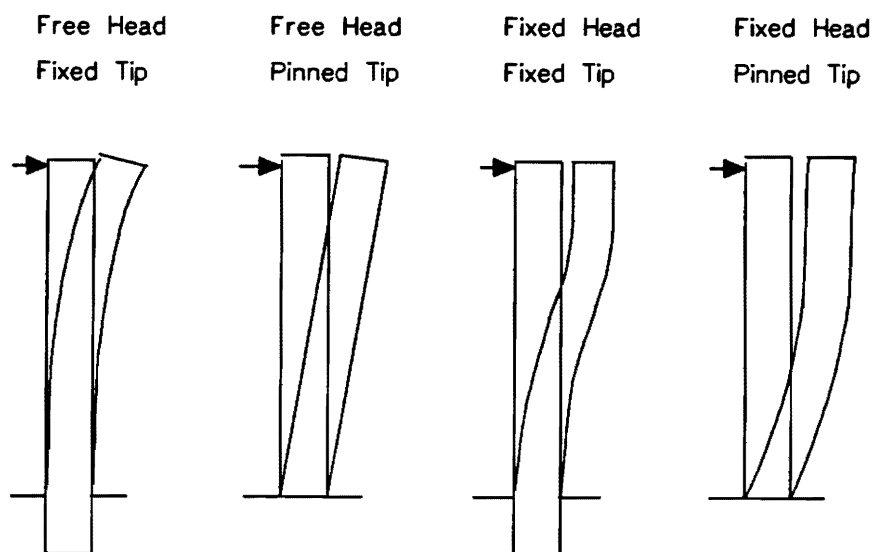


Figure 4.1. Various Boundary conditions for Laterally-Loaded Shafts.

conditions. The condition of interest in this report is the free head-fixed tip pier since this most closely represents the foundations for the LLWAS pole situation. In this case, the tip is restrained from moving by socketing it into rock, and the shaft head is only surrounded by soil so that it is relatively free to move. Solutions for the deflection and rotation of the drilled shaft head and the force and moment developed at the tip are given in the form of design equations and charts. The Poulos solution also includes modifications to allow for soil yielding, soil-shaft separation, and nonuniform soil modulus with depth.

The method involves a boundary element analysis of the drilled shaft. The drilled shaft is modeled as a thin rectangular strip of length, L , and width, d (taken as equivalent to the diameter of a circular drilled shaft). The foundation has a modulus, E_p , and a constant moment of inertia, I_p . The drilled shaft tip is restrained by a tip force, H_t , and a fixing moment, M_t . For the finite difference analysis, the drilled shaft is divided into $n+1$ elements which each have length, δ , except for the two end elements which have length, $\delta/2$. A constant, uniform, horizontal force, H , acts on each element. The soil layer is modeled as a homogeneous, isotropic, elastic medium having modulus E_s and Poisson's ratio ν_s .

The solution is obtained by writing the basic beam equations in finite difference form. The boundary conditions at the drilled shaft head and tip are included and the stress and displacement of each element may be described in the following form:

$$- [p] = \frac{E_p I_p n^4}{d L^4} [\Delta] \cdot [p^o] + \frac{E_p I_p n^4}{d L^4} [c] \quad [4.1]$$

In this equation $[p]$ and $[p^o]$ are $n-1$ column vectors for stresses and drilled shaft displacements, $[\Delta]$ is an $n-1$ by $n+1$ matrix of coefficients of finite difference operators, and $[c]$ is an $n-1$ column vector. The terms of $[\Delta]$ and $[c]$ depend on the tip and head boundary conditions which are defined by the following: (1) free-head means that the moment at the head is equal to the applied moment, (2) fixed-head means that the head rotation is equal to zero, (3) pinned-tip means that the tip displacement is equal to zero,

and (4) fixed-tip means that the tip rotation is equal to zero.

Displacements of the soil along the drilled shaft may be written in the form of:

$$[s^p] = \frac{d}{E_s} [I_s] \cdot [p] \quad [4.2]$$

In this case, $[s^p]$ is the $n+1$ column vector of soil displacements in a semi-infinite mass due to an interior point loading. Poulos (1972) utilizes a fictitious mirror image of the drilled shaft which is loaded by equal and opposite horizontal stresses to solve the equations. The terms in $[I_s]$ are the soil displacement influence factors which may be evaluated with an expression derived by Douglas and Davis (1964) from the integration of the Mindlin equation.

The displacements for the drilled shaft and soil are then equated to each other for each element along the length of the drilled shaft. These equations, along with the appropriate equilibrium equations, are then solved to provide the stresses and displacements of the drilled shaft. The solution depends greatly on the relative stiffness of the drilled shaft and soil. Therefore, a dimensionless factor to describe the relative flexibility of the foundation is introduced. The drilled shaft flexibility factor, K_r , is defined as:

$$K_r = \frac{E_p I_p}{E_s L^4} \quad [4.3]$$

where: E_p is the drilled shaft modulus, I_p is the drilled shaft moment of inertia (for circular sections $I_p = \pi d^4/64$), E_s is the soil modulus, and L is the drilled shaft length. Note that K_r equal to infinity denotes a perfectly stiff drilled shaft and K_r equal to zero means that the drilled shaft is perfectly flexible. For practical applications, if $K_r > 10^1$ the shaft will behave rigidly and if $K_r < 10^2$ then the shaft will behave as a flexible member. The Poulos (1972) solution also includes modifications to allow for local yielding of the soil and for drilled shaft-soil separation.

The method provides equations in a very simple form. Shown here are equations for the displacements and the rotations for free-head-fixed tip drilled shafts:

$$\delta = I_{\rho H} \frac{H}{E_s L} + I_{\rho M} \frac{M}{E_s L^2} \quad [4.4]$$

$$\theta = I_{\theta H} \frac{H}{E_s L^2} + I_{\theta M} \frac{M}{E_s L^3} \quad [4.5]$$

where H is the horizontal load, M is the moment load, and δ and θ are the displacement and rotation of the shaft at the ground surface. The I_{xx} terms in the equations are the displacement and rotation influence factors. They are dimensionless and can be obtained from Figures 4.2, 4.3, and 4.4 where the influence factors are shown to be functions of the shaft flexibility factor, K_r , and slenderness ratio, L/d . Alternatively, for $K_r > 10^{-1}$,

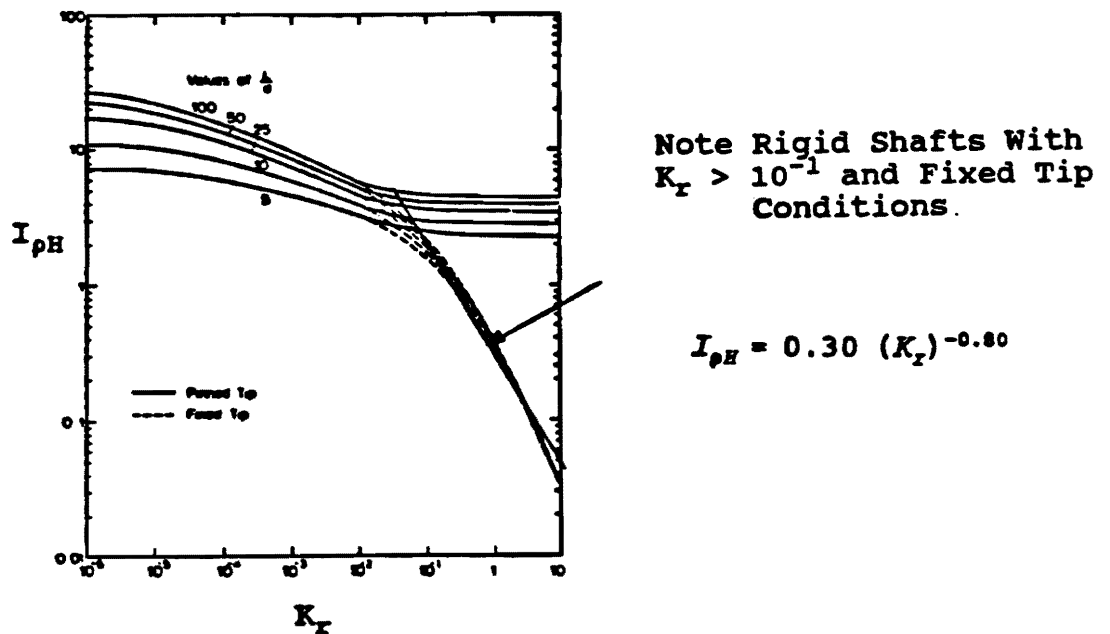
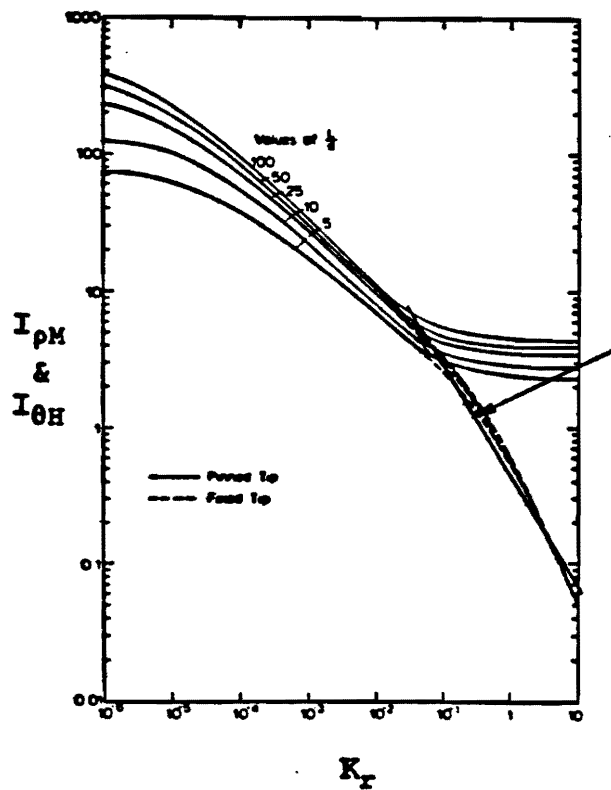


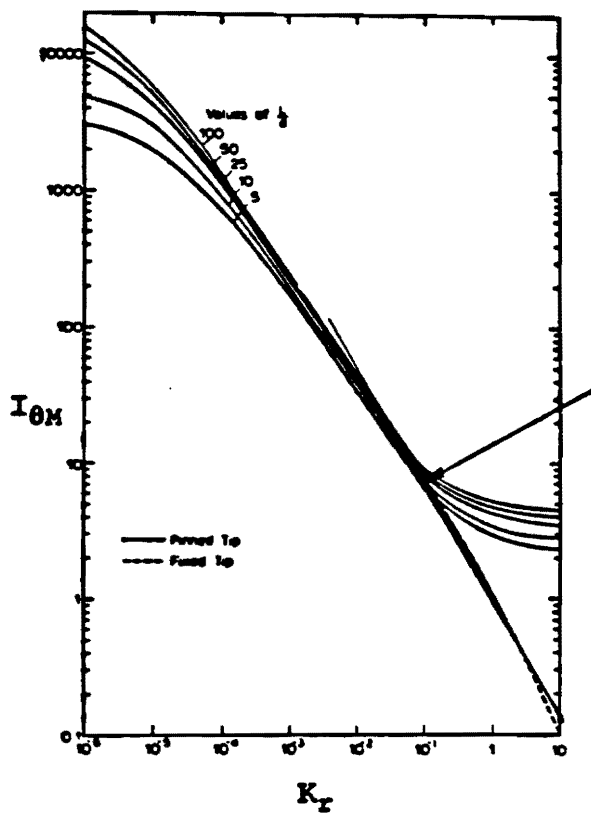
Figure 4.2. Influence factors $I_{\rho H}$ from Poulos (1972).



Note Rigid Shafts With
 $K_r > 10^{-1}$ and Fixed Tip
 Conditions

$$I_{\rho M}, I_{\theta H} = 0.50 (K_r)^{-0.82}$$

Figure 4.3. Influence factors $I_{\rho M}$ and $I_{\theta H}$ from Poulos (1972).



Note Rigid Shafts With
 $K_r > 10^{-1}$ and Fixed Tip
 Conditions

$$I_{\theta M} = 1.0 (K_r)^{-0.86}$$

Figure 4.4. Influence factors $I_{\theta M}$ from Poulos (1972).

an approximation of the curve in the form of an equation may be used. These approximate equations are presented to the right of the charts in Figures 4.2, 4.3, and 4.4. All the charts are for $\nu = 0.5$ because parametric analyses have shown that its influence was very small and could be ignored for practical problems.

As can be seen in Figures 4.2, 4.3, and 4.4 for values of $K_r < 10^2$ the drilled shaft behaves as a flexible member and the influence factors are unaffected by the tip condition. However, as K_r becomes greater than 10^2 , the drilled shaft behaves more as a rigid member and the influence factors decrease dramatically with increasing stiffness. This causes the displacements and rotations to tend toward zero as the drilled shaft becomes infinitely stiff. Consequently, for $K_r < 10^2$, there is no advantage in socketing the drilled shaft as far as lateral behavior is concerned.

In soils with nonuniform modulus with depth, Poulos (1972) suggested that the equivalent constant modulus can be estimated to be the modulus at a depth of $0.25L$ for relatively stiff drilled shafts and at a depth of $0.05L$ for flexible drilled shafts. If the drilled shaft head is fixed, the constant modulus occurs at a depth of about $0.5L$ for stiff drilled shafts and at a depth of about $0.15L$ for flexible drilled shafts.

Poulos (1972) shows that the effect of local yield and drilled shaft-soil separation is less pronounced for rigid drilled shafts than for flexible drilled shafts. However, if the effects are neglected, then the predicted movements will be too small. Four approaches are suggested that may be used to solve practical problems. These include:

1. A complete numerical analysis, including local yield and drilled shaft-soil separation, with E_s determined from laboratory triaxial or horizontal in-situ plate load tests.
2. The elastic solutions presented here can be used with E_s determined from a horizontal in-situ plate load test at an appropriate load level.
3. A simple elastic solution with E_s estimated from empirical correlations.
4. A full-scale lateral load test on a socketed drilled shaft per ASTM D-3966 procedures could be performed.

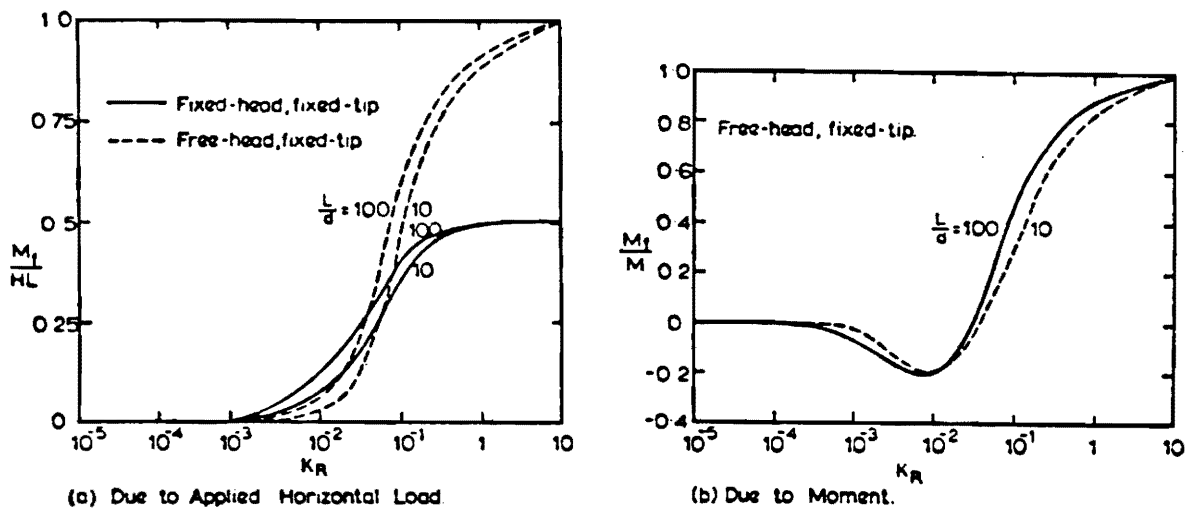


Figure 4.5. Fixing Moment at Drilled Shaft Tip/Base
(Source: Poulos, 1972)

When the tip of a rigid drilled shaft is socketed and restrained from moving, significant moments and forces are developed at the drilled shaft tip. Figure 4.5 gives the fixing moment at the drilled shaft tip and Figure 4.6 gives the horizontal force at the tip. The forces and moments are small for flexible drilled shafts and only become significant as K_t increases above 10^{-2} . In some cases, such as moment loading of a rigid, free head-fixed tip drilled shaft, the force can decrease and even become negative. The figures give moments and forces for either moment or horizontal loading only. In cases which involve both loadings, superposition may be used to combine the two.

4.1.2. CARTER AND KULHAWY (1988) SOLUTION

The aim of the Carter and Kulhawy (1988) solution method is to provide an approximate closed-form method of analysis of the behavior of socketed drilled shaft foundations under lateral and moment loading. The equations provided here are approximations to

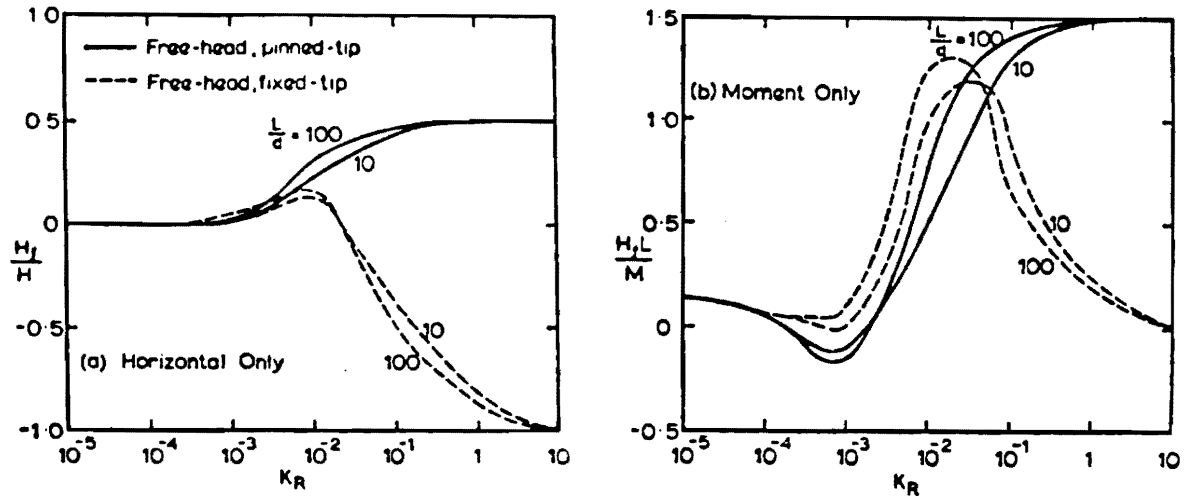


Figure 4.6. Horizontal Force at Drilled Shaft Tip/Base.

(Source: Poulos, 1972)

the results of a finite element study of the behavior of axisymmetric bodies subjected to nonsymmetric loading. Eight noded, isoparametric, quadrilateral elements with 3 X 3 Gaussian integration, were used in the finite element study. The analysis showed that the effects of variations in Poisson's ratio of the rock mass ν_r , could be accounted for by the use of an equivalent shear modulus of the rock, G^* , given as:

$$G^* = G_r \left(1 + \frac{3\nu_r}{4}\right) \quad [4.6]$$

in which:

$$G_r = \frac{E_r}{2(1+\nu_r)} \quad [4.7]$$

is the actual shear modulus of the rock mass. In this equation, E_r is the rock mass

modulus and ν_r is the Poisson's ratio of the rock mass.

A new parameter, the modulus ratio, was defined as the ratio of the foundation elastic modulus to the equivalent rock shear modulus (E_e/G^*). The modulus ratio and slenderness ratio of the shaft, L/d , were found to influence the behavior of the shaft. For different values of the modulus ratio, a shaft may behave as an infinitely long flexible member, as a rigid member, or as an intermediate stiffness member. The finite element analysis showed that if:

$$\frac{L}{d} \geq \left(\frac{E_e}{G^*} \right)^{2/7} \quad [4.8]$$

then the shaft will behave as a flexible member. Under this condition, the shaft behavior is dependent only on the modulus ratio and on Poisson's ratio of the rock. When $L/d > (E_e/G^*)^{2/7}$, shaft response is independent of L/d . For this case the following equations are valid:

$$\rho = 0.5 \frac{H}{G^* d} \left(\frac{E_e}{G^*} \right)^{-1/7} + 1.08 \frac{M}{G^* d^2} \left(\frac{E_e}{G^*} \right)^{-3/7} \quad [4.9]$$

$$\theta = 1.08 \frac{H}{G^* d^2} \left(\frac{E_e}{G^*} \right)^{-3/7} + 6.4 \frac{M}{G^* d^3} \left(\frac{E_e}{G^*} \right)^{-5/7} \quad [4.10]$$

These equations are appropriate for the ranges of modulus ratio, $1 \leq E_e/G^* \leq 10^6$ and slenderness ratio, $L/d \geq 1$.

A rigid shaft condition occurs when:

$$\left(\frac{L}{d} \right) \leq 0.05 \left(\frac{E_e}{G^*} \right)^{1/2} \quad [4.11]$$

Under these circumstances, the shaft behavior depends only on the slenderness ratio (L/d)

and Poisson's ratio of the rock (ν_r) and is independent of the modulus ratio. The following equations are valid for rigid shafts:

$$\rho = 0.4 \frac{H}{G^* d} \left(\frac{2L}{d} \right)^{-1/3} + 0.3 \frac{M}{G^* d^2} \left(\frac{2L}{d} \right)^{-7/8} \quad [4.12]$$

$$\theta = 0.3 \frac{H}{G^* d^2} \left(\frac{2L}{d} \right)^{-7/8} + 0.8 \frac{M}{G^* d^3} \left(\frac{2L}{d} \right)^{-5/3} \quad [4.13]$$

The applicable ranges for the rigid shaft case are $1 \leq L/d \leq 10$ and $E_r/G^* \geq 1$.

The intermediate stiffness case occurs when the slenderness ratio is in the following range:

$$0.05 \left(\frac{E_r}{G^*} \right)^{1/2} \geq \frac{L}{d} \geq \left(\frac{E_r}{G^*} \right)^{2/7} \quad [4.14]$$

For cases of intermediate stiffness, the deflections predicted by finite element analysis exceed those given by the equations for flexible or rigid drilled shafts by about 25%. To simplify the analysis, Carter and Kulhawy (1988) suggested that the deflection of an intermediate stiffness shaft be taken as 1.25 times the deflection of the maximum of the flexible or rigid case.

The previous section dealt with the case of a rock layer at the ground surface. Carter and Kulhawy (1988) also present a method for dealing with a soil layer overlying the rock. However, the modeling of the lateral soil reaction resistance utilizes the Broms (1964) solution for purely cohesive or purely cohesionless soils. It is only applicable for the ultimate lateral soil reaction and is not suitable for the analysis of drilled shafts under loadings less than ultimate. Therefore, the method has not been included in further studies herein.

4.1.3. DEFPIG COMPUTER SOLUTION

The DEFPIG computer program (Poulos, 1978) utilizes much of the previous boundary element work on elastic solutions for axially and laterally loaded piles. The program incorporates the elastic solutions for axially and laterally loaded single piles into the DEFPIG program to provide solutions for pile groups. Whereas the program is set up mainly to analyze pile groups, analysis of single piles is also possible.

An advantage of the DEFPIG program is that the inclusion of a nonhomogeneous soil profile is possible. This capability makes DEFPIG directly applicable to the analysis of rock-socketed shafts. The rock-socketed shaft case is modeled by including a two-layer profile with the upper layer having the modulus of the soil and the lower layer having the modulus of the rock.

For the theoretical basis, DEFPIG combines the following five analyses:

1. Settlement behavior of single axially-loaded shafts (Mattes and Poulos, 1969);
2. Settlement of a group of shafts, using superposition of pile interaction factors, presented by Poulos and Mattes (1971);
3. Lateral response of an isolated shaft, developed by Poulos (1971);
4. The lateral response of a group of deep foundations, using superposition of pile interaction factors, (Poulos, 1971);
5. Analysis of a pile group containing batter piles under lateral, vertical, and moment loading, developed by Poulos and Madhav (1971).

Of specific interest for the LLWAS tower foundation is the Poulos (1971) solution for the lateral response of single piles. This solution is theoretically very similar to the method described in Section 4.1.1 for rock-socketed piles and will not be described further here. A summary of these elastic continuum solutions is also given by Poulos and Davis (1980).

4.2. LOAD TEST DATA

There are relatively few published reports and papers concerning the analysis of rock-socketed laterally-loaded drilled shafts. In most construction projects, such as buildings and bridges, the important critical loading is often axial compression. However, in the design of foundations for transmission line towers, offshore oil drilling platforms, LLWAS towers, and other types of pole foundations, the lateral and/or moment loading is often the most important mode.

The limited theoretical work is followed closely by a lack of full scale load tests on socketed shafts. These tests are the final confirmation of any design method and without them, any theoretical method is in question. In the literature search, eight drilled shaft load tests were found where rock-socketed tips had been installed. Table 4.1 contains a summary of the shaft geometries for these load tested shafts. The drilled shaft length to diameter ratios, L/d , range from 2.1 to 8.9 and are similar to the $L/d = 5$ currently used for drilled shaft foundations in LLWAS pole support structures. This section will describe the load tests and provide the load-deflection curves.

Table 4.1. Summary of Load Tests on Rock-Socketed Drilled Shafts.

Shaft	Ref. No.	L (feet)	d (feet)	L/d	L_s (feet)	L_s/d	Reference
A	1-N	11.4	4.0	2.8	5.0	1.7	Davisson and Salley (1969)
B	1-S	8.5	4.0	2.1	4.0	1.0	Davisson and Salley (1969)
C	2-N	40.1	4.5	8.9	5.0	1.1	Davisson and Salley (1969)
D	2-S	32.1	4.5	7.1	5.5	1.2	Davisson and Salley (1969)
E	1200	34.4	3.9	8.8	7.7	1.9	Lyndon et al. (1989)
F	1500	32.7	4.9	6.7	8.2	1.7	Lyndon et al. (1989)
G	14-U	-	3.0	-	6.0	2.0	Carter and Kulhawy (1988)
H	14-D	-	4.0	-	8.0	2.0	Carter and Kulhawy (1988)

4.2.1. Load Tests in Texas

Four lateral drilled shaft load tests in Texas are described by Davisson and Salley (1969) and include two short drilled shafts and two longer drilled shafts. The short drilled shafts, designated A and B, have L/d ratios of 2.8 and 2.1, respectively. The longer drilled shafts designated C and D have L/d ratios of 8.9 and 7.1, respectively. The

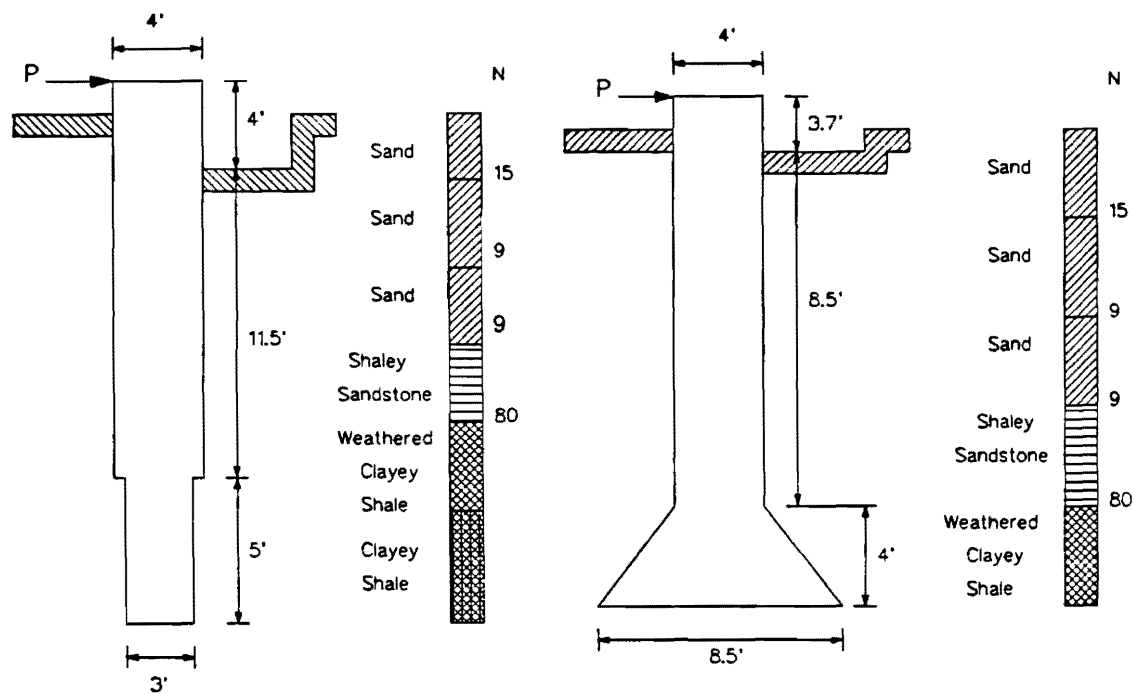


Figure 4.7. Profiles for Socketed Shafts A and B.
(Adapted from Davisson and Salley (1969).)

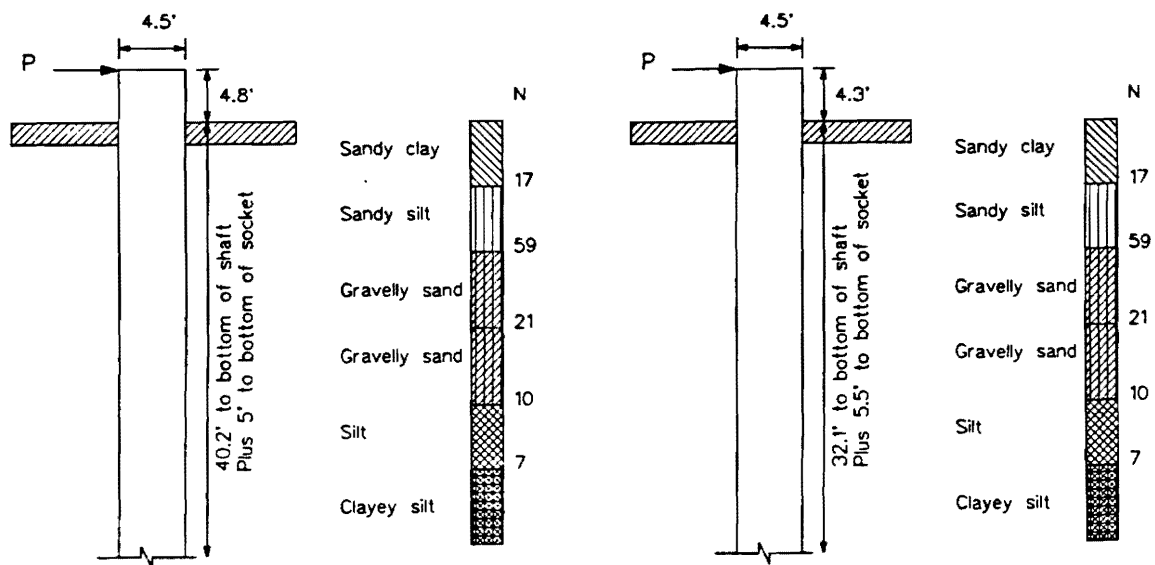


Figure 4.8. Profiles for Socketed Shafts C and D.
(Adapted from Davisson and Salley (1969).)

ground conditions at this site consist primarily of medium sands overlying a shale bedrock with the water table at a depth of 10 feet. Shaft dimensions and geotechnical data for shafts A and B are given in Figure 4.7, and the information for shafts C and D are given in Figure 4.8. Note that shaft A was built with a socket diameter slightly smaller than the shaft diameter and that shaft B was constructed with a belled base. The loading sequence consisted of increasing the lateral load in 25-kip increments up to 100 kips. Subsequently, the load was cycled 80 to 100 times from 0 to 100 kips. The effect of the cyclic loading was to approximately double the deflection of the first cycle. After the cyclic loading, the shafts were loaded to a maximum of 170 kips (A and B) or 200 kips (C and D). The load-deflection curves are presented in Figures 4.9-4.12.

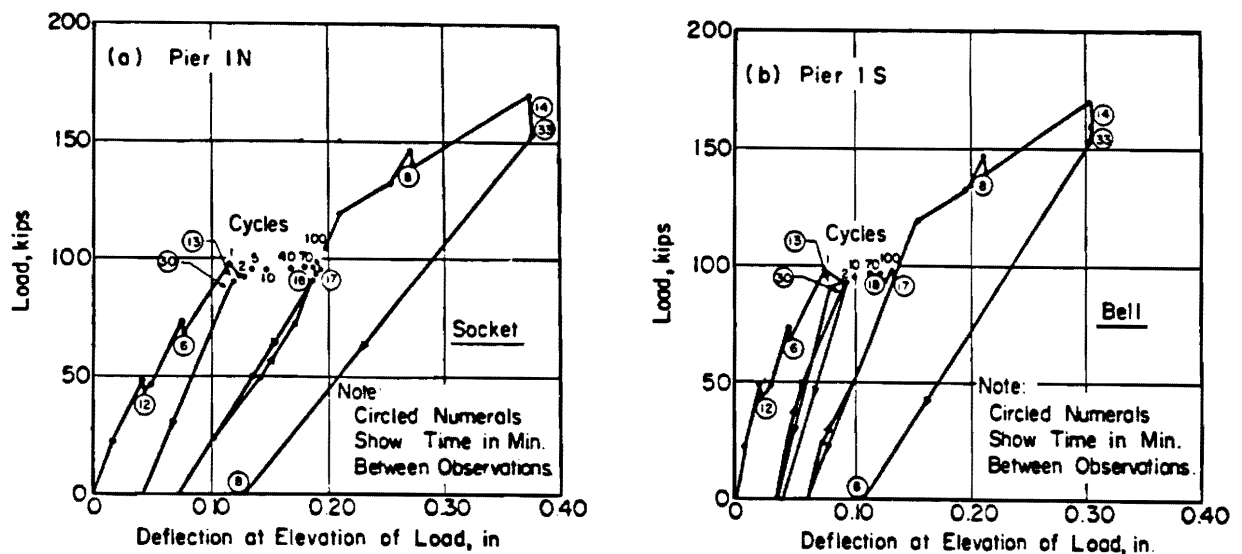


Figure 4.9. Load-Deflection Curve for Socketed Shaft A.

(from Davisson and Salley, 1969)

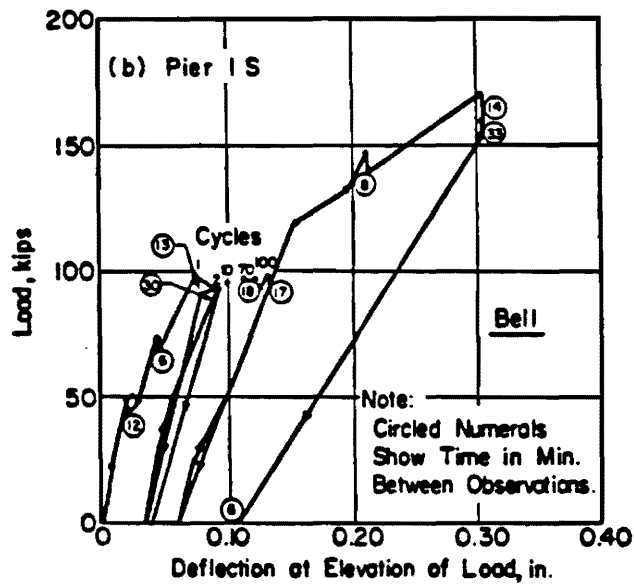


Figure 4.10. Load-Deflection Curve for Socketed Shaft B.
(from Davisson and Salley, 1969)

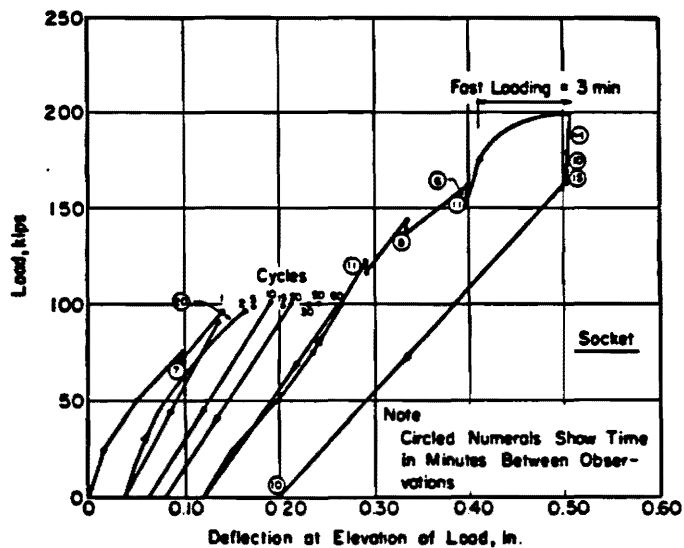


Figure 4.11. Load-Deflection Curve for Socketed Shaft C.
(from Davisson and Salley, 1969)

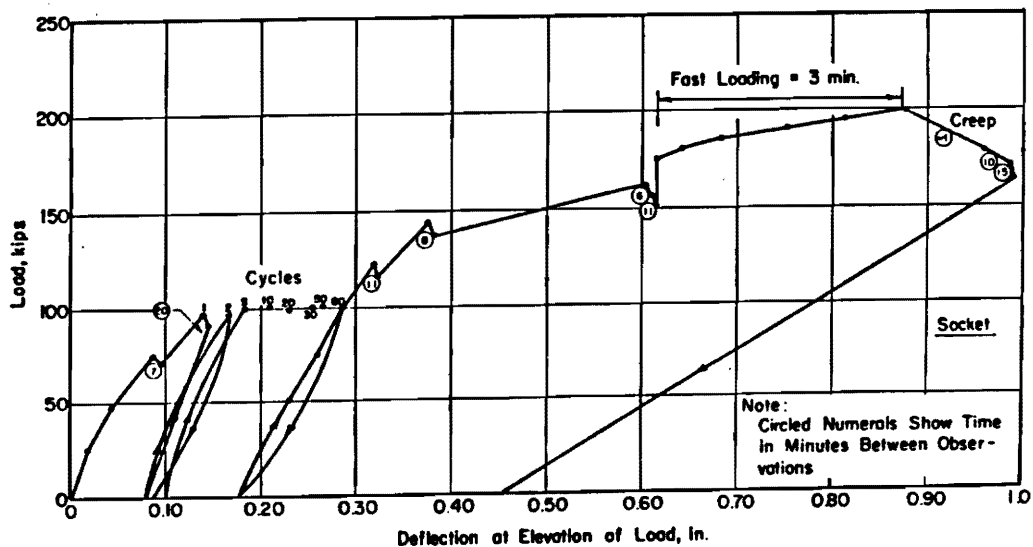


Figure 4.12. Load-Deflection Curve for Socketed Shaft D.
(from Davisson and Salley, 1969)

4.2.2. Load Tests in the United Kingdom

Two drilled shaft load tests on socketed-piers in the U.K. are described in a paper by Lyndon, et al (1989). The two shafts, designated shaft E and F, have L/d ratios of 8.4 and 7.0. The site conditions consist of dense sand and gravel overlying weathered sandstone bedrock with the groundwater table located at a depth of 11.5 feet. The boring logs for three holes adjacent to the drilled shafts and the shaft details are presented in Figure 4.13. The soils consist of dense to very dense sands, gravels, and boulders underlain by very highly weathered sandstone.

The load-deflection curves are presented in Figure 4.14. It can be seen in these figures that shaft E deflected almost four times as much as shaft F at the higher load levels. Lyndon et al. (1989) attribute some of this difference to the fact that shaft E was axially loaded up to 3600 kips before the lateral load test was performed. No axial load was applied to shaft F before the lateral testing.

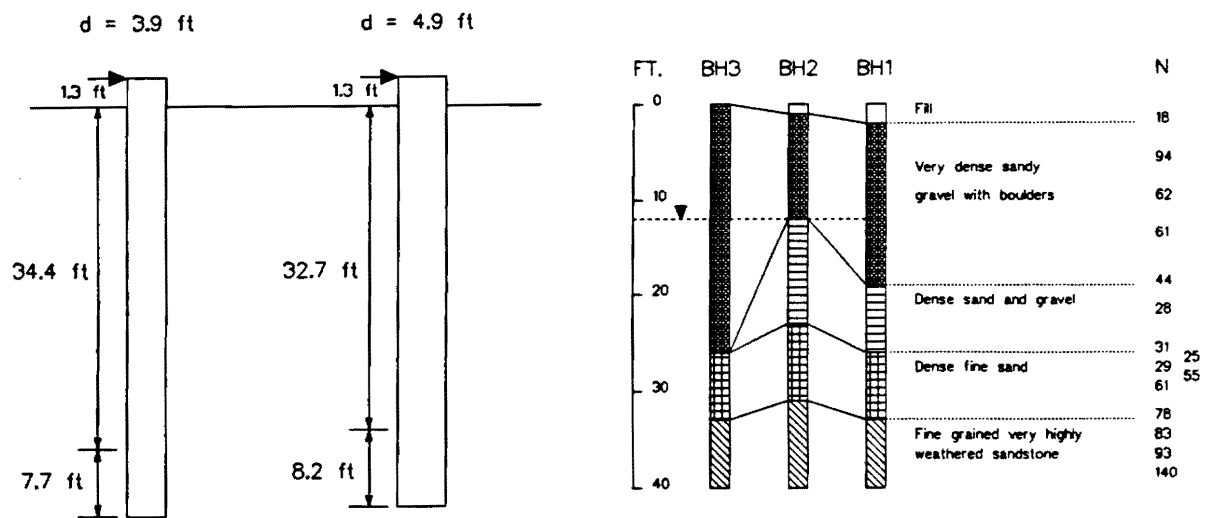


Figure 4.13. Geotechnical Information and Shaft Details for Socketed Drilled Shafts E and F in the U.K. (from Lyndon, et al., 1989).

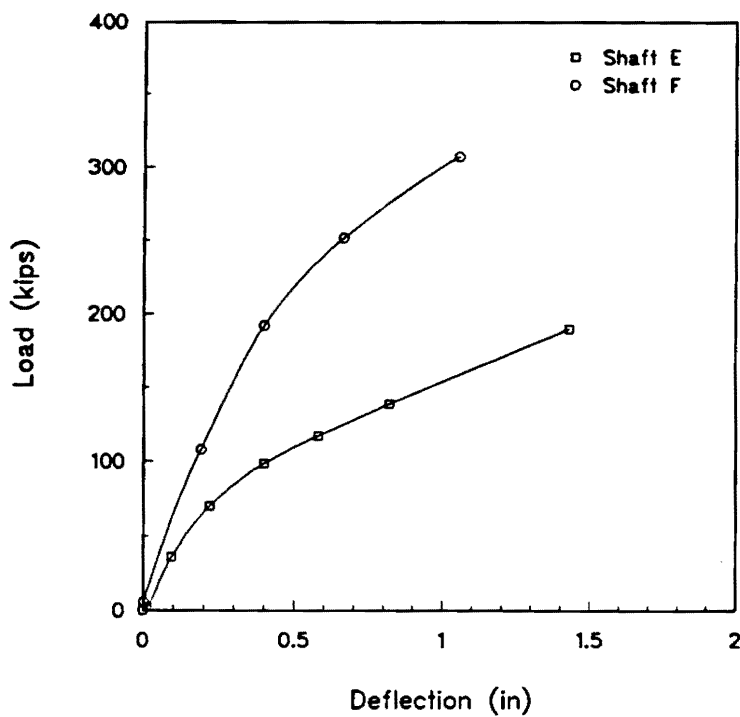


Figure 4.14. Load-Deflection Curves for Socketed Shafts E and F (Lyndon, et al. 1989).

4.2.3. Load Tests on Shafts Embedded in Surface Exposed Rock

Load tests for two short drilled shafts ($L/d \approx 2.0$ for both shafts) are presented in Carter and Kulhawy (1988). These load tests (designated G and H) involved the jacking together of two drilled shafts which once formed the foundation of a transmission line tower. The shafts are founded in a surface-exposed granite bedrock. The details of these rock-socketed shafts are shown in Figure 4.15.

The load-deflection curves are in Figure 4.16. The rock modulus was backcalculated for each load test using the equations presented in Section 4.1.2 by Carter and Kulhawy (1988) and was determined to be 8650 ksf for shaft G and 2100 ksf for shaft H. Note that the enlarged base of shaft G and the sloping rock surface between the two shafts was not taken into account in the calculation of E_r .

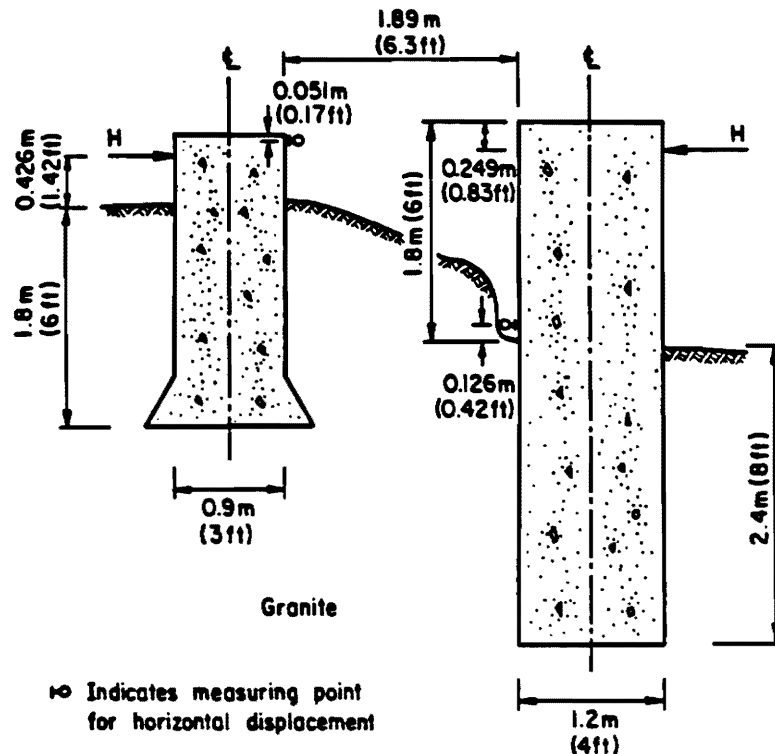


Figure 4.15. Details for Rock-Socketed Shafts G and H.
(from Carter and Kulhawy, 1988)

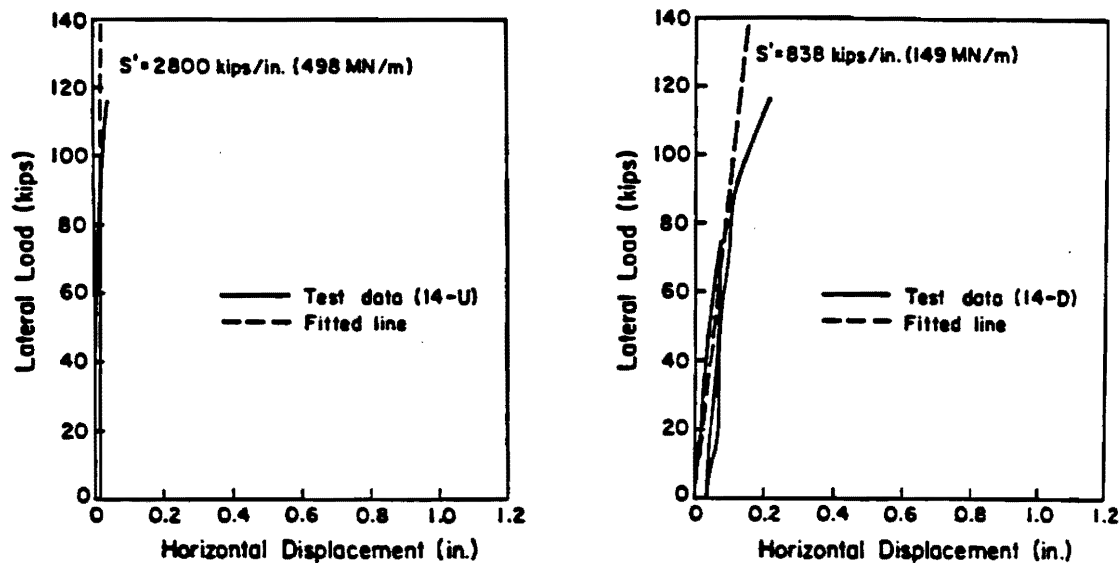


Figure 4.16. Load-deflection Curves for Socketed Shafts G and H.
(from Carter and Kulhawy, 1988)

4.3. DETERMINATION OF MATERIAL PARAMETERS

The increased use of numerical and computer methods in modern civil engineering practice has greatly enhanced a designer's ability to analyze a problem, and at the same time has increased the ability to make mistakes if the application of the computer method is not understood fully. Given the necessary parameters, very accurate solutions can be made of previously unsolvable problems. However, any solution is only as accurate as the material properties (i.e. E and ν) of the soil, rock, and construction materials. In other words, the solution can only be as accurate as the numbers used in the analysis.

In most cases, the only way to accurately determine material properties is with relatively expensive field and laboratory tests. Given the economic constraints of most projects, a full analysis of the material properties is not warranted. In these cases, simple inexpensive tests such as standard penetration test, SPT, and rock quality designation,

RQD, are assumed to be available and methods for determining material properties empirically from them will be presented here.

4.3.1. ELASTIC PARAMETERS FOR SOILS

The research on lateral behavior of LLWAS foundations for the FAA conducted at Georgia Tech included an extensive study of available load test data on drilled shaft foundations. These results have been reported in Section 2 of this report. The load tests included in this study were limited to rigid or very nearly rigid drilled shafts. By using a hyperbolic model of the load deflection behavior of a laterally loaded shaft and by employing elastic continuum theory it was possible to backcalculate the soil modulus which fit the load deflection curves for these load tests. Consequently, the derived relationships between the soil modulus (E_s) and SPT-N value have been utilized in this section as well for consistency.

Poisson's ratio of soil has a very small effect on the elastic solution, as stated by Poulos (1972). The design charts use $\nu = 0.5$ and this should be suitable for most calculations requiring Poisson's ratio.

4.3.2 ELASTIC PARAMETERS FOR ROCK MASSES

Kulhawy (1975) compiled a large database of E and ν values for intact cores of 154 different rock types. In this study, the range of modulus was only two orders of magnitude for all rock types studied (20,800 ksf to 2,080,000 ksf) and the average ν was 0.2, which is a commonly accepted value. Table 4.2 is adapted from this paper and gives average intact moduli for different rock types and should provide a reasonable estimate of the modulus if laboratory tests are unavailable. The Poisson's ratio average of 0.2 is considered sufficient for general use.

Once an intact rock modulus determined from a uniaxial compression test or from Table 4.2 is selected, a reduction factor should be used to convert the intact modulus to that of the rock mass modulus. Figure 4.17 relates the rock quality designation, RQD, to a reduction factor, $E_{\text{mass}}/E_{\text{intact}}$. This is necessary in order to take into account the strength

Table 4.2. Intact Rock Modulus Values.

(adapted from Kulhawy, 1975)

Rock Type	No. of Samples	Range (10 ⁶ ksf)	Average (10 ⁶ ksf)
Igneous:	51	0.16-2.08	1.17
Metamorphic			
Nonfoliated:	12	0.75-1.84	1.24
Foliated:			
Gneiss	11	0.97-1.70	1.37
Schist	13	0.12-1.44	0.72
Phyllite	3	0.18-0.36	0.25
Sedimentary:			
Clastic	35	0.10-0.82	0.40
Chemical	30	0.09-1.88	0.98

reduction caused by weathering and the discontinuities in the rock mass. The RQD provides a rough estimate of the quality of the rock mass.

Alternatively, Figure 4.18 shows a correlation from Bieniawski (1984) which gives the rock mass modulus vs. the geomechanics rock mass rating (RMR). The lower bound of this data for a very poor quality rock mass is approximately 20,000 ksf. As a comparison, if the low value of the range of intact sedimentary rock in Table 4.2 is combined with the maximum reduction factor, 0.14, from Figure 4.19, then the resulting rock mass modulus is 14,000 ksf which agrees with the value of 20,000 ksf from Bieniawski (1984).

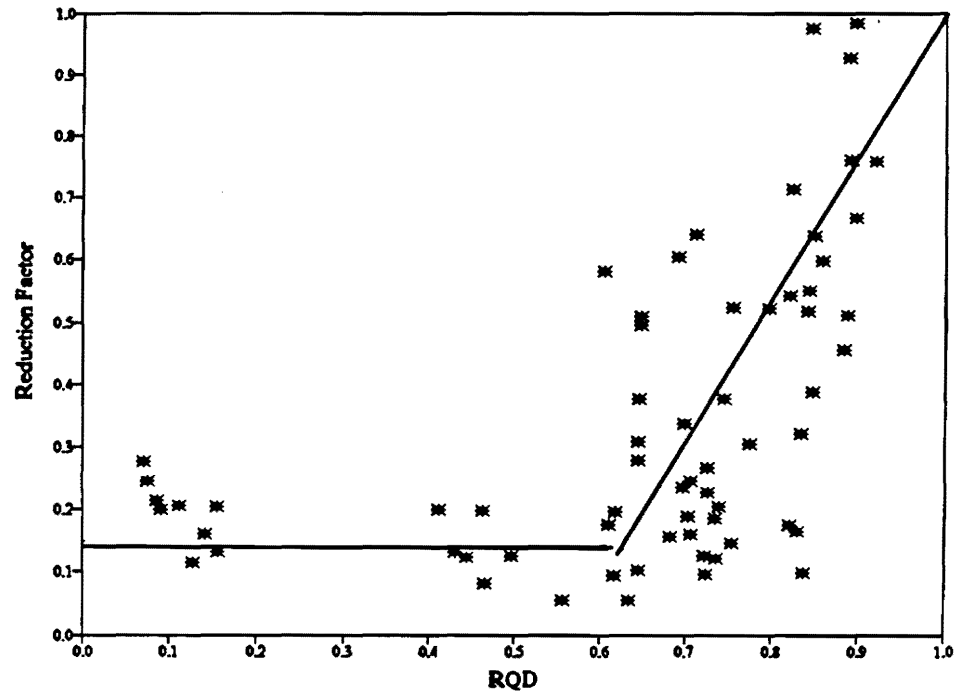


Figure 4.17. Modulus Reduction Factor Versus Rock Quality Designation (RQD).
(from Hall, Newmark, and Hendron, 1974).

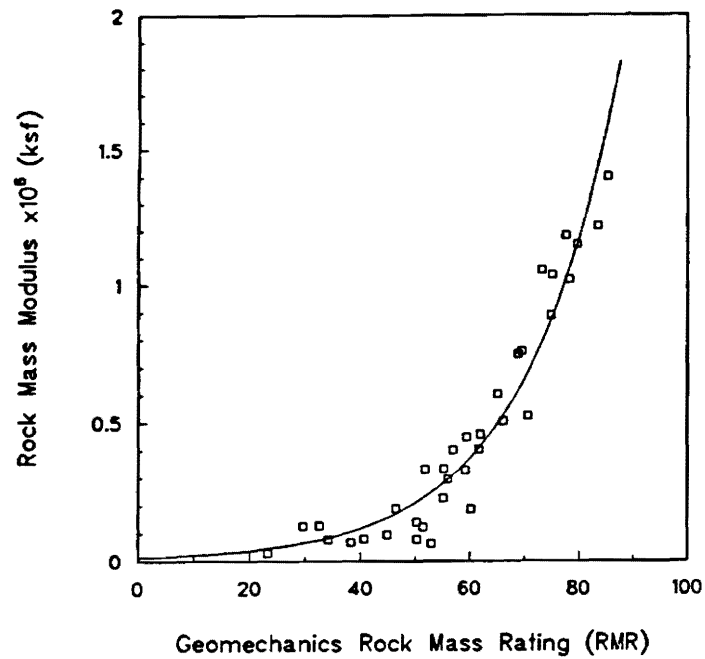


Figure 4.18. Rock Mass Modulus Versus Rock Mass Rating (RMR).
(After Bieniawski, 1984)

4.4. ANALYSIS AND DISCUSSION

The analysis of the Poulos (1972) solution, the Carter and Kulhawy (1988) solution, and the DEFPIG computer program (Poulos, 1978), consists of a comparison of the three methods, development of a recommended method of analysis, analysis of the load test data using the recommended method, and the development of design charts for rock socketed drilled shaft foundations.

4.4.1. Comparison of Methods

The solution provided by Poulos (1972) is the result of a boundary element analysis of the socketed pile case. Finite difference equations with 21 elements per pile were used to solve the problem and the results were published in 1972. Therefore, the development of the methodology had to take place during the late 1960's to early 1970's. During this time period, the computing power to handle rigorous numerical solutions was not available. For this reason, the Poulos (1972) solution is expected to be somewhat less accurate than later work. Another weakness with the Poulos (1972) solution is that the shaft tip is assumed to be fixed. No analysis is performed to take into account the length of socket or the quality of the rock mass on the overall shaft behavior. Because of this, an error occurs in the analysis of short stubby shafts where the socket may not be sufficient to fully fix the tip. In these cases, the Poulos (1972) solution predicts a deflection which is too low.

Carter and Kulhawy (1988) used a finite element numerical solution of the rock-socketed, drilled shaft case. In a finite element analysis, the actual number of elements used to model the pile is variable, but is considerably more than the 21 elements used by Poulos (1972). The series of approximate closed-form equations provided from this solution have been developed from a rigorous finite element study specifically for drilled shaft foundations in rock and should provide a good model for drilled shaft behavior.

The weak point of the Carter and Kulhawy (1988) solution lies in the analysis of the case of soil over rock. The models used for the lateral soil reaction resistance on the shaft are from Broms (1964). The ultimate lateral resistance in a clay soil is assumed to be

a constant $p_u = 9s_u$, where s_u is the soil undrained shear strength, starting at a depth of $1.5B$ and continuing to the rock interface. In sands, the reaction stress is taken as a triangular distribution, and the stress, p_u , at any depth is $p_u = 3K_p\sigma_v'$ where σ_v' is the vertical effective overburden stress and K_p is the Rankine passive earth pressure coefficient defined as $K_p = (1 + \sin\phi')/(1 - \sin\phi')$, where ϕ' is the soil effective stress friction angle.

There are two main difficulties with the Broms (1964) models. The first is that the model is oversimplified and not an accurate representation. The second problem is that in order for the full reaction stress to develop, the shaft must move laterally, along its entire length, enough to fully develop these limiting stresses. The purpose of the LLWAS foundation, to limit the amount of lateral deflection, dictates that in most cases the limiting earth pressure will not be developed. Due to this limitation of the Carter and Kulhawy (1988) solution, it does not seem appropriate to compare the two methods for a soil over rock case. Therefore, the comparison will only include analysis of full rock sockets with no overlying soil.

In addition, there is a difficulty with the analysis of an intermediate stiffness shaft. The Carter and Kulhawy (1988) solution provides explicit equations for deflections and rotations of rigid and flexible shafts. However, deflections and rotations for the intermediate stiffness shaft taken as less than or equal to 1.25 times the maximum of either the rigid or flexible case. The reasoning is that it simplifies the solution of the intermediate stiffness case considerably. Consequently, it is not possible to compare the two methods for an intermediate stiffness shaft because the Carter and Kulhawy method does not actually analyze the intermediate shaft.

Additionally, cases of a drilled shaft behaving as a rigid member when socketed in rock are not very common. This is due to the fact that the shaft modulus and the rock modulus are close to being equal. Because of this, it takes a very short socket length or a very weak rock to have the rigid case.

The DEFPIG computer program, Poulos (1978), has none of the limitations which make it difficult to analyze certain cases with the other solutions. The socket and soil sections of the shaft are both taken fully into account, and there are no practical limits on the ranges of the input data.

The comparison of the Poulos (1972), the Carter and Kulhawy (1988), and the DEFPIG program, Poulos (1978) solution methods will only cover the effects of rock modulus and shaft length for shafts embedded in surface exposed rock. The analysis revealed that the three solutions agree quite closely, with the Poulos (1972) and the DEFPIG, Poulos (1978), solutions being almost the same and the Carter and Kulhawy (1988) solution giving deflections which are about 25% to 30% lower than the other two solutions. Figure 4.19 shows the deflection predicted by each of the three solution methods. These numbers are for shafts which are just long enough to be classified as flexible members for the given rock modulus. The comparison of the three solution methods also showed a difference in the predicted deflections for shafts which are well into the flexible range.

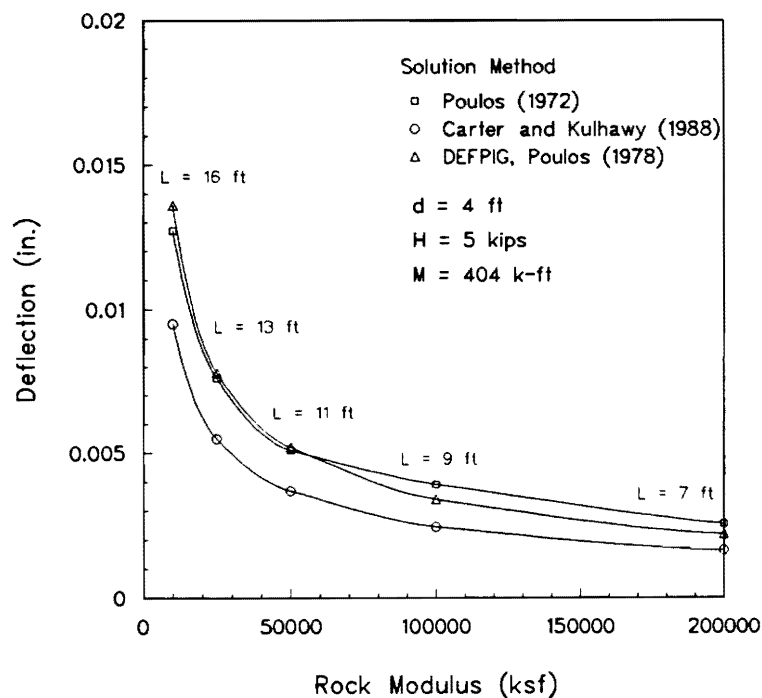


Figure 4.19. Comparison of Predicted Deflections from the Three Solutions for Flexible Socketed Shafts.

For these cases, the Carter and Kulhawy solution gives no reduction in deflection as the socketed length increases for a flexible shaft because in the Carter and Kulhawy (1988) solution deflection is independent of shaft length for the flexible case. The Poulos (1972) solution, however, gives decreasing deflections with increasing length, even for shafts which classify as flexible. The DEFPIG program also gives decreasing deflections when the socket length of a flexible shaft is increased, but the decrease is much less than for the Poulos (1972) solution. Data from the comparison of the three solution methods were obtained using the design loading of an LLWAS tower, and the diameter for all shafts was four feet.

4.4.2. Recommended Design Procedure

If the time, facilities, and understanding to run the DEFPIG computer program are available, it is recommended that it be used for the analysis of specific LLWAS foundations requiring rock sockets. The theory behind the program is sound and the limiting assumptions of the Poulos (1972) and the Carter and Kulhawy (1988) solutions are not present in the DEFPIG solution. However, it is recognized that in some instances it may be helpful to have a hand solution available. In these cases, the following hybrid solution which combines the Poulos (1972) and the Carter and Kulhawy (1988) solutions is also presented. This solution utilizes the Poulos (1972) method to analyze the soil section of the shaft and uses the Carter and Kulhawy (1988) method to analyze the socket section of the shaft. Then the two solutions are superimposed to give the overall groundline deflection.

An exception to the recommendation of the DEFPIG computer program exists for the case of rock which is exposed at the surface with no soil cover. In this case, the equations of Carter and Kulhawy (1988) for shafts embedded in surface exposed rock are recommended. These equations were developed from finite element analysis specifically for drilled shaft foundations. The use of these equations requires much less time than the computer solution and in the limited load tests available, agree with the actual measured data.

The deficiencies of both the Poulos (1972) and the Carter and Kulhawy (1988) methods suggest that neither method is sufficient by itself. The Poulos method because it limits the analysis to a completely fixed tip case and the Carter and Kulhawy solution because of the poor modeling of the soil reaction stress. When combined, the two methods can provide a reasonable model of the laterally loaded, rock socketed, drilled shaft problem.

The approximations of the Poulos (1972) influence factor charts in Section 4.1.1 (Figures 4.2, 4.3, and 4.4) are valid for $K_r > 10^1$. In most cases the soil section will have a K_r greater than 10^1 . Therefore, the approximations of the charts of Poulos (1972) in Section 4.1.1 will be valid most of the time for the analysis of the soil section of the shaft. The influence factors are then used in Equations 4.5 and 4.6 to obtain the deflection and rotation of the soil section. The equations provided by Carter and Kulhawy (1988) in Section 4.1.2 (Equations 4.9, 4.10, 4.12, and 4.13) can then be used to analyze the rock socket using the horizontal and moment loads at the end of a fixed tip shaft given by Poulos (1972) in Section 4.1.1 (Figures 4.5 and 4.6).

4.4.3. Example Application

To illustrate the proposed hybrid solution for rock-socketed shafts, an analysis of shaft A, under the conditions of the field load test, is included. Refer to Figure 4.7 for the shaft details and geotechnical data and to Figure 4.9 for the load-deflection curve.

The first objective is to determine the material parameters from the available information. The average N-value for the soil was 11, and using Figure 4.17, the approximate soil modulus is 1706 ksf. The bedrock is a weathered shale. Using the low value of the range of modulus for clastic sedimentary rocks in Table 4.2 and assuming a modulus reduction factor of 0.14, the rock mass modulus is $100,000 \text{ ksf} \times 0.14 = 14,000 \text{ ksf}$.

The method of Poulos (1972) is used to analyze the soil section of the shaft. In order to calculate the shaft rigidity factor, K_r , the shaft properties are needed. The assumed modulus for a lightly reinforced concrete shaft is 570,000 ksf, and the moment of inertia for a four foot diameter circular shaft is 12.5 ft^4 . Given these values, the flexibility

factor is:

$$K_r = \frac{570,000 \times 12.5}{1706 \times 11.4^4} = 0.24$$

$$\frac{L}{d} = \frac{11.4 \text{ ft}}{4 \text{ ft}} = 2.85$$

Because this value of K_r is greater than 0.1, the approximate solution of the Poulos (1972) charts, valid for $K_r > 0.1$ may be used.

$$I_{\rho H} = 0.30 (K_r)^{-0.80} = 0.93$$

$$I_{\theta H} = 0.50 (K_r)^{-0.82} = 1.61$$

The level of loading for this example will be compatible with that used in the load test so that the two may be compared. The horizontal load is 100 kips at an eccentricity of 4 feet to give a moment of 400 kip-feet. These values are used in Equation 4.4 to give the deflection at the shaft head (groundline):

$$\rho = 0.91 \frac{100}{1706 \times 11.4} + 1.56 \frac{400}{1706 \times 11.4^2} = 0.092 \text{ inch.}$$

The socket section is analyzed by determining the approximate loading on the socket head by the charts of Poulos (1972) in Figures 4.5 and 4.6.

Moment:

$$M_r/HL = 0.62$$

$$M_r = 0.62 \times 100 \text{ kips} \times 11.4 \text{ ft} = 706 \text{ kip-ft}$$

$$M_r/M = 0.52$$

$$M_f = 0.52 \times 400 \text{ kip-ft} = 208 \text{ kip-ft}$$

$$M_{TOT} = \underline{914} \text{ kip-ft}$$

Shear:

$$H_f/H = -0.5$$

$$H_f = -0.5 \times 100 \text{ kips} = -50 \text{ kips}$$

$$H_f L/M = 0.7$$

$$H_f = (0.7 \times 400 \text{ kip-ft})/11.4 \text{ ft} = 24 \text{ kips}$$

$$H_{TOT} = \underline{-26} \text{ kips}$$

Once the loading on the socket head is calculated, the equations of Carter and Kulhawy (1988) are used to calculate the deflection of the socket. The rock modulus is estimated as 14,000 ksf and ν is assumed = 0.2, therefore:

$$G_r = 14000 \text{ ksf}/(2 \times 1.2) = 5833 \text{ ksf}$$

$$G^* = 5833 \text{ ksf} \times (1 + 0.15) = 6708 \text{ ksf}$$

The L/d for this shaft is between $(E_c/G^*)^{2/7}$ and $0.05(E_c/G^*)^{1/2}$, therefore, the section is an intermediate stiffness member. The Carter and Kulhawy (1988) solution solves the intermediate case by taking the deflection to be 1.25 times the maximum of the flexible or rigid case. For this shaft, the flexible case gives the greater deflection, and using Equation 4.9 the deflection is:

$$\rho = 0.5 \frac{-26}{6708 \times 3} \left(\frac{570000}{6708} \right)^{-1/7} + 1.08 \frac{914}{6708 \times 3^2} \left(\frac{570000}{6708} \right)^{-3/7}$$

$$\rho = \delta = 0.014 \text{ in.} \quad (\text{flexible case})$$

$$\rho = \delta = 0.014 \times 1.25 = 0.0175 \text{ in.} \quad (\text{intermediate case})$$

$$\text{Total Deflection} = 0.092 + 0.0175 = \underline{0.109} \text{ in.}$$

$$\text{Actual Deflection} = 0.12 \text{ in.}$$

4.4.4. Analysis of the Load Test Data

The load test data from the eight available load tests were analyzed using the two recommended solutions and the results along with the actual measured deflections are presented in Table 4.3. In this analysis very close agreement between the predicted values and the actual measured deflection is shown. The only real discrepancies are in the values predicted for shafts E and H. The authors who describe the load test of shaft E, Lyndon et al. (1989), attribute the abnormally large deflection of shaft E to the fact that shaft E was loaded axially to failure before the lateral load test was run. Both solutions underpredicted the deflection of shaft H by more than 50%. However, no reason for this error is readily apparent.

Table 4.3. Analysis of the Load Test Data on Socketed Shafts Using the DEFPIG Program and the Poulos/Carter & Kulhawy Hybrid Solution.

Shaft No.	Ref. No.	Actual Defl. (in)	Poulos/Carter & Kulhawy Solution (in)	DEFPIG Computer Solution (in)
A	1-N	0.120	0.109	0.123
B	1-S	0.075	0.066	0.096
C	2-N	0.140	0.093	0.104
D	2-S	0.140	0.084	0.104
E	1200	1.300*	0.117	0.354
F	1500	0.310	0.143	0.270
G	14-U	0.020	0.025	0.024
H	14-D	0.120	0.028	0.029

* Note: Shaft axially loaded before lateral load test.

4.5. DESIGN CHARTS

For quick reference and for ease in designing LLWAS foundations at sites with shallow bedrock, the following design charts are included in this section. The data points for these charts were calculated using the DEFPIG computer program.

The first three charts present data for four values of rock modulus (1000, 10,000, 100,000, and 1,000,000 ksf) and assume a soil modulus of 100 ksf for all cases. Figures 4.20 to 4.22 show the deflection vs. socket length for a depth to rock of 5 feet, 10 feet, and 15 feet. Figure 4.23 combines this information assuming a conservative value of rock modulus = 1000 ksf. This is necessary since specific rock type and quality will not

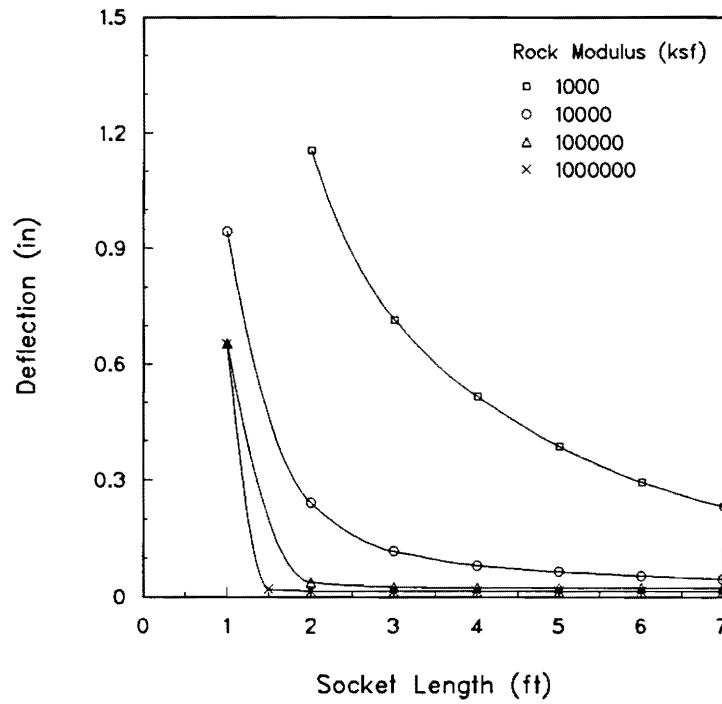


Figure 4.20. Theoretical Deflection Versus Socket Length for
Depth to Rock = 5 ft.

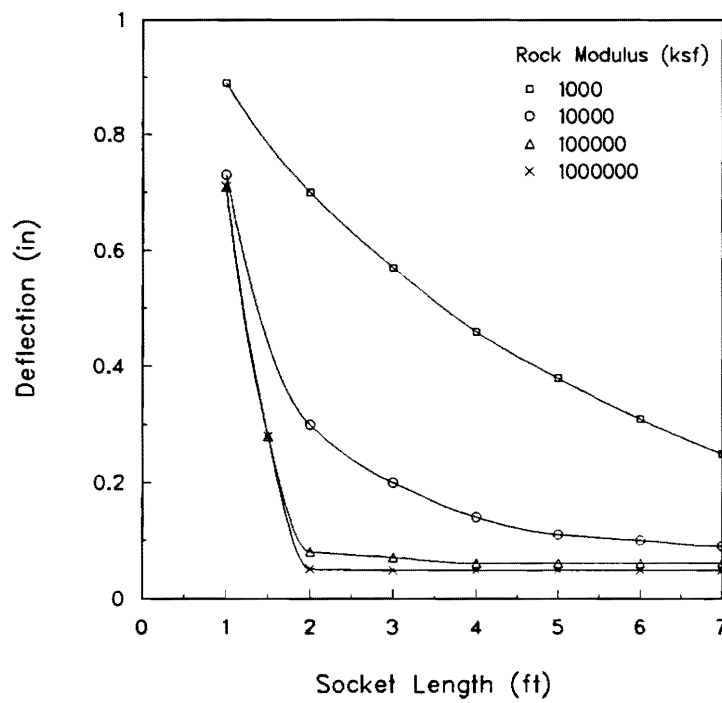


Figure 4.21. Theoretical Deflection Versus Socket Length for
Depth to Rock = 10 ft.

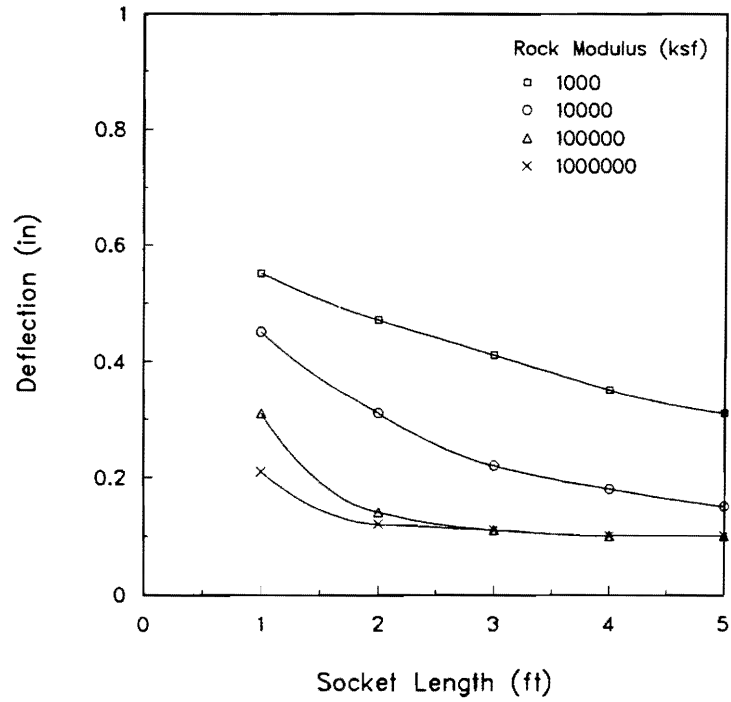


Figure 4.22. Theoretical Deflection Versus Socket Length for
Depth to Rock = 15 ft.

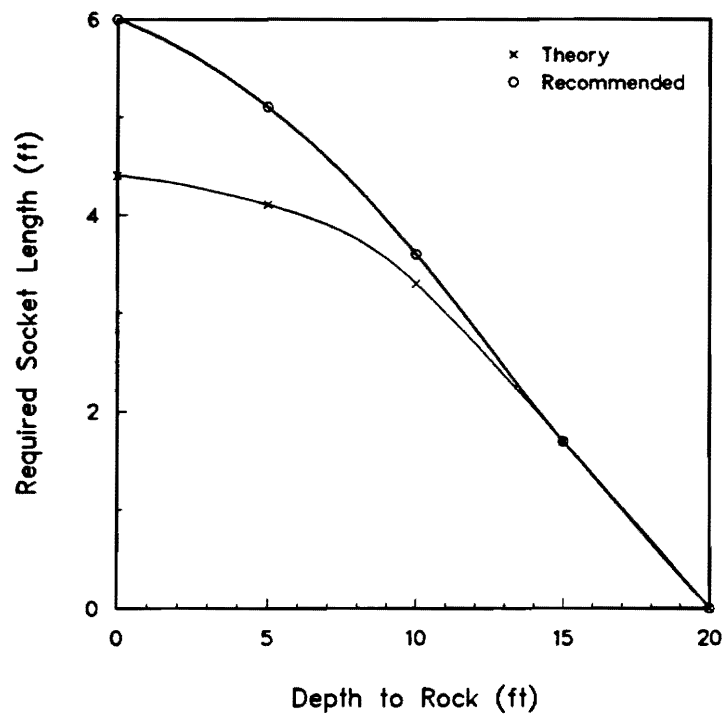


Figure 4.23. Recommended Minimum Required Socket Length Versus Depth to Rock.

normally be distinguished on LLWAS projects. Figure 4.23 shows the recommended minimum socket lengths versus the depth to rock. The recommended socket length is higher than the theoretical length for shallow depths to rock to take into account the very high stresses which would be applied at shallow depths and may cause yielding of the rock at the surface. In addition, the average L_e/d from Table 4.1 is 1.5 which would correspond to a 6 foot rock socket.

4.6. CONCLUSIONS

Rock-socketed shafts under lateral and moment loading may be analyzed using either a hybrid solution based on boundary element/finite element methods or a 2-layer system solved via the DEFPIG program. The few reported load test results on rock-socketed shafts have been reviewed and evaluated in this context. Based on conservative estimates of soil and rock moduli, design charts have been presented to ascertain the minimum required length of rock socket for LLWAS sites where shallow bedrock is encountered.

4.7 REFERENCES

Bieniawski, Z.T. (1984), Rock Mechanics Design in Mining and Tunneling, Balkema Publishers, Rotterdam, Netherlands, 272 p.

Broms, B.B. (1964), "Lateral Resistance of Piles in Cohesive Soils", Journal of the Soil Mechanics and Foundations Division, ASCE, Vol. 90, No. SM2, pp. 27-63.

Broms, B.B. (1964), "Lateral Resistance of Piles in Cohesionless Soils", Journal of the Soil Mechanics and Foundations Division, ASCE, Vol. 90, No. SM3, pp. 123-156.

Carter, J.P. and Kulhawy, F.H. (1988), "Analysis and Design of Drilled Shaft Foundations Socketed Into Rock", Report EL-5918, Electric Power Research Institute, Palo Alto, 134 p.

Davisson, M.T. and Salley, J.R. (1969), "Lateral Load Tests on Drilled Piers", Performance of Deep Foundations (ASTM STP 444), American Society for Testing and Materials, Philadelphia, PA, pp. 68-83.

Douglas, D.J. and Davis, E.H. (1964), "The Movement of Buried Footings Due To Moment and Horizontal Load and the Movement of Anchor Plates", Geotechnique, Vol. 14, No. 1, pp. 115-132.

Hall, W.J., Newmark, N.M., and Hendron, A.J. (1974), "Classification, Engineering

Properties, and Field Exploration of Soils, Intact Rock, and In-Situ Rock Masses", Report WASH-1301, Directorate of Regulatory Standards, U.S. Atomic Energy Commission, Washington, D.C., 260 p.

Kulhawy, F.H. (1975), "Stress Deformation Properties of Rock and Rock Discontinuities", Engineering Geology, Vol. 9, No. 2, pp. 327-350.

Kulhawy, F.H. and Mayne, P.W. (1990), "Manual on Estimating Soil Properties for Foundation Design", Report EL-6800, Electric Power Research Inst., Palo Alto, 306 p.

Lee, S.L., Kog, Y.C., and Karunaratne, G.P. (1987), "Laterally-Loaded Piles in Layered Soil", Japanese Society of Soil Mechanics and Foundation Engineering, Vol. 27, No. 4, pp. 1-10.

Lyndon, A., et. al. (1989), "The Effect of Vertical Pile Loading on Subsequent Lateral Behavior", Piling and Deep Foundations, Proceedings of the International Conference on Piling and Deep Foundations, London, pp. 377-382.

Mattes, N.S., and Poulos, H.G. (1969), "Settlement of Single Compressible Pile", Journal of the Soil Mechanics and Foundations Division Vol. 95, No. SM1, pp. 189-207.

Pise, P.J. (1982), "Laterally Loaded Piles in a Two Layer Soil System", Journal of the Soil Mechanics and Foundations Division ASCE, Vol. 108, No. GT9, pp. 1177-1181.

Poulos, H.G. (1971a), "Behavior of Laterally Loaded Piles: I. Single Piles", Journal of the Soil Mechanics and Foundations Division ASCE, Vol. 97, No. SM5, pp. 711-731.

Poulos, H.G. (1971b), "Behavior of Laterally Loaded Piles: II. Pile Groups", Journal of the Soil Mechanics and Foundations Division ASCE, Vol. 97, No. SM5, pp. 733-751.

Poulos, H.G. (1972), "Behavior of Laterally Loaded Piles: III. Socketed Piles", Journal of the Soil Mechanics and Foundations Division ASCE, Vol. 98, No. SM4, pp. 341-360.

Poulos, H.G. (1978), Users Guide to Program DEFPIG, The University of Sydney, School of Civil Engineering, Sydney, Australia, 77 p.

Poulos, H.G. and Davis, E.H. (1980), Pile Foundation Analysis and Design, John Wiley and Sons, New York, 379 p.

Poulos, H.G. and Madhav, M.R. (1971), "Analysis of the Movement of Battered Piles", Proceedings, First Australian - New Zealand Conference on Geomechanics, Vol. 1, Wellington, pp. 268-275.

Poulos, H.G. and Mattes, N.S. (1971), "Settlement and Load Distribution Analysis of Pile Groups", Australian Geomechanics Journal, Vol. G1, No. 1, pp. 18-28.

SECTION 5

EXECUTIVE SUMMARY

Current practice for supporting a 150-foot high FAA LLWAS tower involves the construction of a single drilled shaft foundation with a 4-foot diameter embedded 20 feet into soil and/or rock, depending upon the specific site and local geology. Large overturning moments are imposed on the shafts during storm events. Specific concerns include the ultimate lateral capacity and groundline displacements of the foundations during wind shear and microbursts, since the LLWAS system must perform as a warning system for these conditions.

In the FAA Southern Region, a total of 37 airports have been outfitted with a basic array of 6 LLWAS towers. For most of these sites, the LLWAS tower foundation systems have proven to be adequate in capacity and overall performance. At 16 of these airports, an additional 5 LLWAS towers have been installed or are currently under construction. The remaining 21 airports will also be provided with additional LLWAS towers over the next few years. Of particular interest to FAA are sites where: (1) the standard foundation design may be inadequate for load-deflection response due to poor soil conditions and (2) shallow bedrock conditions which result in significant cost overruns during construction in order to achieve the standard design foundation lengths.

This design manual summarizes procedures to be taken by field personnel during the initiation and construction of future LLWAS towers. The text of this manual is a synopsis of a companion *Final Report* addressing a geotechnical analysis of the LLWAS drilled shaft foundation system which has been prepared by GTRC for the FAA Southern Region. The geotechnical study was performed to evaluate the probable lateral capacity and load-deflection response under a variety of common geologic settings, soil types, and bedrock conditions. The effort was separated into three primary tasks to address specific issues raised by the FAA Technical Officer, including: (1) the expected performance of standard LLWAS foundations under critical loading conditions, (2) an assessment of available analytical and numerical modelling capabilities, and (3) recommendations for

minimum required socket lengths of shaft foundations at sites where shallow rock is encountered. These task items are discussed in detail in the *Final Report*.

5.1. SOIL PROFILES

5.1.1 Analytical Design Charts

For LLWAS towers installed at sites underlain by firm soils, the standard 4-foot diameter by 20-foot long drilled shaft foundations appear adequate. These dimensions constitute relatively rigid foundation members due to their low length to diameter ratio ($L/d = 5$). Their anticipated performance has been evaluated from a load test database on rigid drilled shaft foundations subjected to lateral/moment loading that were compiled from the geotechnical literature and published reports. These load test results have been analyzed within a framework of elastic continuum mechanics, and a simple hyperbolic model was shown to effectively describe the nonlinear load-deflection behavior. Backcalculated design parameters were formulated in terms of soil strength and soil modulus, which in turn have been related to the simple and common standard penetration test (SPT).

The results of the analytical study are summarized in Figures 5.1 and 5.2 for clayey soils and sandy soils, respectively. As discussed in the *Final Report*, a maximum groundline deflection $\delta = 0.5$ inches has been established as the acceptance criterion for foundation performance. The analyses show that, in general, the standard LLWAS foundation is capable of adequate or superior performance under critical loading conditions, except where the soil overburden profile consists of soft/firm clays or loose sands below the water table.

5.1.2 Problem Soils

Specifically, the numerical analysis indicated problems could exist where the results of soil test borings (ASTM D-1586) showed standard penetration test (SPT) resistances consistently less than 7 blows per foot in clays and less than 8 blows per foot in sands. For LLWAS sites not meeting these criteria, more extensive geotechnical analyses should be performed to evaluate the need for installing deeper (or wider) foundations at these sites.

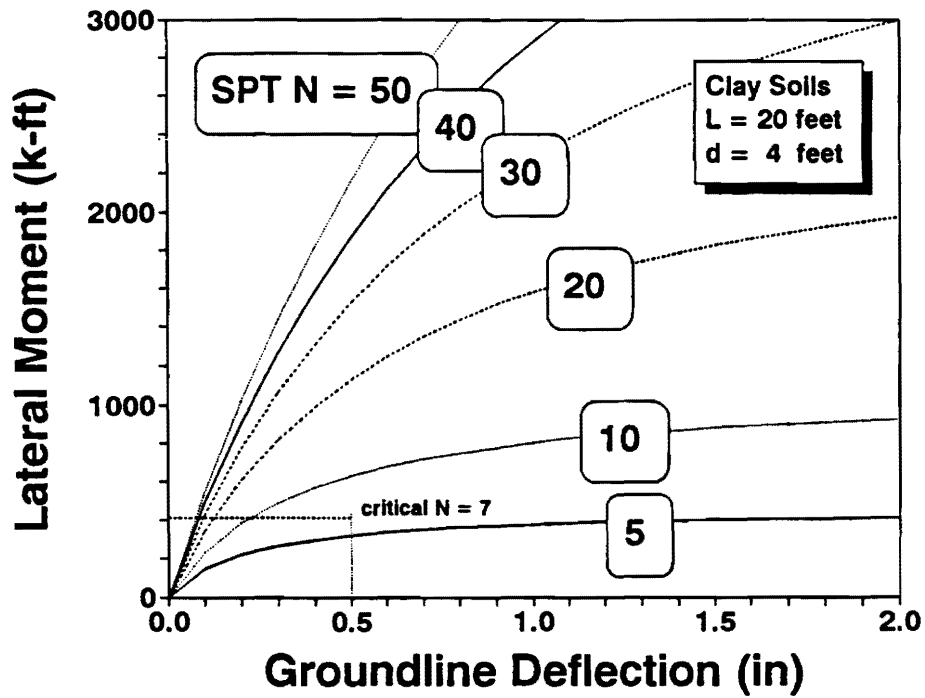


Figure 5.1. Predicted Moment-Deflection Behavior of Shafts at Clay Sites.

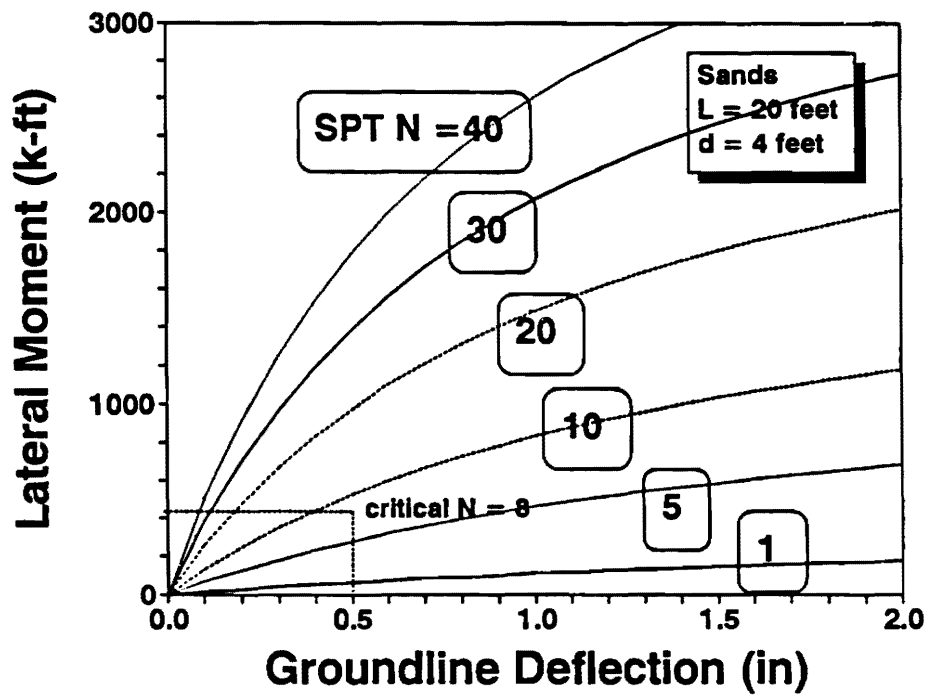


Figure 5.2. Predicted Moment-Deflection Behavior of Shafts at Sand Sites.

5.1.3 Field Inspection

Visual examination of auger cuttings of excavated soils should provide warning to the FAA field inspector as to the necessity for more detailed geotechnical analyses and possible need for a modified foundation design. Of particular concern, the field inspector should be wary of wet, soft, and plastic clays, black and dark-colored clays with organics, peats, uniform silts, loose clean to silty sands, and soils which cave upon excavation by the caisson rig (Reference ASTM D-2488 standards for soil classification). Also, sites having been previously filled and containing debris, rubble, waste, and man-made buried objects should be suspect as not meeting the criteria for acceptable ground.

In many cases, the field inspector may be able to discern the problem soil types, yet not be confident in estimating the degree of penetration resistance without actually performing an SPT. For these situations, the helix probe test (HPT) may provide a simple and economical means of obtaining a numerical value of the soil consistency. The HPT measures the torque required to advance a 0.75-inch diameter auger (Yokel and Mayne, 1988). Approximately five feet of soil depth can be investigated in about 5 to 10 minutes with readings typically taken on 0.5-foot increments. The measured torque (t_{12}) has been correlated with standard penetration test (SPT) resistance, as well as cone penetration test (CPT), dilatometer test (DMT), and in-place density measurements. The entire instrument weighs only 5 lbs and easily carried by a field inspector. A modified version with rod extensions has also been built which is capable of achieving test depths of up to 20 feet.

5.1.4 Advanced Geotechnical Analyses

If the field inspector has determined the need for additional and more extensive foundation analyses, a qualified geotechnical consultant should be retained to perform the necessary in-situ testing and computer simulations. Based on the findings of the *Final Report*, it is recommended that the consultant perform a series of flat dilatometer tests (DMT) or pressuremeter tests (PMT) at the LLWAS site in question. Test procedures for the DMT and PMT are given by Schmertmann (1986) and ASTM (1990). The results of these tests provide information on the soil strength and modulus properties.

The use of the computer programs: LTBASE (North Carolina State University, Raleigh, NC) or MFAD (Electric Power Research Institute, Palo Alto, CA) appear appropriate for analyzing LLWAS foundations because both have been specifically developed for short and rigid drilled shafts.

In the event that the standard design is suspected to be inadequate, the following remedial measures may be considered: (1) increase foundation length, (2) increase foundation diameter, (3) soil improvement, or (4) move the tower location. Considering the practicality of drilling operations and feasibility of construction, selection of choice (1) appears the most economical. Therefore, modified designs and analyses should be directed at solutions which investigate $L = 30$ feet, or longer, or similar such alternatives.

5.2 SHALLOW BEDROCK PROFILES

5.2.1 Analytical Approach

The design and construction of LLWAS foundations at sites with soil over shallow bedrock has also been addressed in the *Final Report*. In the LLWAS program, no current procedures or guidelines exist for terminating shaft lengths less than the standard design length of 20 feet, even if sound rock is encountered beforehand. Available analytical tools for evaluating rock-socketed shafts have been reviewed and these are based on boundary element and finite element solutions to elastic continuum formulations of the problem. A computer program (DEFPIG) has been used to develop a design chart, presented as Figure 5.3, which rationally minimizes the required length of the rock socket. The chart is valuable to the FAA field inspector in selecting a suitable total length of shaft and mitigating cost overruns during drilled shaft construction.

In the event that bedrock is encountered at the ground surface, the recommended minimum length of the shaft should be 1.5 times the foundation diameter. Recent unpublished moment load tests on rock-socketed shafts conducted by EPRI support this recommendation. Therefore, for the standard 4-foot diameter shaft, a minimum 6-foot embedment length is recommended.

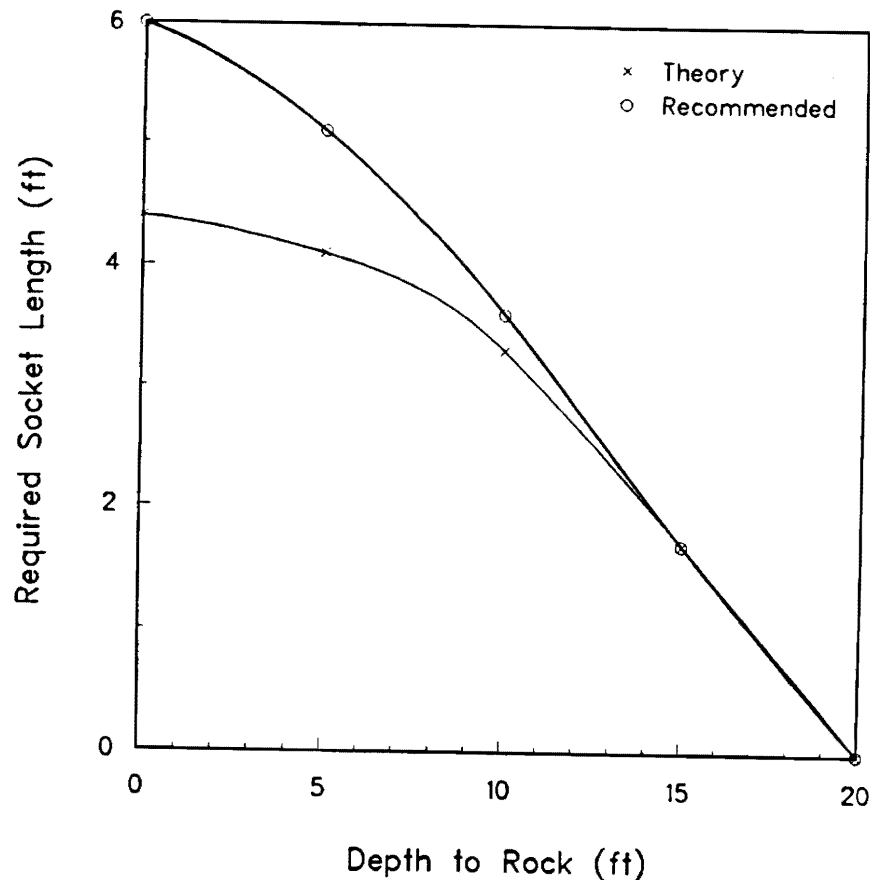


Figure 5.3. Recommended Minimum Length of Rock Socket for Drilled Shaft Foundations Constructed at Shallow Bedrock Sites.

5.2.2 Detailed Geotechnical Analysis

If more detailed analyses are desired, the following procedure is suggested for implementation by a qualified geotechnical consultant. Soil test borings with standard penetration testing (SPT) should be advanced to the top of bedrock (ASTM D-1586). The SPT values may be used to evaluate the relevant soil moduli from relationships given in Section 2 of the *Final Report*. Upon SPT refusal, core samples of the underlying rock should be taken (ASTM D-2113) and the rock quality designation (RQD) should be determined. Selected specimens from the recovered core should be subjected to uniaxial compression tests to determine the elastic modulus of the intact rock (ASTM D-3148). The RQD value should be utilized to obtain a reduction factor per Section 4 of the *Final Report* and appropriate value of the modulus of the rock mass in-situ. Finally, the computer program DEFPIG (University of Sydney, Australia) should be used to evaluate the load-deflection behavior of the rock-socketed foundations.

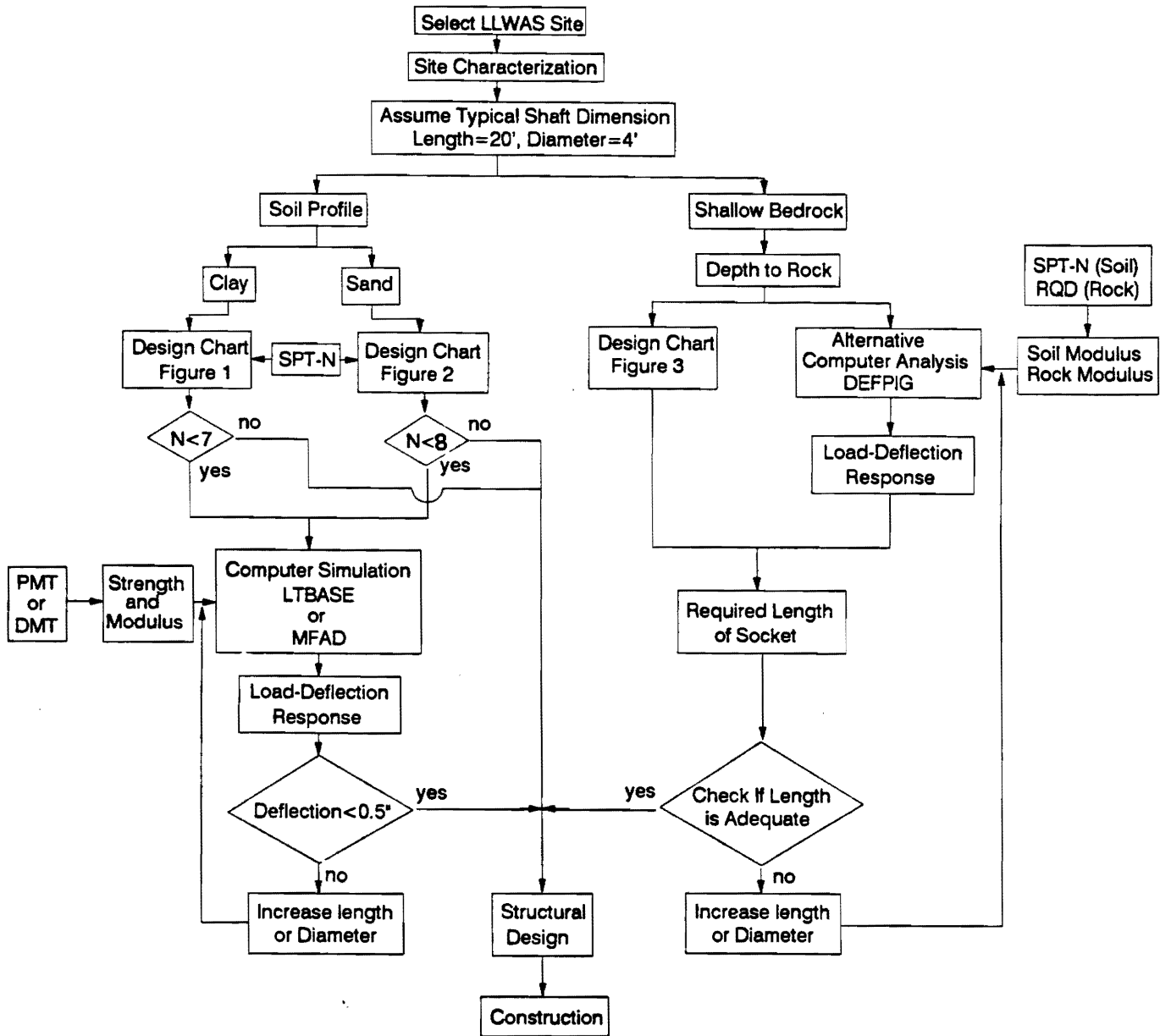


Figure 5.4. Systematic Procedure for Geotechnical Evaluation of LLWAS Site.

5.3 FLOW CHART

A synopsis of the recommended procedures for evaluating the suitability of geotechnical conditions at specific LLWAS tower foundation locations is given on the flow chart in Figure 5.4. This flow chart may be used by the field inspection and FAA engineer in

assessing the adequacy of the standard LLWAS foundation design, the need for more extensive geotechnical studies, and/or the modification of the drilled shaft foundation to meet the desired performance.

Based on numerical and analytical calculations, the standard LLWAS drilled foundation ($L = 20$ feet, $d = 4$ feet) appears adequate or superior for its intended use, except at sites underlain by soft/firm clays and silts or loose sands below the water table. The field inspector should be trained to discern unacceptable soil conditions and may find assistance in evaluating poor ground conditions by use of the helix probe test (HPT).

At shallow bedrock sites, conservative estimates of rock mass properties and numerical analyses indicate that the total length of the LLWAS foundation may be reduced. The required length of the rock socket will depend upon the particular depth to bedrock.

5.4 REFERENCES

American Society for Testing and Materials (1990), ASTM D-3148: "Standard Test Method for Elastic Moduli of Intact Rock Core Specimens", Annual Book of ASTM Standards, Vol. 04.08, Philadelphia, PA, 391-394.

American Society for Testing and Materials (1990), ASTM D-2113: "Standard Practice for Diamond Core Drilling for Site Investigation", Annual Book of ASTM Standards, Vol. 04.08, Philadelphia, PA, 256-259.

American Society for Testing and Materials (1990), ASTM D-1586: "Standard Method for Penetration Test and Split-Barrel Sampling of Soils", Annual Book of ASTM Standards, Vol. 04.08, Philadelphia, PA, 228-232.

American Society for Testing and Materials (1990), ASTM D-4719: "Standard Test Method for Pressuremeter Testing in Soils", Annual Book of ASTM Standards, Vol. 04.08, Philadelphia, PA, 896-903.

American Society for Testing and Materials (1990), ASTM D-2488: "Standard Practice for Description and Identification of Soils", Annual Book of ASTM Standards, Vol. 04.08, Philadelphia, PA, 305-314.

Borden, R.H. and Gabr, M.A. (1987), "LTBASE: Computer Program for Laterally-Loaded Pier Analysis Including Base and Slope Effects", Research No. HRP 86-5, North Carolina State University, Raleigh, NC, 48 p.

Chen, B.S-Y., Fang, J.S., Blaydes, D.G., and Mayne, P.W. (1991), "Final Report, Geotechnical Evaluation of LLWAS Tower Foundations Under Lateral and Moment Loading", Georgia Tech Research Corporation Report E-20-622 to FAA Southern Region, Atlanta, Georgia, 113 p.

Davidson, H.L., et al. (1990), "TL Workstation Code: Version 2.0, Volume 17, MFAD Manual", EPRI Report EL-6420, Electric Power Research Institute, Palo Alto, CA.

Poulos, H.G. (1978), "User's Guide to Program DEFPIG", University of Sydney, School of Civil Engineering, Australia, 77 p.

Schmertmann, J.H. (1986), "Suggested Method for Performing the Flat Dilatometer Test", ASTM Geotechnical Testing Journal, Vol. 9 (2), 93-101.

Yokel, F.Y. and Mayne, P.W. (1988), "Helical Probe Tests: Initial Test Calibration", ASTM Geotechnical Testing Journal, Vol. 11 (3), 179-186.